JNCC/Cefas Partnership Report Series

Report No. 14

CEND 19x/12: Offshore seabed survey of Braemar Pockmarks SCI and Scanner Pockmark SCI

Rance, J., Barrio Froján, C. & Schinaia, S.Ju

June 2017

ISSN 2051-6711

CEND 19x/12: Offshore seabed survey of Braemar Pockmarks SCI and Scanner Pockmark SCI

Rance, J., Barrio Froján, C. & Schinaia, S.

Report completed 2013 and published June 2017

ISSN 2051-6711

For further information please contact:

Joint Nature Conservation Committee
Monkstone House
City Road
Peterborough PE1 1JY
www.jncc.defra.gov.uk

This report should be cited as:

Rance, J., Barrio Froján, C. & Schinaia, S. 2017. CEND 19x/12: Offshore seabed survey of Braemar Pockmarks SCI and Scanner Pockmark SCI. *JNCC/Cefas Partnership Report Series*, **No. 14**. JNCC, Peterborough.

Executive Summary

This report presents the findings from the analyses of the data gathered during the seabed survey of the Braemar Pockmarks and Scanner Pockmark Sites of Community Importance (SCI), as defined in the European Commission Habitats Directive 92/43/EEC. The pockmark features present within both of the SCIs are a series of crater-like depressions on the seafloor, and can include the Directive's Annex I habitat 'Submarine structures made by leaking gases'. These structures consist of large blocks, pavements, slabs and smaller fragments of carbonate rock, including methane-derived authigenic carbonate (MDAC).

The report describes the presence, location and extent of the pockmark features, along with detail relating to the presence and location of any associated seafloor carbonate structures where they are observed to occur. A physical and biological characterisation of the wider area, surrounding the pockmark features, is also provided.

Full-coverage acoustic multibeam bathymetry and backscatter data were acquired at the two SCIs and data quality was found to be good. Additionally, sidescan sonar data were collected, however the quality of these data was affected by the survey conditions during acquisition, and was considered to be of low quality. Areas of distinct acoustic signatures from multibeam data were delineated using the semi-automated eCognition software. Standard univariate and multivariate analyses on the taxa abundance data have been performed to identify distinct faunal assemblages.

Combined analysis of the acoustic and groundtruthing data enabled the identification of two distinct sediment types within both SCIs, namely mud and mixed sediments. Further interpretation led to the assignment of the biotopes A5.36 Circalittoral Fine Mud and A5.44 Circalittoral Mixed Sediment to these sediment types.

Presence of the Annex I habitat 'Submarine structures made by leaking gases' within the Braemar Pockmark SCI was suggested through observations of seabed structures on the video and still image data, and confirmed following laboratory analysis of carbonate samples (MDAC) collected in a number of grab samples. Sidescan sonar records also provided evidence of gas bubbles in the water column, which appeared to be venting from one of the pockmarks. No Annex I habitat 'Submarine structures made by leaking gases' (MDAC) was observed in either the underwater video footage, still images or grab samples at the Scanner Pockmark SCI, and no evidence of active venting was observed on the sidescan sonar data.

Table of Contents

List of Figures

List of Tables

1 Background

Two Sites of Community Importance (SCIs, as defined in the European Commission Habitats Directive 92/43/EEC), namely the Braemar Pockmarks SCI and the Scanner Pockmark SCI, were approved following submission to the European Commission in August 2008. At the time of writing, the SCIs were awaiting formal designation as Special Areas of Conservation (SACs) by the UK Government[1] (JNCC 2011a & 2011b). Both sites were proposed for designation, as existing evidence suggested that they contain the Annex I habitat 'Submarine structures made by leaking gases'.

In November 2012 the Joint Nature Conservation Committee (JNCC) in partnership with Cefas, conducted an acoustic and benthic sampling survey of both SCIs to gather additional evidence to support the development of fisheries management measures under the Common Fisheries Policy (CFP). The survey was completed successfully in December 2012, and a cruise report (Cefas & JNCC 2013) was delivered shortly after. The present report describes the findings from the analyses of the data gathered during the survey.

2 Introduction

Both the Braemar Pockmarks SCI (area: 518ha) and the Scanner Pockmark SCI (area: 335ha) are situated within the Witch Ground Basin in the northern North Sea. The Braemar Pockmarks SCI is situated approximately 240km east of the Orkney Islands (Figure 1). The Scanner Pockmark SAC is located further south, 185km northeast of the Scottish mainland (Figure 2). Both sites lie at depths between 120 and 150m.

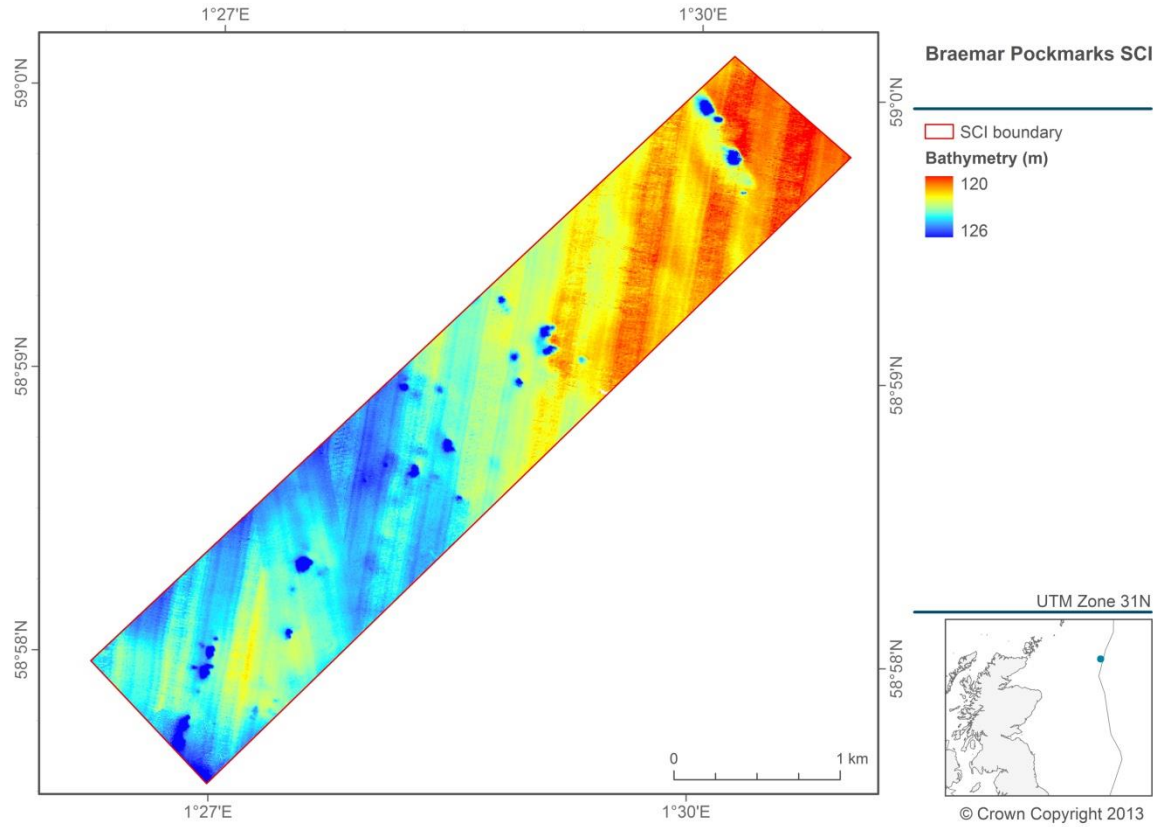

Figure 1. The Braemar Pockmarks SCI. Bathymetry data collected by the offshore energy industry.

[1] At time of writing the sites were awaiting designation. Both Braemar Pockmarks and Scanner Pockmark were designated as SACs in December 2015.

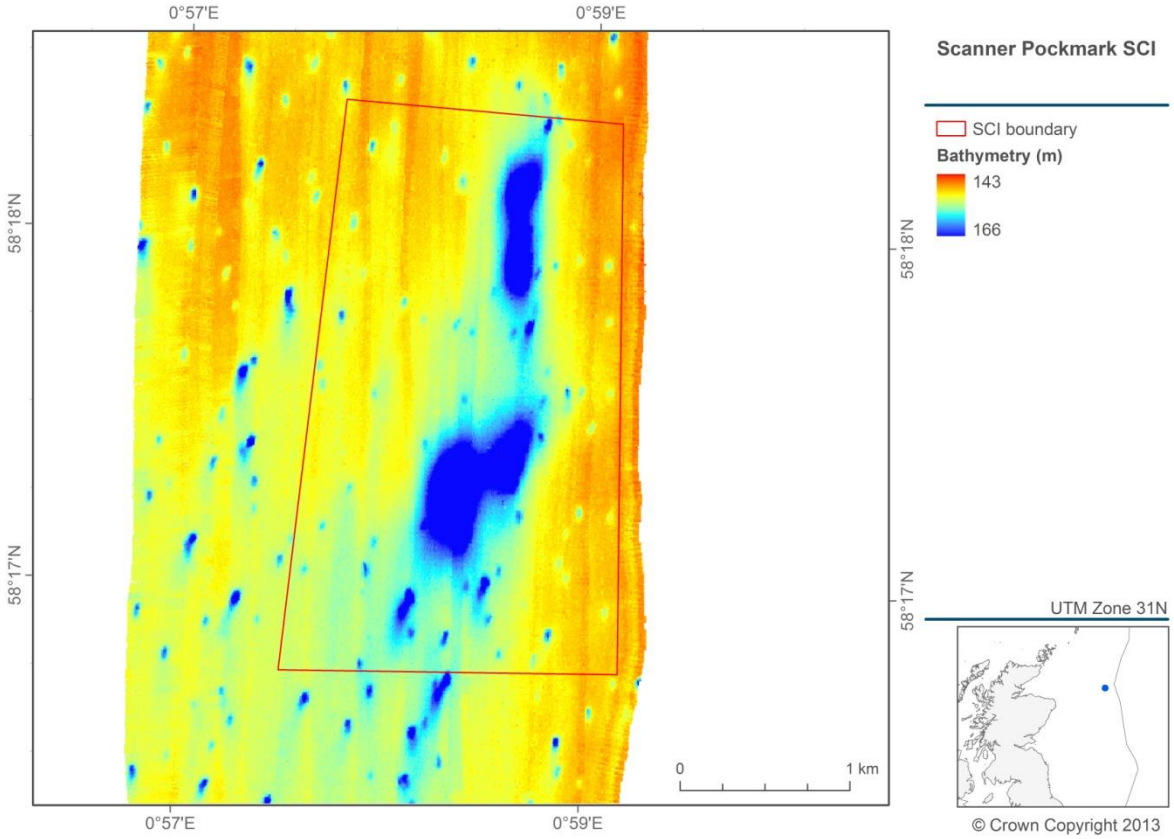

Figure 2. The Scanner Pockmark SCI. Bathymetry data collected by the offshore energy industry.

The pockmark features present within both of the SCIs are of a series of crater-like depressions on the seafloor, some of which have been shown to contain the Annex I habitat 'Submarine structures made by leaking gases' (Hartley 2005) or methane-derived authigenic carbonate (MDAC). These carbonates are formed by precipitation during the anaerobic oxidation of methane gas within sediments close to the seafloor (Boetius *et al* 2000), and when exposed provide a habitat for marine fauna usually associated with hard substrates (Dando *et al* 1991) (see Annex 1 for a review of their geological origin and properties). Such methane-derived authigenic carbonate (MDAC) structures provide a habitat for marine fauna usually associated with rocky reef, as well as for chemosynthetic micro-organisms, which utilise methane and hydrogen sulphide as an alternative energy source to solar-derived energy. Larger blocks of carbonate also provide shelter for large fish species such as wolf-fish and cod (Hartley 2005). Existing evidences suggests that MDAC structures at the Braemar Pockmarks SCI are more abundant and diverse in form than those at the Scanner Pockmark SCI, and appear to be characterised by slightly different species assemblages (JNCC 2008, 2012a).

The MDAC structures and associated biological communities at both SCIs are currently assessed as *moderately vulnerable* (Braemar) and *highly vulnerable* (Scanner) to damage by physical disturbance or abrasion, and biological disturbance by selective extraction of species (both by demersal fishing activities) (JNCC 2012b, 2012c). There is, however, a lack of detailed information on (i) the condition of Annex I features within these sites, (ii) the levels of exposure to human activities, and (iii) the potential ecological impact of such activities on their associated Annex I features.

The present investigation aims to provide additional evidence to support the development of fisheries management measures under the Common Fisheries Policy (CFP), whilst also enabling a better understanding of the extent and condition of the qualifying features within

each site prior to any management measures being developed and implemented. Collected data have been analysed and the results are presented here.

3 Survey Design and Methods

3.1 Acoustic and geophysical data acquisition

Acoustic data were collected onboard RV *Cefas Endeavour* using a Kongsberg EM2040 dual head multibeam echosounder. A Kongsberg Seapath 330+ with Seatex MRU5 system was used to provide positional and motion compensation data.

The raw MBES files (.ALL files) were acquired using the Kongsberg SIS operating system. Bathymetry data were processed using the CARIS HIPS and SIPS 7.1 SP2 hydrographic data processing system. Tidal data were modelled using Cefas' tidal model software TStide and the offsets from MSL to Chart Datum were subsequently applied. Backscatter mosaics were produced using QPS Fledermaus Geocoder Toolkit (FMGT) software.

Dual frequency sidescan sonar data were collected using Edgetech FS4200 sidescan sonar (SSS). TEIs ISIS and Tritonmap software were used to process the raw SSS data (.XTF files). The best gain settings were established and applied across the geophysical dataset to enable outputs in the form of geotiff images.

Full details on the collection and processing of acoustic data can be found in Cefas and JNCC (2013).

3.2 Groundtruth sampling station selection

Sampling of the seabed, using underwater cameras and sediment sampling devices, was conducted to acquire data from in and around each of the SCI areas. These data serve to groundtruth the results from analysis of the acoustic data, as well as to enable the characterisation of habitats and benthic communities within the pockmark features and the surrounding areas.

3.3 Sampling methods

3.3.1 Video and still images

The underwater drop-camera system comprised a video camera with capability to also capture still images. Illumination was provided by two high intensity LED striplights and a flash unit. The system was fitted with a four-spot laser scaling device (lasers separated by 17cm) to provide a reference scale in the video image. Setup and operation followed the MESH 'Recommended Operating Guidelines (ROG) for underwater video and photographic imaging techniques' (Coggan *et al* 2007). Video was recorded simultaneously to a Sony GV-HD700 DV tape recorded and a computer hard drive. A video overlay was used to provide station metadata, time and GPS position of the vessel in the recorded video image.
Video and still sampling site selection was targeted to the pockmark features themselves (Figure 3 and Figure 4). Camera deployments lasted a minimum of 10 minutes, with the vessel executing a controlled drift using Dynamic Positioning at c.0.5knots (c.0.25ms $^{-1}$) across a 100m 'bullring' centred on the sampling station position. Still photographic images were captured at one minute intervals and opportunistically if features or species of interest were observed. The height of the camera off the seabed was controlled by a winch operator with sight of the video monitor.

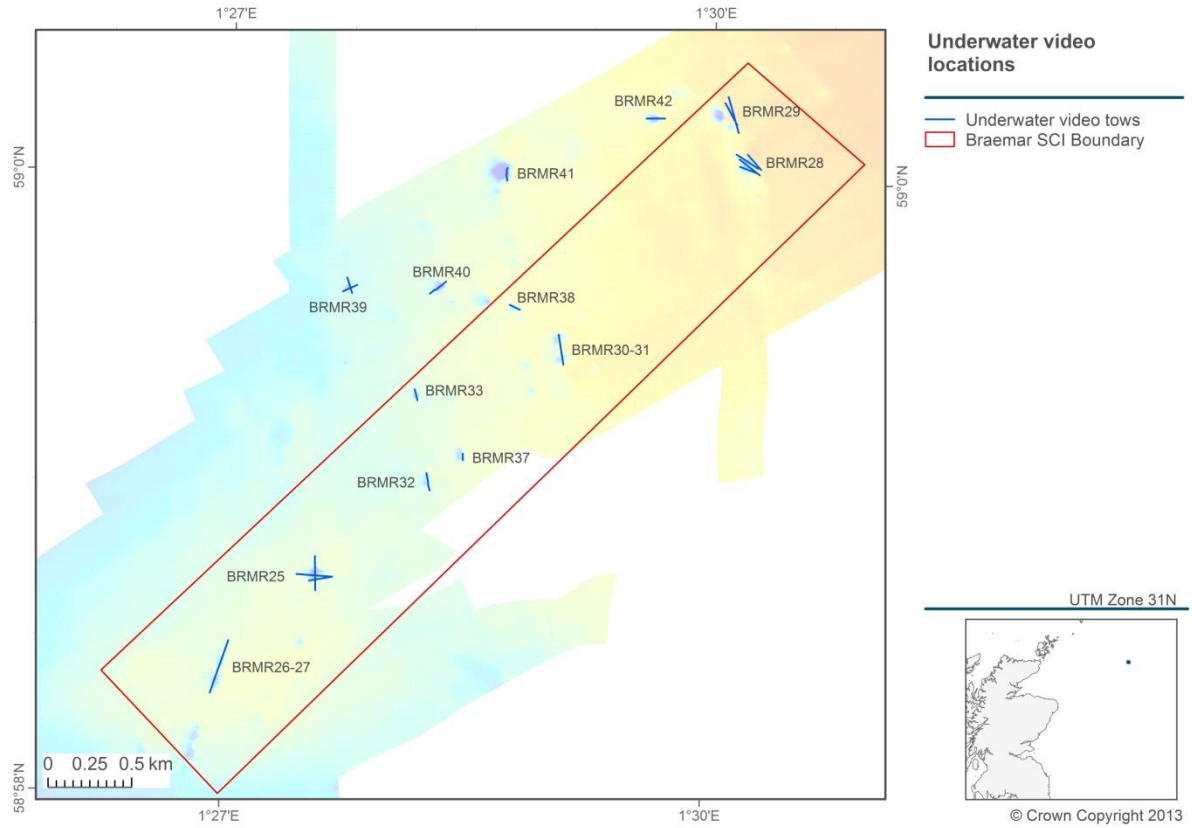

Figure 3. Location of underwater video tows at the Braemar Pockmarks SCI, with background bathymetry from Figure 8.

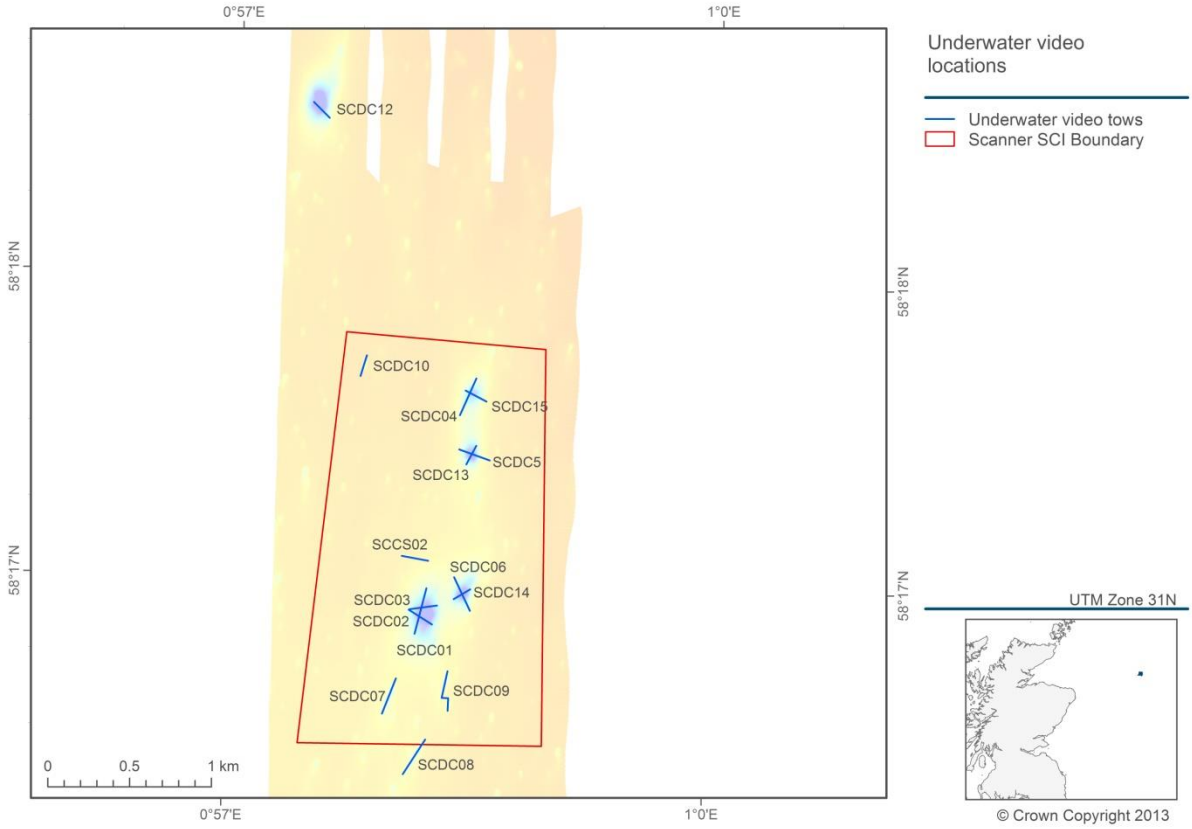

Figure 4. Location of underwater video tows at the Scanner Pockmark SCI, with background bathymetry from Figure 28.

3.3.2 Grab sampling for fauna and particle size analysis (PSA)

Grab sampling station selection at each SCI was based on a triangular lattice pattern, with stations placed approximately 1km apart, to allow for even spatial coverage of each site. Additional sampling stations were placed specifically on features of interest, such as pockmarks, falling outside of the grid pattern (Figure 5 and Figure 6).

Replicate grab samples (three samples separated by a distance of approximately 5m) were collected at a sub-set of stations to explore the effects of survey design and sampling density on the species accumulation curve within the site.

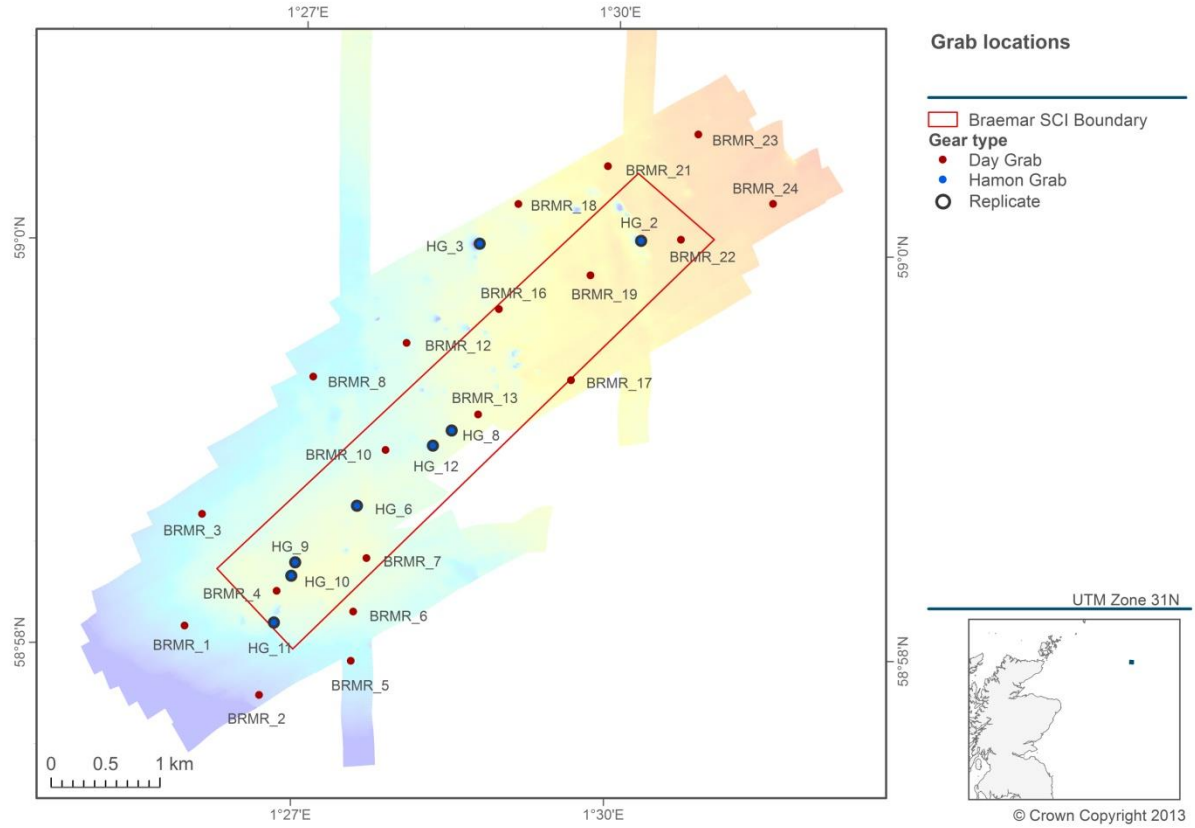

Figure 5. Locations of grab sampling stations at the Braemar Pockmarks SCI, with background bathymetry from Figure 8.

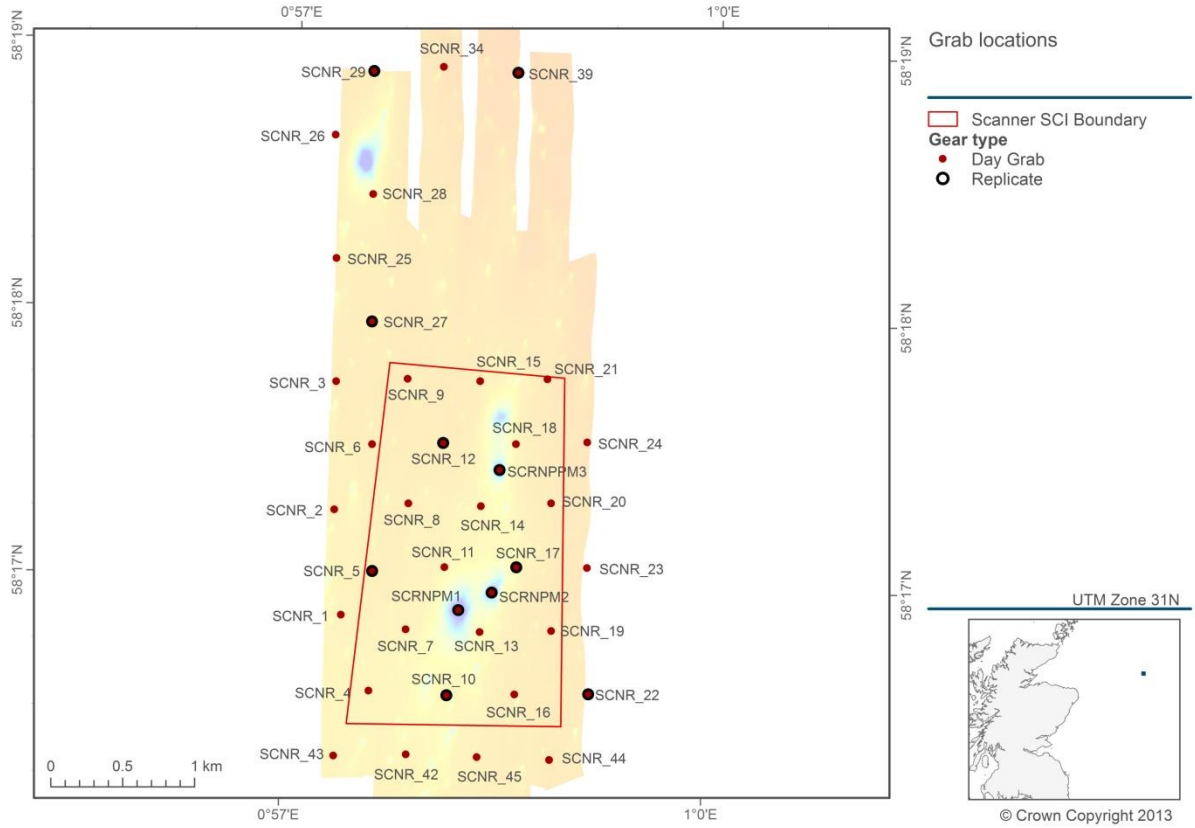

Figure 6. Location of grab sampling stations at the Scanner Pockmark SCI, with background bathymetry from Figure 28.

Preliminary observations indicated that sediments across both SCIs were characterised mostly by soft mud, therefore, a Day grab was chosen for the acquisition of sediment samples and macro/meiofaunal collection. On recovery of the Day grab, a photograph was taken of the intact sediment surface, and the depth of the sediment within the deepest area of the grab was recorded. The sample was sub-sampled, using a full depth corer (diameter 30mm), for particle size analysis (PSA). The same corer was used to collect a second sub-sample (to a depth of 5cm) for the extraction of meiofauna. Sub-sampling for meiofauna was carried out to determine the presence of the chemosynthetic gutless nematode *Astomonema southwardorum*. Macrofauna were separated from the remaining sample by washing it with seawater over a 1mm mesh sieve. The retained material was transferred to a labelled container and preserved in 4% buffered formaldehyde for later taxonomic processing.

Sampling was also undertaken at specific stations where MDAC was anticipated from the acoustic data. This was intended to confirm the presence of carbonate structures (following detailed laboratory analysis), particularly in case they were present just beneath the sediment surface, where they may not be visible using conventional seabed imagery techniques. The predicted coarser sediment from these areas was sampled using a sampling gear consisting of a 0.1m^2 mini Hamon grab fitted with a video camera, the combined gear being known as a HamCam. The camera relayed an image of the undisturbed seabed surface prior to each grab sample being obtained. On recovery, the grab contents were emptied into a large plastic bin, photographed, the volume recorded, and a representative sub-sample of sediment (c.500ml) taken for particle size analysis (PSA). Fragments of possible MDAC collected in the grab samples were placed into a separate storage container for further analysis of their composition. No meiofaunal sub-sample was taken from Hamon grab samples because this sampler does not yield an undisturbed seabed surface necessary for meiofaunal sample acquisition. Further processing of Hamon grab samples for macrofauna followed the same procedure as for Day grab samples. Finally, grab samples collected from a subset of sites within the Scanner Pockmark SCI were also sub-sampled for organic contaminant analysis.

3.4 Seabed sample and data processing

3.4.1 Particle Size Analysis (PSA)

PSA was carried out by Cefas following standard laboratory practice and the results checked by specialist Cefas staff following the recommendations of the National Marine Biological Analytical Quality Control (NMBAQC) scheme (Mason 2011).

3.4.2 Macrofaunal samples from grabs

Macrofaunal samples were processed by APEM Ltd (Braemar) and Seastar Survey Ltd (Scanner) following standard laboratory practices, and the results were checked following the recommendations of the National Marine Biological Analytical Quality Control (NMBAQC) scheme (Worsfold *et al* 2010).

3.4.3 Meiofaunal samples from grabs

Meiofaunal samples were processed by Physalia Consultant and Forensic Ecologists specifically for the extraction and identification of the Nematoda. Processing and extraction techniques followed standard laboratory protocols. Total sample volume was recorded and the sample homogenised in c.800ml of fresh water. A modified, multiple Boisseau apparatus was used to elutriate the meiofaunal organisms, thus separating most of them from the bulk of the inorganic matrix. The meiofaunal fractions were retained on 38µm mesh sieves

immersed in flowing tap water. Pooled meiofaunal/silt fractions for each sample were further concentrated by a polymer density separation technique and centrifugation, with the meiofauna re-collected onto 38µm mesh sieves. For a full description of the meiofaunal sample processing protocol, see the dedicated meiofaunal sample analysis report (Physalia 2013).

3.4.4 MDAC samples from grabs

Suspected MDAC fragments obtained from sediment grab samples were sent for petrographic and stable isotope analysis to the British Geological Survey (BGS). A detailed description of the methodologies undertaken by the BGS is presented in Milodowski and Sloane (2013) (see Appendix 7).

3.4.5 Video and still image analysis

Video and photographic stills were processed by Envision Mapping Ltd in accordance with the guidance documents developed by Cefas and JNCC for the acquisition and processing of video and stills data (Coggan & Howell 2005; JNCC, in prep.).

3.5 Data analysis methodologies

3.5.1 Acoustic data interpretation

Multibeam bathymetry and backscatter data were used in combination to enable a semi-automated interpretation of the Braemar Pockmarks and Scanner Pockmark SCIs. Habitat maps were produced using object-based image analysis (OBIA; Blaschke 2010), implemented in the software package eCognition® v8.7.2. OBIA is a two-step approach consisting of the segmentation and classification of an image, in this case the MBES bathymetry and backscatter floating point geotiff images. A similar approach in eCognition® was adopted for both the Braemar and Scanner SCIs. The process is summarised in Figure 7.

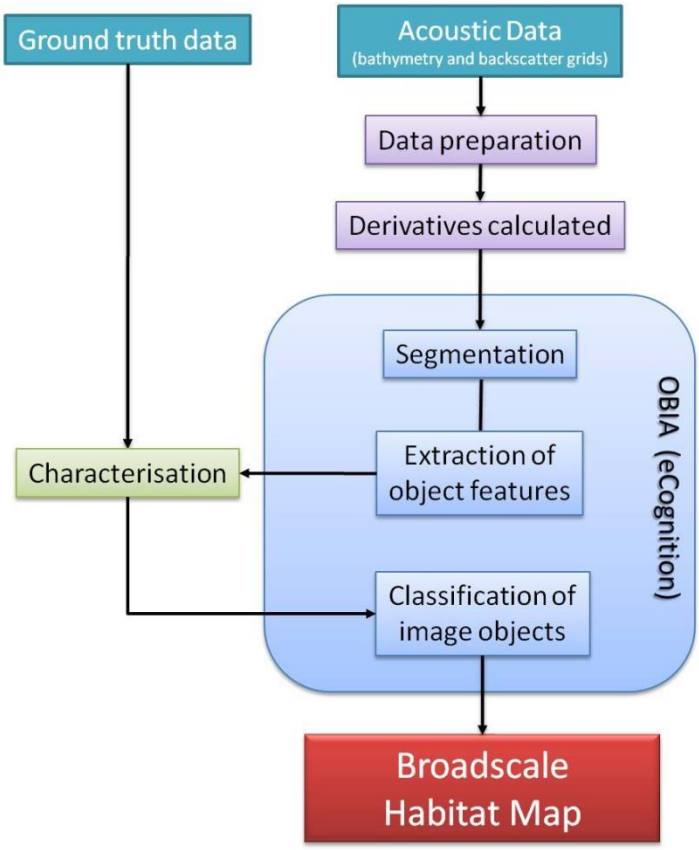

Figure 7. Flowchart outlining the process of producing a broadscale habitat map.

The acoustic data were assessed and derivatives were produced. The most applicable derivative for both SCIs was Bathymetric Position Index (BPI), and this was used for all subsequent analyses and interpretation. The next step in OBIA is segmentation, resulting in the creation of meaningful objects in the map image. The input layers used in the segmentation were primary acoustic data layers (bathymetry and backscatter). Segmentation was carried out using the multi-resolution segmentation algorithm in eCognition® with the scale parameter set at 10. This is an optimisation procedure enabling individual pixels to be merged with neighbouring pixels based on a set threshold.
The classification of the image objects was based on the roughness of the seabed (i.e. objects with a positive BPI). Both grab sample data (PSA) and seabed imagery were used to aid class assignments. Using object asymmetry and main object direction, it was possible to exclude areas of poor quality data and trawl tracks. Further manual editing was carried out in ArcGIS 9.3 to account for the misclassification of certain objects. The broadscale habitat map produced was based on the classification of sediment type derived from the PSA and video and still image data.

3.5.2 Faunal data analysis

Standard univariate and multivariate analyses have been performed on the taxon abundance-by-sample matrix produced by the grab sample processors. Prior to analyses, the data matrices were checked for inconsistencies and spurious identifications. Metrics calculated for each sample included total macrofaunal abundance (N), total wet weight biomass (B), total number of taxa (S) and Hill's (1973) taxon diversity index (N1). Multivariate analyses were performed using the PRIMER 6 software package (Clarke and Gorley, 2006). These analyses included calculations of faunal similarity (using the Bray-Curtis similarity coefficient applied to square root transformed data). Sample clustering techniques (SIMPROF) were also employed to identify significantly significant groups of

samples and SIMPER analyses were performed to identify which taxa contributed to the similarity between these statistically defined groups.

3.6 Data QA/QC

All activities in the field were performed according to the recommendations in the following documents:

- Biological Monitoring: General Guidelines for Quality Assurance document (ICES 2004)
- Quality Assurance in Marine Biological Monitoring (Addison 2010)
- MESH Recommended operating guidelines for underwater video and photographic imaging techniques[2].

4 Results and Discussion

4.1 Braemar Pockmarks SCI

4.1.1 Multibeam bathymetry and backscatter

Full bathymetry and backscatter data were acquired at Braemar Pockmarks SCI with the exception of an area midway along the south-eastern boundary, where the obstruction of a well head prevented data collection in a small area (Figure 8).

The seabed at the Braemar Pockmarks SCI presents a series of crater-like depressions lying at an average depth of approximately 125m (CD). The crater-like depressions – or pockmarks – vary in size, ranging from larger examples of around 50-100m in diameter to smaller pockmarks of between 5 and 10m in diameter.

[2] Reference URL: http://www.searchmesh.net/PDF/GMHM3_Video_ROG.pdf

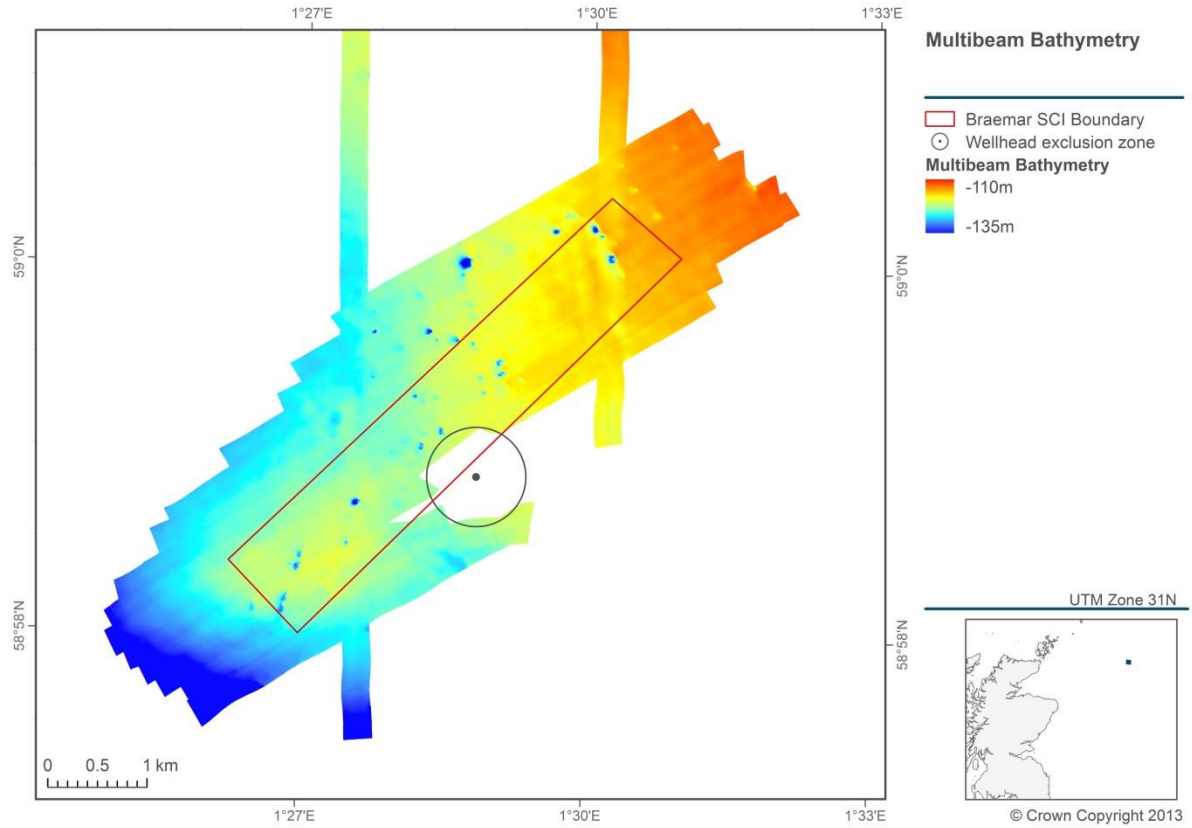

Figure 8. Display of multibeam bathymetry data collected at the Braemar Pockmarks SCI.

Aside from the pockmarks, the seabed within the SCI boundary itself is relatively flat, sloping gently from northeast to southwest. The acoustic coverage extends outside of the SCI boundary and shows the seabed to the southwest deepening to around 135m.

The size, density and distribution of pockmarks are not uniform and vary greatly across the site. One notably large pockmark can be seen on the multibeam bathymetry data to the north of the SCI boundary. No pockmarks were observed in the deeper water to the southwest of the SCI. This may suggest that pockmarks are more likely to occur in slightly shallower water depths at this site, although the lack of more extensive data coverage may equally explain this.

The multibeam backscatter data show a relatively homogeneous seabed with very little difference in backscatter strength across the site (Figure 9). No change in backscatter strength was observed between the shallower and deeper parts of the site, suggesting similar sediments occur throughout the wider area. Whereas the general area has a low backscatter return, the pockmarks themselves are associated with high backscatter intensity, indicative of a coarser or harder substrate in these areas. No other features of note are recognised on the multibeam bathymetry or backscatter data.

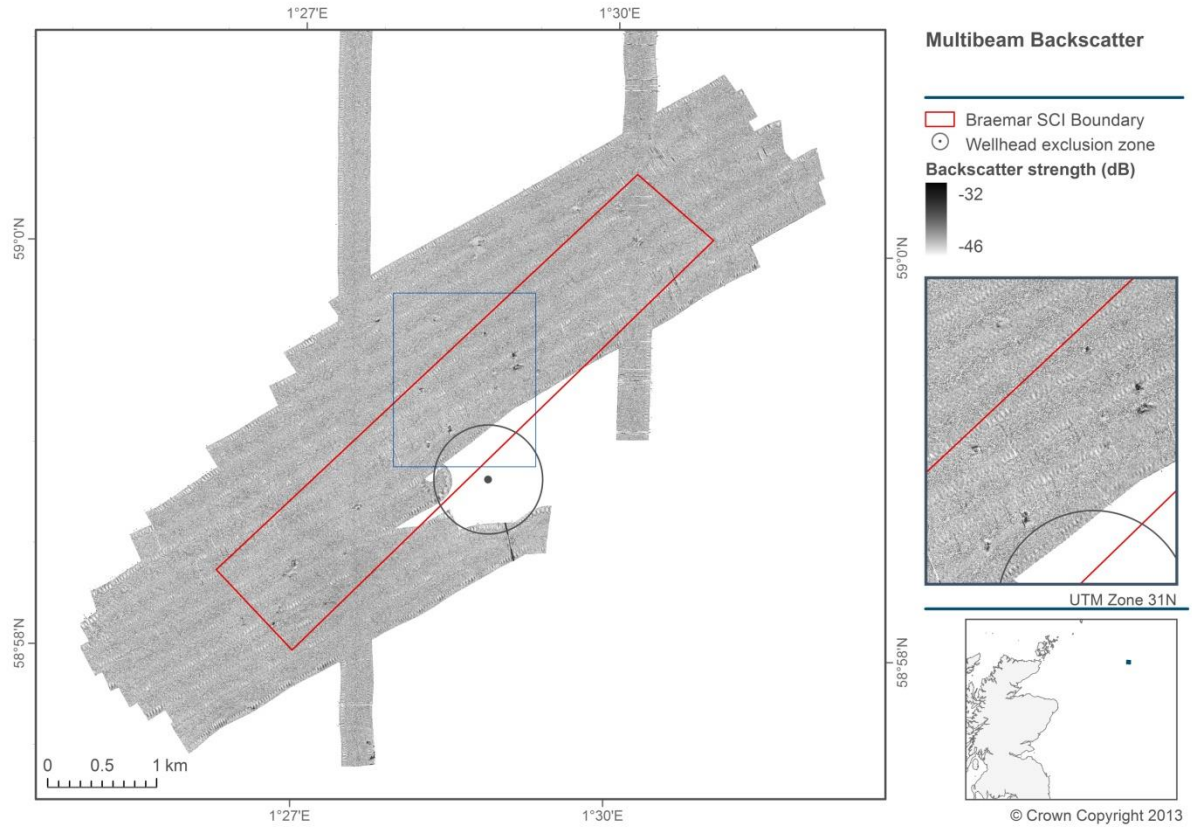

Figure 9. Display of multibeam backscatter data collected at the Braemar Pockmarks SCI with detail insert.

4.1.2 Sidescan sonar

Full sidescan sonar coverage was achieved at the Braemar Pockmarks SCI, however, there is a gap in data coverage due to the obstruction of a well head. Significant swell was experienced during survey operations, which also affected the quality of the acquired sidescan data. Figure 10 illustrates the low frequency sidescan sonar data within the SCI boundary. The low frequency data were chosen over the high frequency data due to increased swath width and better data quality. Pockmarks with a diameter of approximately 50m or more can be seen against the surrounding featureless seabed.

Bubbles were also identified on the sidescan sonar record, which may indicate an active pockmark within the Braemar Pockmarks SCI. See Section 4.1.9 and Annex 1 for further information.

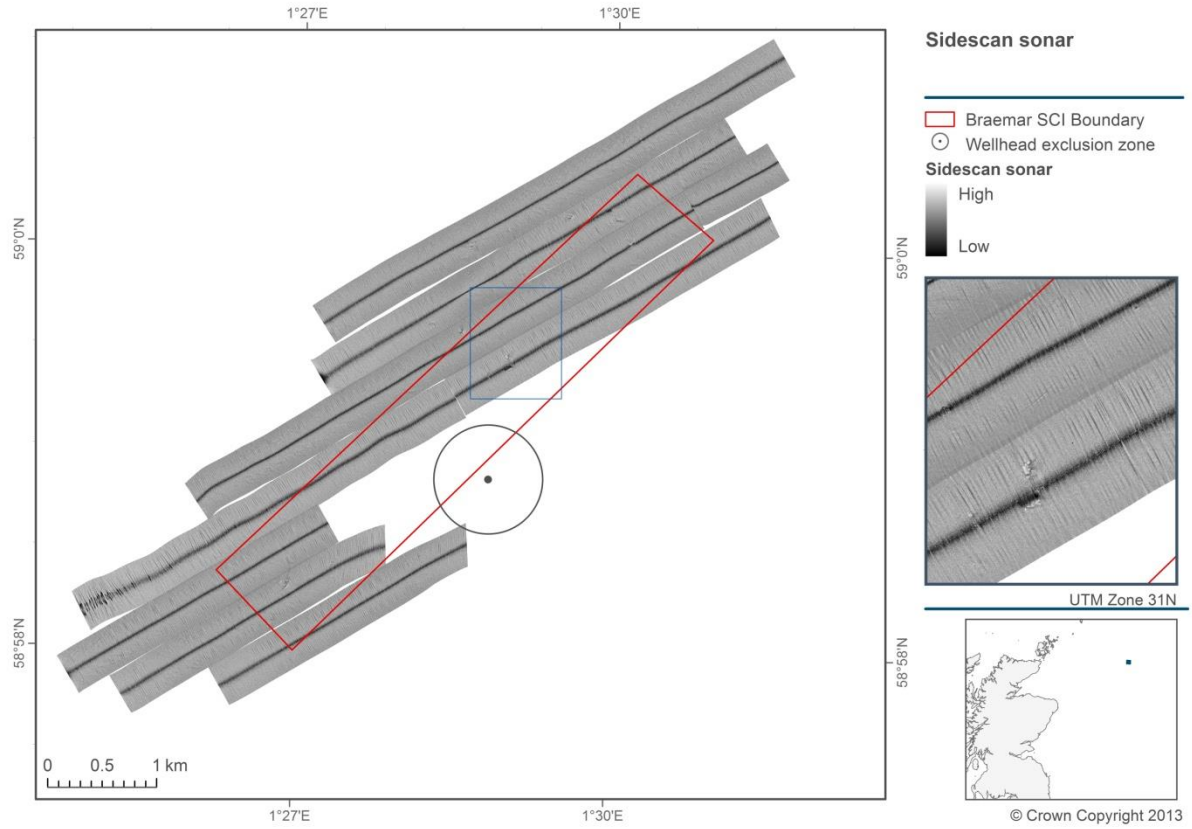

Figure 10. Display of low frequency sidescan sonar data collected at the Braemar Pockmarks SCI with detail insert.

4.1.3 Surficial sediments

Multibeam bathymetry and backscatter data, in combination with video and grab groundtruthing PSA samples, have been used to produce a sediment distribution map according to the EUNIS sediment classification system, which is based on the modified Folk trigon (Long 2006; see Annex 5). PSA results from the Braemar Pockmarks SCI indicate a predominance of sand and mud fractions within the samples, with only a handful of samples having a noticeable proportion of gravel (Figure 11). Using the same data to inform the EUNIS classification system, the sediment types most commonly found were mud and sandy mud (Figure 12). These results concur with the low backscatter strength that was observed from the multibeam echosounder data. Sampling stations showing an elevated proportion of gravel were classified as either mixed or coarse sediments in the EUNIS classification system.

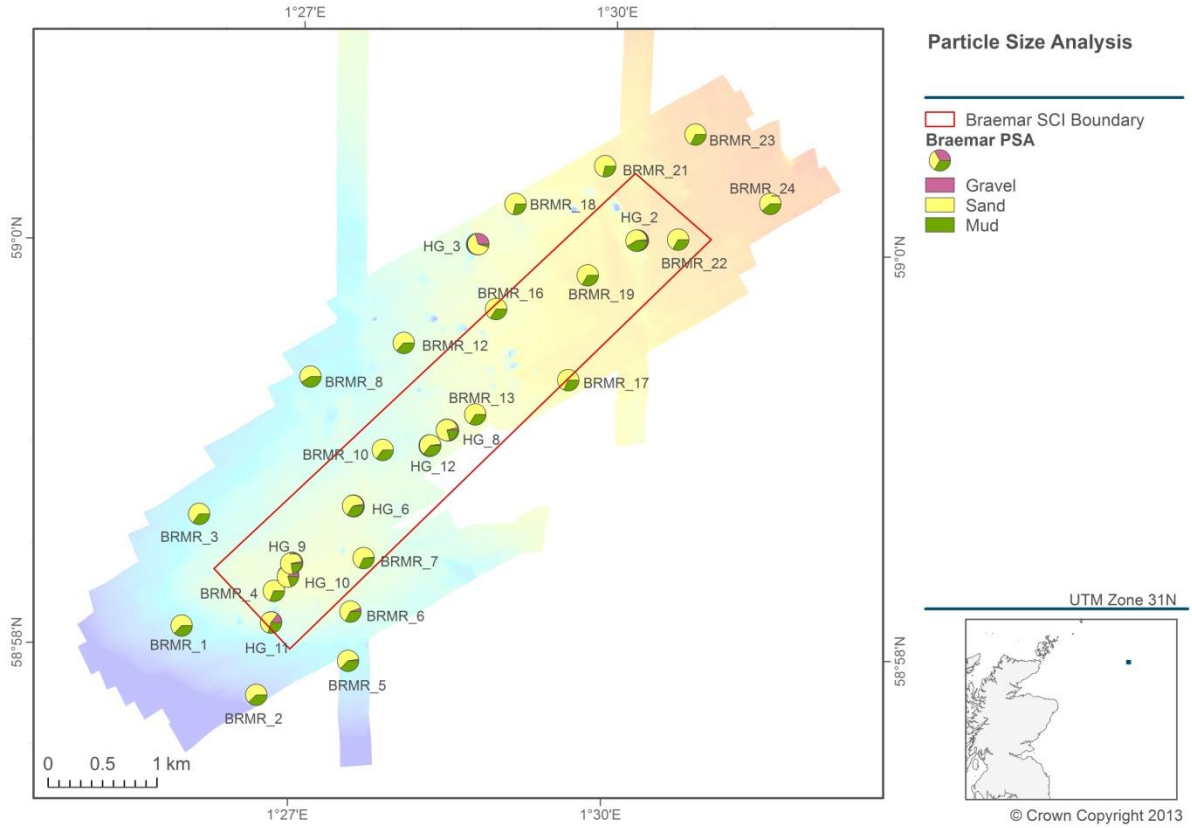

Figure 11. Results from PSA displayed as pie charts at the Braemar Pockmarks SCI, with background bathymetry from Figure 8.

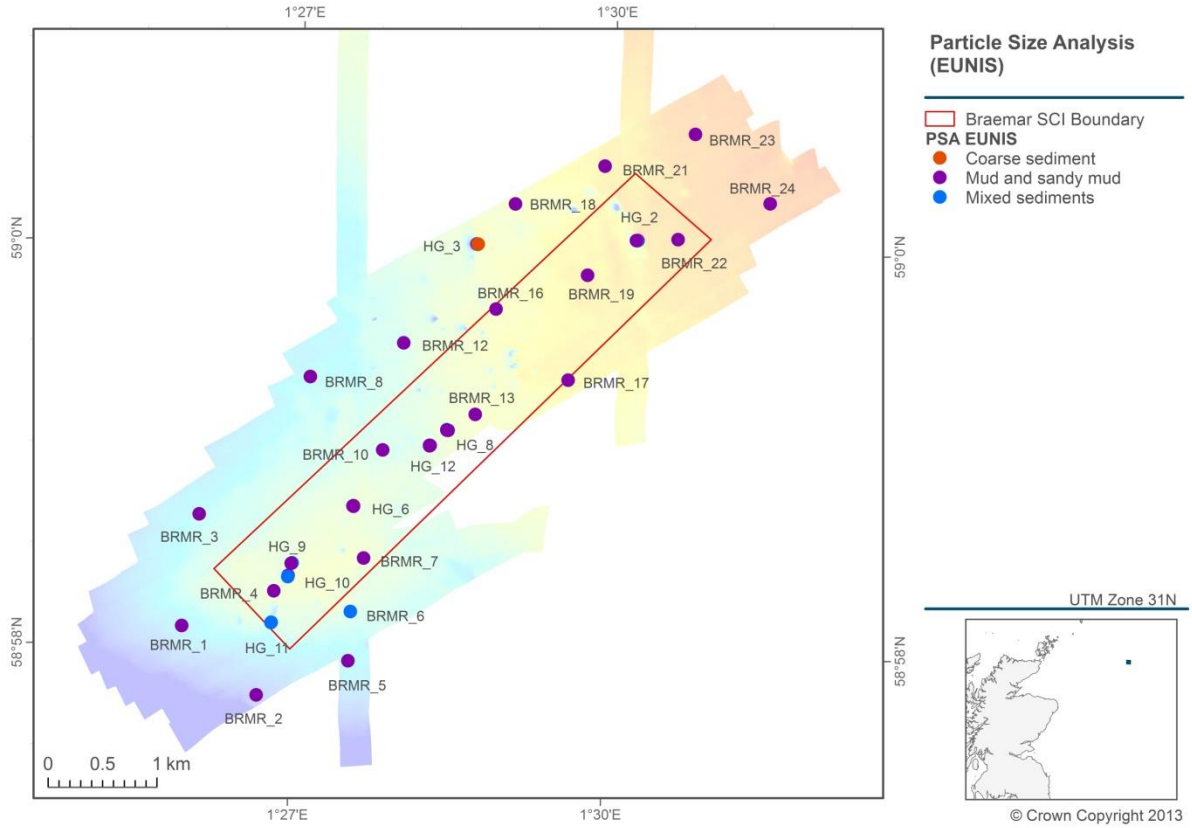

Figure 12. EUNIS sediment classification map of the Braemar Pockmarks SCI, with background bathymetry from Figure 8.

Combining all multibeam acoustic and sample data using the OBIA approach, only two classifications of sediment type within the SCI boundary were identified: (i) mud, and (ii) mixed coarse sediments (Figure 13).

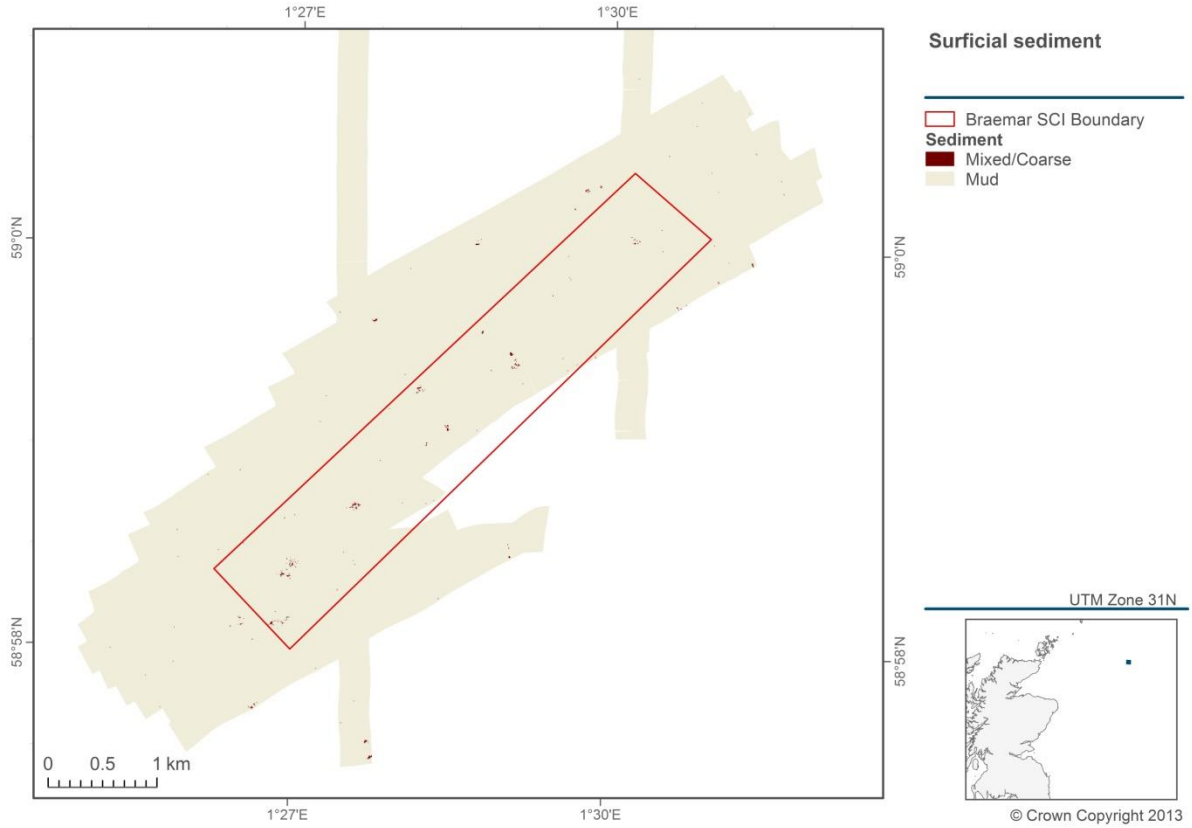

Figure 13. Sediment classification map of the Braemar Pockmarks SCI based on the combination of acoustic and groundtruthing data.

Previous modelling studies have suggested that the most readily pockmarked sediment is soft, silty mud (Judd 2001). Newly acquired data from the Braemar Pockmarks SCI supports this suggestion, as the predominant sediment type observed was mud. Using eCognition, the areas defined as mixed sediment were distinguishable from the surrounding muddy sediment due to the strong multibeam backscatter return associated with such a ground type. Mixed sediments were found predominantly at the bottom of some the pockmark depressions, but were not exclusive to those features. A single sample (HG_3) was found to contain coarse sediment and was situated outside of the site boundary to the north (Figure 12). The mixed sediment signature also includes shell beds, which were supported by observations made from the underwater video footage and still images. Patches of dense shell hash observed in the video footage and still images (see Image 1 in Figure 23) are thought to form as a result of sediment sorting induced by the sporadic emission of gas bubbles from below the sediment surface (Hartley 2005).

MDAC is significantly harder than other seabed sediments and, therefore, would also be represented by a strong acoustic return. However, patches of MDAC cannot be differentiated from coarse and mixed sediments using the acoustic data in isolation.Therefore, the location of areas comprising possible MDAC were informed using a combination of the acoustic, video footage and still image data and observation of fragments of possible MDAC present in the grab samples. These were also subject to further laboratory analysis.

4.1.4 Grab sample analysis

Macrofaunal abundance values per grab sample ranged between 22 and 422 individuals. The same samples which contained the extreme low and high abundance values also contained the lowest and highest values for number of taxa (14 and 72 taxa, respectively). Wet weight biomass ranged from 0.403g to 284.74g per sample. Taxon diversity was between 11.9 and 41.0 per sample. All calculated metrics per sample are presented in Appendix 1.

The distribution of selected calculated metrics across the Braemar Pockmarks SCI is displayed in Figure 14 and Figure 15. At sampling stations where replicate grabs were taken, an average across replicates has been calculated for each metric at each station.

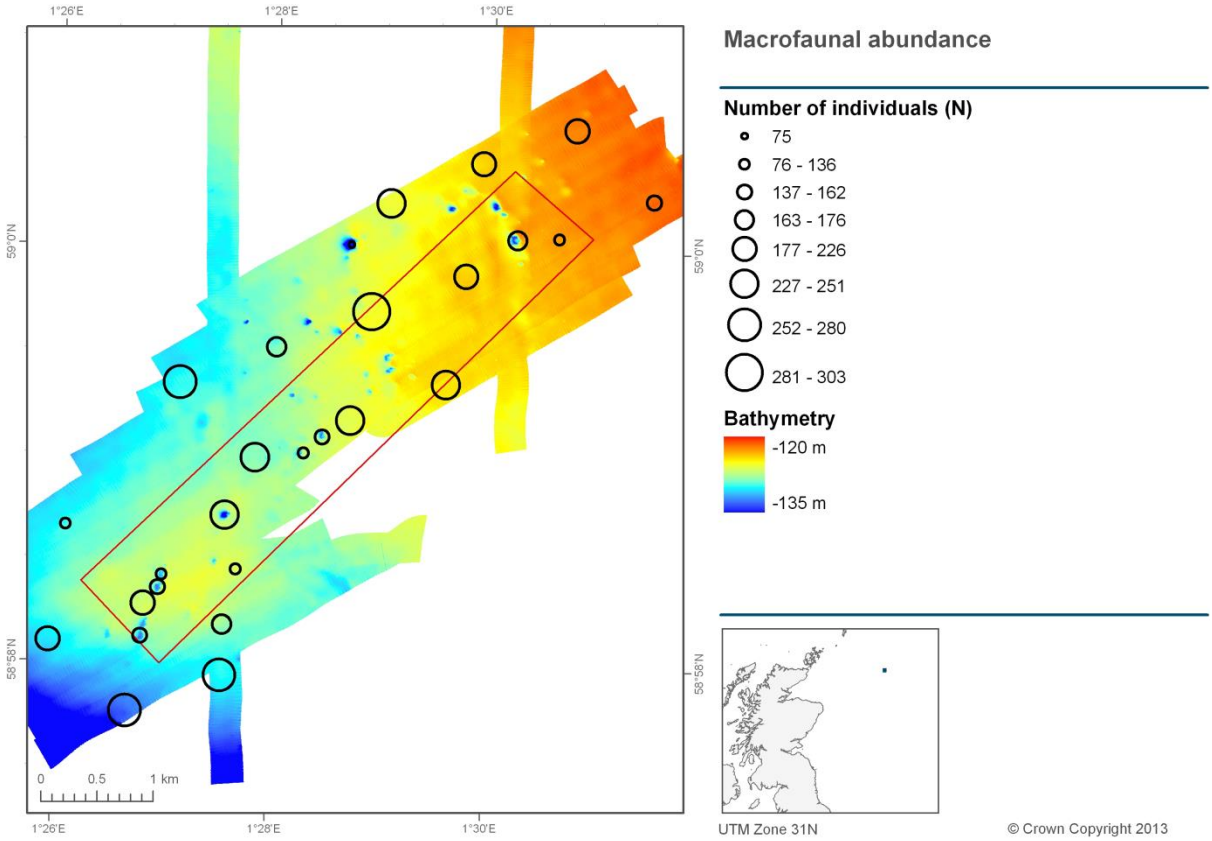

Figure 14. Spatial distribution of mean macrofaunal abundance values per station at the Braemar Pockmarks SCI.

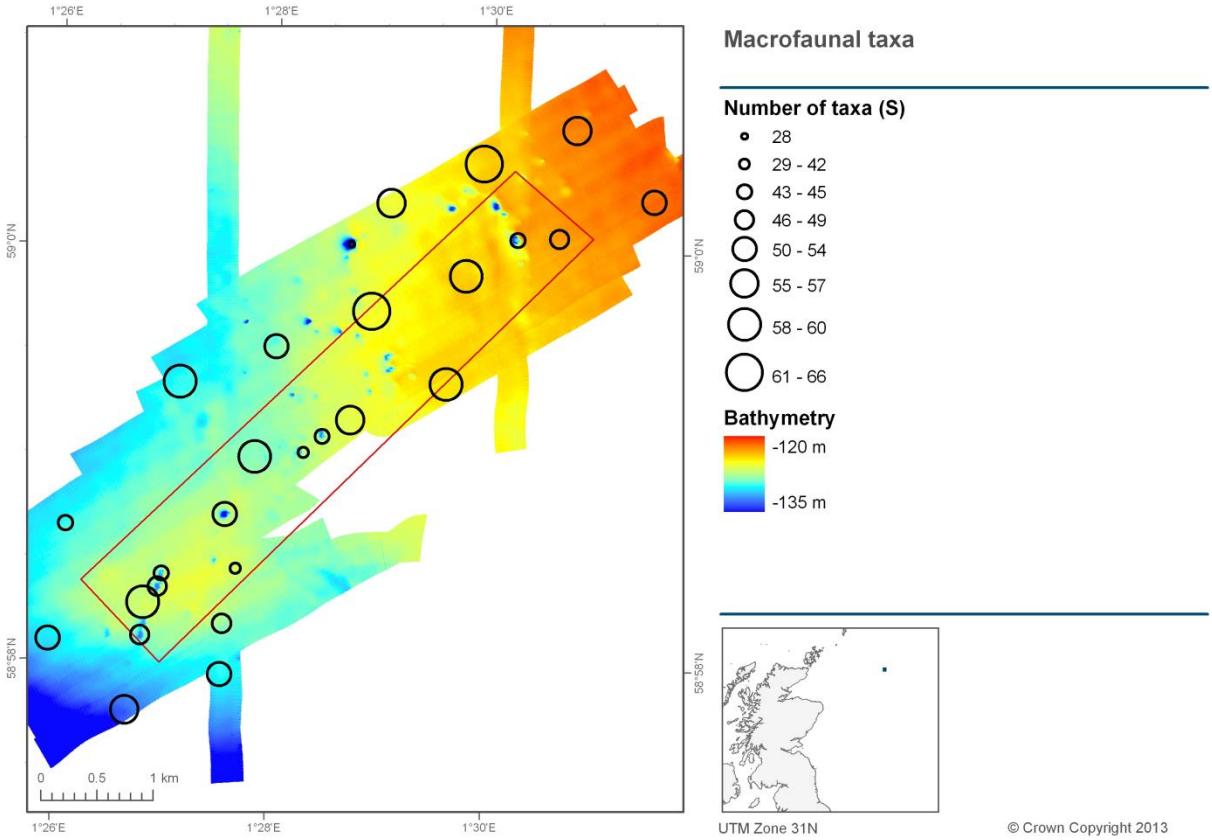

Figure 15. Spatial distribution of the mean number of macrofaunal taxa recorded per station at the Braemar Pockmarks SCI.

The number of macrofaunal taxa and of individuals was variable across the survey area, with pockmark features harbouring relatively low values for the various metrics calculated, and the surrounding sediments harbouring a range of low and high values for each calculated metric. The pattern in variation which is observed in the distribution of the number of taxa (Figure 15) is also reflected in the distribution of diversity, evenness and biomass values (data not shown). Samples targeting pockmarks (sampled with mini Hamon grab) harbour significantly ($p<0.05$) fewer taxa, fewer individuals, have lower diversity and lower biomass than samples from surrounding areas (sampled with Day grab). Because of the difference in sampling gear targeting pockmarks and the surrounding areas, any difference in macrofaunal assemblage metrics observed between pockmark features and their surroundings cannot be explained categorically by potential differences in habitat between the features sampled. Any difference observed may be caused by sampler bias.

Because sampling effort was different across sampling stations (i.e., some stations were sampled in triplicate whilst others only sampled once), only the first acquired replicate from each station was subjected to multivariate analysis. This step (in contrast to averaging data across replicates where they exist) avoids the detection of difference caused by increased sampling effort at sites sampled in triplicate.

Six statistically defined assemblages (*a* to *f*) were identified from the multivariate clustering analysis of macrofaunal samples (see dendrogram insert in Figure 16). One of these distinct assemblages (*a*), represented by a single sample, contained the least number of taxa (S = 20) and coincided with a pockmark feature. The most widespread assemblage (*e*) was observed across the whole sampling area and contained the most number of taxa (S = 158). Assemblage *b* occurred exclusively at stations representing pockmarks, although not all samples from pockmarks were included in that assemblage (Figure 16). The number of taxa represented in assemblage *b* was relatively high (S = 117). All other assemblages were

represented by just two or three stations and contained relatively few taxa (S: 62-84). Taxa characterising each of the assemblages identified are listed in Appendix 2.

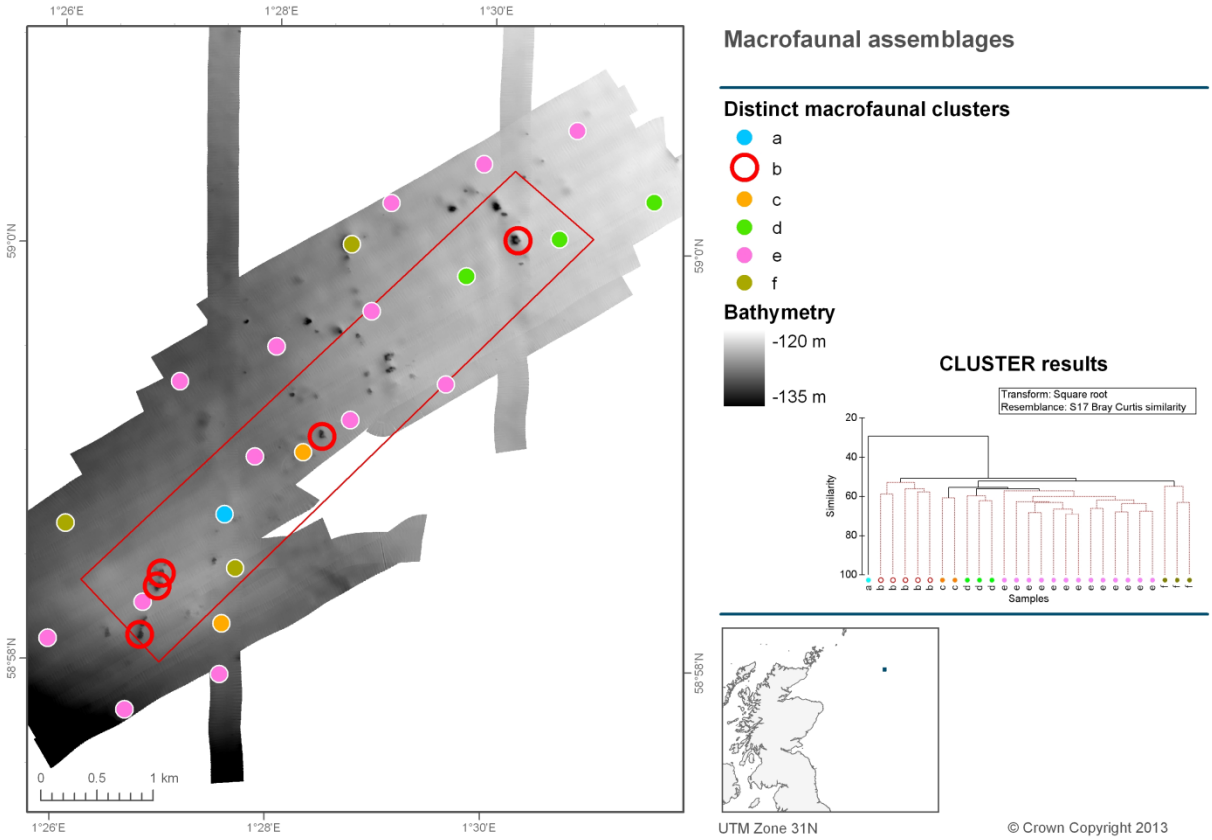

Figure 16. Spatial distribution of the distinct macrofaunal assemblages identified at the Braemar Pockmarks SCI.

An ANOSIM test to look for differences in macrofaunal assemblage composition between samples targeting pockmarks and those sampling the surrounding area revealed a significant difference in assemblage composition between the two (R value = 0.574, 0.1% significance), however, this difference may be caused by the different sampling gears used to target each of the two targeted habitats. A further ANOSIM test comparing the assemblage composition between samples in which MDAC was observed and in which it was not, revealed a significant difference in assemblage composition between the two test treatments (R value = 0.521, 0.1% significance), though again, differences in sampling gear confound this result.

The relative proportion of particle size classes within each sample can also be subjected to multivariate analyses; results from which are presented here. Since the number and identity of particle size classes is fixed (unlike the number and identity of taxa that may be captured in a grab sample), an average value for each size class can be calculated across replicate samples without consideration for differences in sampling effort at different sampling stations. Data from the same particle size class from each station sampled in triplicate have therefore been averaged across replicates.

Cluster analysis of the different proportions of particle size classes across stations revealed several statistically distinct clusters of stations; these are displayed spatially in Figure 17. The most striking pattern in the distribution of the identified clusters is the differentiation between stations representing pockmark features (cluster *m*) and all other stations. Cluster *m* samples were characterised by having a greater proportion of coarser particles (sands and gravels) and conversely, a lower proportion of fine particles (silts). All other clusters were characterised cumulatively by a higher proportion of fine particles and lower proportion

of coarse particles, with variability in the relative proportions of each particle size class responsible for differentiating the distinct clusters. Almost 80% of the variability in the particle size dataset was explained by the two axes in the PCA plot (see insert, Figure 17).

It should be noted that whilst the difference observed in sediment composition between samples from pockmarks and surrounding sediments is revealing, caution must still be applied in the interpretation of such a finding. Stations falling within pockmark features (showing coarser sediments) were sampled using a mini Hamon grab capable of reliably sampling coarse sediments, whereas all other stations were sampled with a Day grab, unsuitable for sampling coarser sediments effectively. It is impossible at present to eliminate the notion that the observed sedimentary differences between pockmarks and their surroundings could be a result of sampler bias.

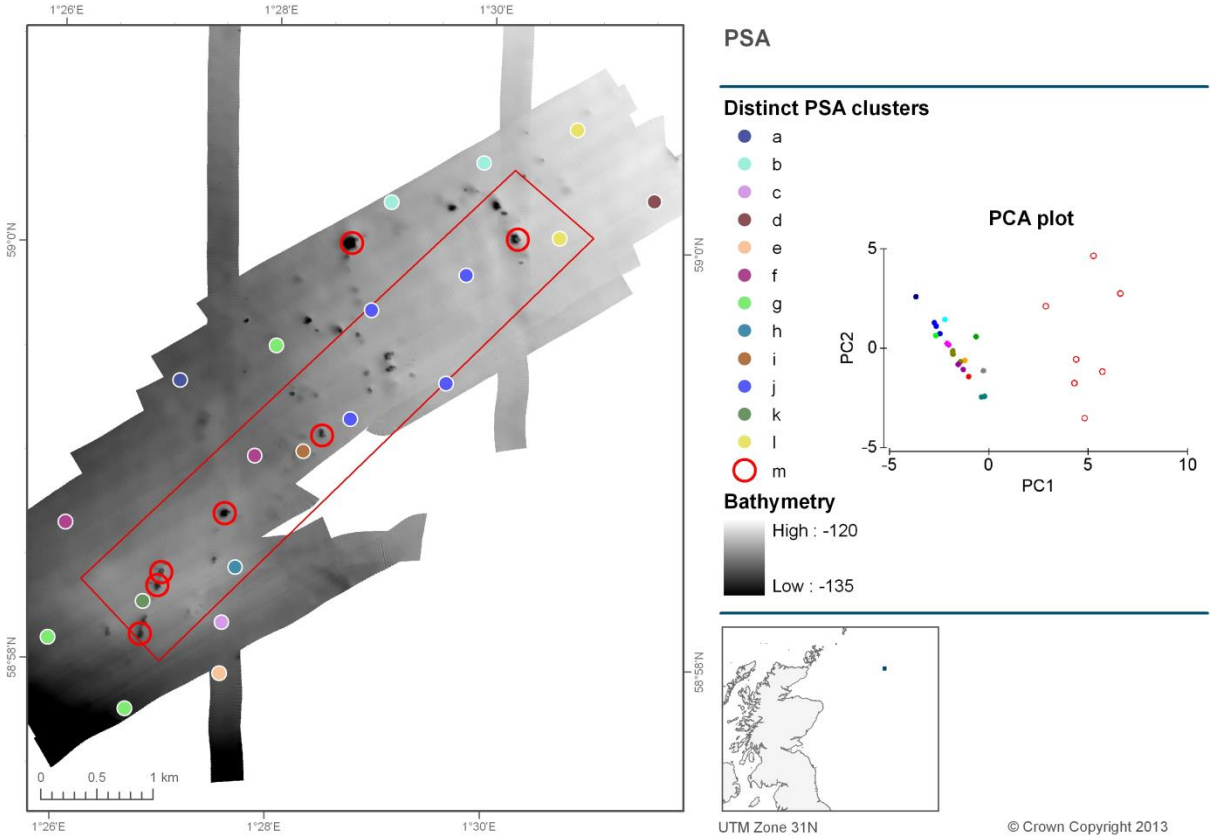

Figure 17. Distribution of distinct clusters of sampling stations based on multivariate PSA. Insert Principle Component Analysis (PCA) plot of stations.

The extent to which the pattern in sediment variables across the survey area explains patterns observed in the biological data was explored using the BIO-ENV routine. The single most influential sediment variable responsible for the pattern observed in the macrofaunal dataset was % Coarse Sand (rho value: 0.648). However, there were at least 10 different combinations of variables which showed a stronger in-combination correlation (i.e. higher rho value) with observed patterns in the macrofaunal dataset. Most of the variable combinations included the coarser components of the samples, suggesting that these components cumulatively have the most influence over the distribution of macrofaunal assemblages in the survey area.

4.1.5 Video and still sample analysis

A total of 17 video clips and 370 stills were analysed. Many of the images analysed had poor or moderate visibility due to the sediment being disturbed and/or the camera occasionally drifting too far from the seafloor for a clear image. Three stations were comprised of different

'segments' as there were significant changes in substrate throughout the video tow. The 14 remaining stations comprised of one 'segment' as there were no significant changes in substrate throughout each of the video tows.

Subtidal Mud and Subtidal Mixed Sediment were the broadscale habitats represented in and around the Braemar Pockmarks SCI. Two different biotopes were identified from the video clips, Circalittoral Fine Mud (SS.SMu.CFiMu) at all 17 sites, and Circalittoral Mixed Sediment (SS.SMx.CMx) recorded at two sections within two sites (BRMR_32 & BRMR_40) and at two sections within a third site (BRMR_41A). An additional biotope was recorded during the analysis of stills that was not assigned during the video analysis. This was Seapens and Burrowing Megafauna in Circalittoral Fine Mud (SS.SMu.CFiMu.SpnMeg), and was characterised by the seapen species *Virgularia mirabilis* and *Pennatula phosphorea* (both recorded as Common on the SACFOR scale in the stills where they occurred). Taxa observed within each of the biotopes recorded on the video footage are listed in Table 1. Numerous and often substantial burrows were also observed consistently throughout all the video tows. White patches on the sediment surface, presumed to be chemosynthetic bacterial mats, were observed in some video and still images (see see Image 1 in Figure 23). All epifaunal taxa recorded from the analysis of both video and still samples are listed in Appendix 4.

Table 1. Taxa/features recording each of the biotopes identified from the collected video footage.

Taxon/feature	A5.3 - Subtidal Mud	A5.4 - Subtidal Mixed Sediment
Anthozoa	x	x
Asterias rubens	x	x
Cnidaria	x	x
Hydrozoa	x	x
Mysida	x	x
Myxinidae	x	x
Pagurus	x	x
Sabella	x	x
Trisopterus luscus	x	x
Asteroidea	x	
Buccinidae	x	
Caridea	x	
Crustacea	x	
Echinus acutus	x	
Gadidae	x	
Glyptocephalus cynoglossus	x	
Hippasteria phrygiana	x	
Lophius piscatorius		x
Nephrops norvegicus	x	
Ophiuroidea	x	
Pectinidae	x	
Pennatula phosphorea	x	
Pleuronectiformes	x	
Pollachius	x	
Urticina	x	
Virgularia mirabilis	x	
Bacterial mat	x	
Burrows	x	

4.1.6 Meiofaunal analysis

A total of 137 discrete (discernible) nematode taxa were recorded during the meiofaunal analyses, 108 of which were represented at the Braemar Pokcmarks SCI. The mean value for the Simpson's diversity index in samples from Braemar was 42.25 (Physalia 2013). There were a high proportion of nematode taxa that did not conform to published descriptions of species recorded from British marine waters.

No specimens of *Astomonema southwardarum* – a characteristic species of methane seep habitats (Austen *et al* 1993) – were documented in the Braemar Pockmarks samples. One symbiotic relationship was documented in the sample BRMR_45A; a *Leptonemella* species (most probably *L. aphanothecae*) was characterised by ectosymbiotic bacteria that adhered to and colonised the cuticle of the adults.

4.1.7 Biotopes

A further assessment of the acoustic data with the associated benthic habitats within the underwater video tows was undertaken to enable the allocation of EUNIS Level 4 biotopes.

The two classifications used to distinguish the surficial sediment map in Section 4.1.3 (Figure 13) have been integrated to allow the EUNIS classifications shown in Figure 18. Two different biotopes were identified in the biotope map, namely A5.36 Circalittoral Fine Mud and A5.44 Circalittoral Mixed Sediment.

The Braemar Pockmarks SCI is characterised by a sedimentary habitat of subtidal mud interspersed with mixed sediment. The mixed sediment is commonly associated with pockmarks and includes the shell hash observed in the video tows and, in some cases, possible MDAC fragments (as observed in Hamon grab samples; see insert image in Figure 18).

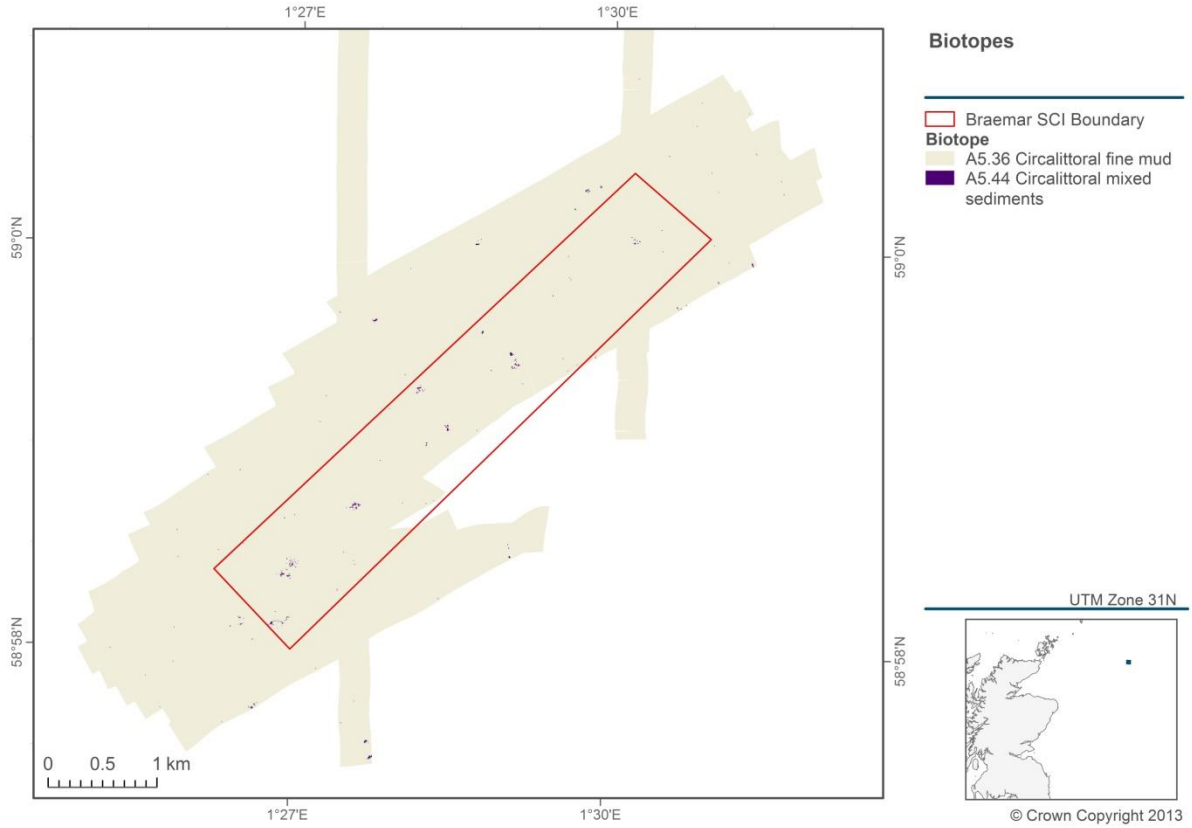

Figure 18. Biotope map based on acoustic and groundtruthing data from the Braemar Pockmarks SCI. Photograph of fragments, including possible MDAC, on 5mm mesh collected at BRMR_30A.

Figure 19 shows an example of the multibeam backscatter data and the location of underwater video stills overlaid with the corresponding biotope as identified during video analysis. The subtidal mixed sediment results in the high backscatter signature observed from the multibeam data.

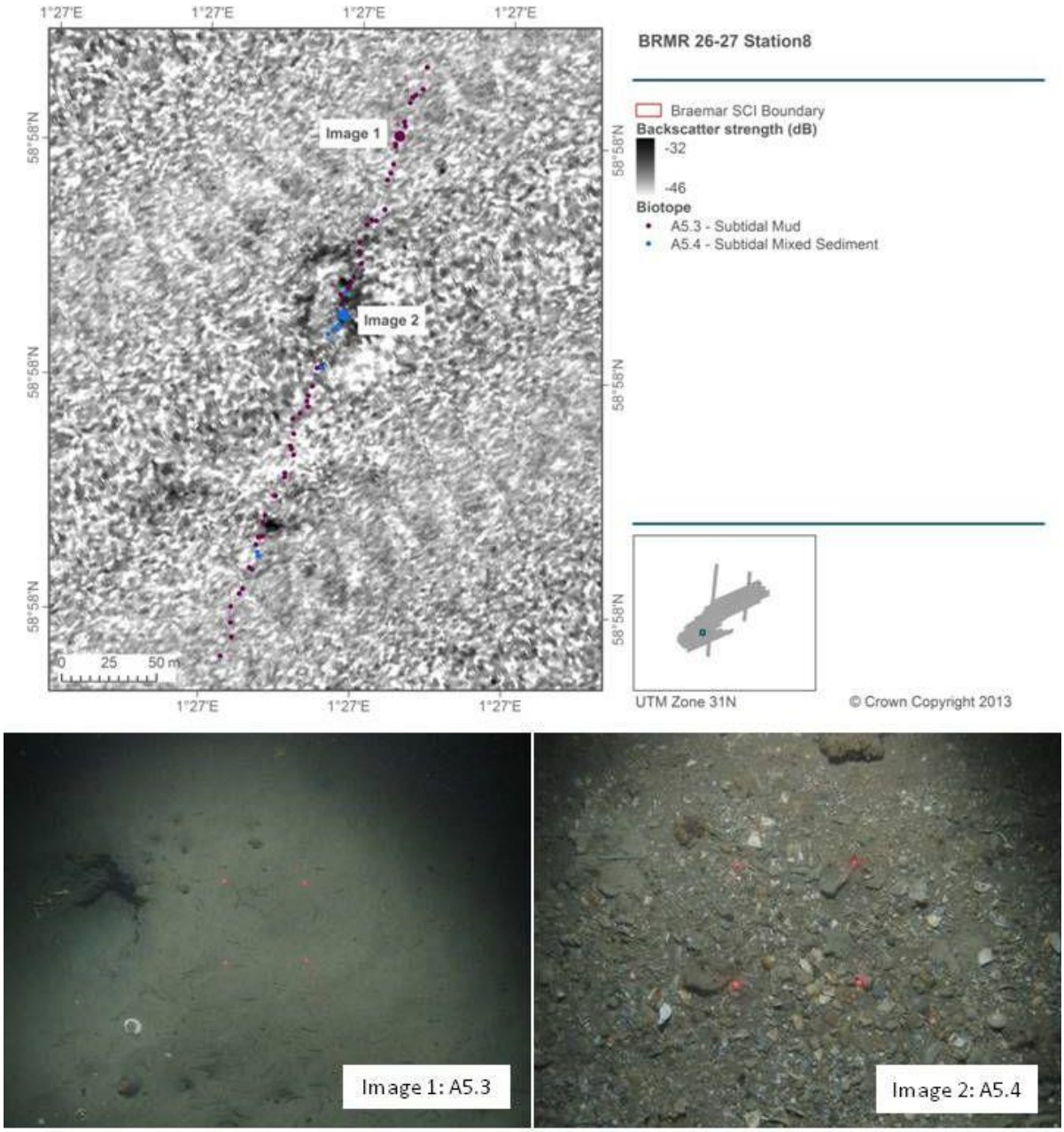

Figure 19. Display of multibeam backscatter data overlaid with underwater video information on the biotope attributed to each still. The four red spot laser scaling device spacing is 17cm.

4.1.8 Pockmark features

The feature of interest targeted for investigation at the Braemar Pockmarks SCI is a series of crater-like depressions which can contain the Annex I habitat 'Submarine structures made by leaking gases'. By combining the acoustic datasets and their derivatives it was possible to identify the presence and extent of pockmarks within the Braemar Pockmarks SCI. To enable the capture of both the smaller and larger pockmarks, a range of bathymetric position index (BPI) 20 and BPI 40 outputs were used to identify likely pockmark signatures on the seabed (Figure 20).

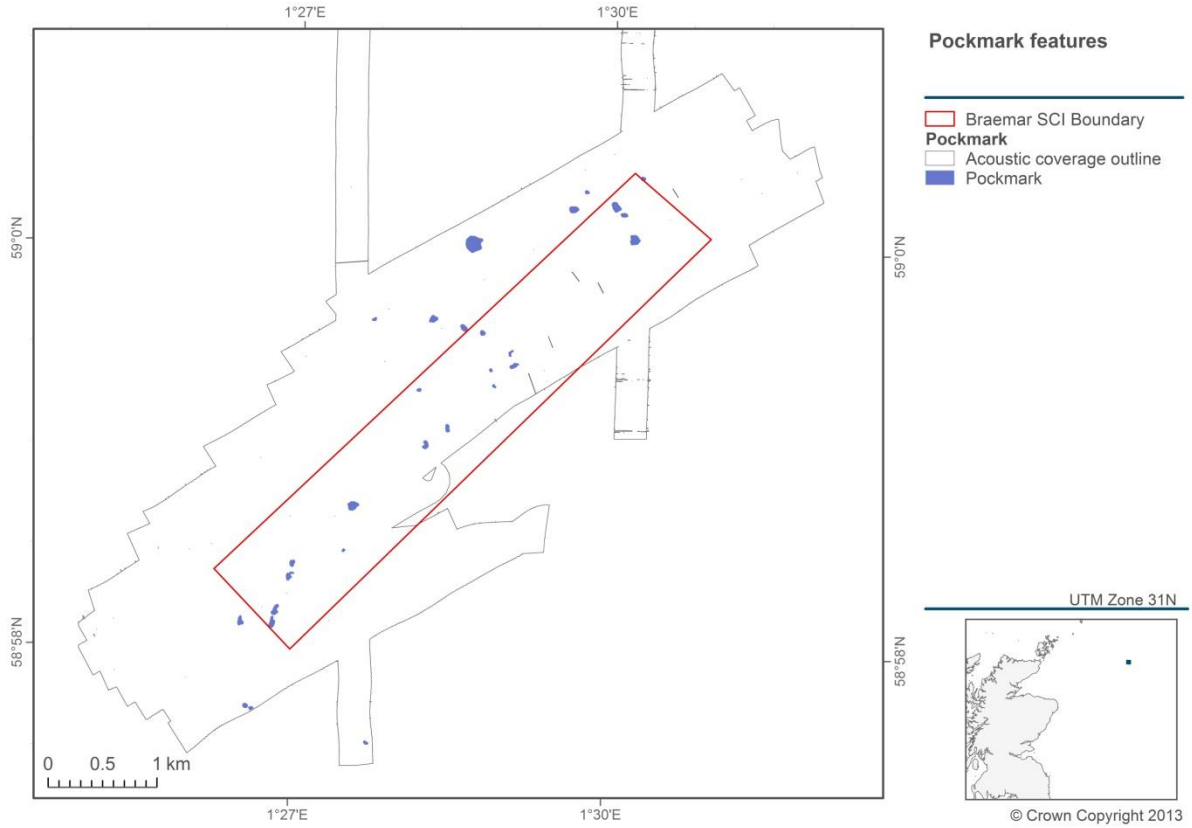

Figure 20. Pockmark locations across the Braemar Pockmarks SCI.

Figure 21 shows a map with the location of four pockmarks identified. The Fledermaus v7 software was used to create profile sections of the pockmarks alongside the bathymetry image. The pockmarks vary in depth from 2 to 5m from the surrounding seabed. The average diameter of the pockmarks in Images 2, 3 and 4 is 100m; the pockmarks in Image 1 are smaller in comparison (40m diameter) and only 2m deep. The four pockmark locations were chosen because of the presence of possible MDAC in the video and grab data (Figure 22).

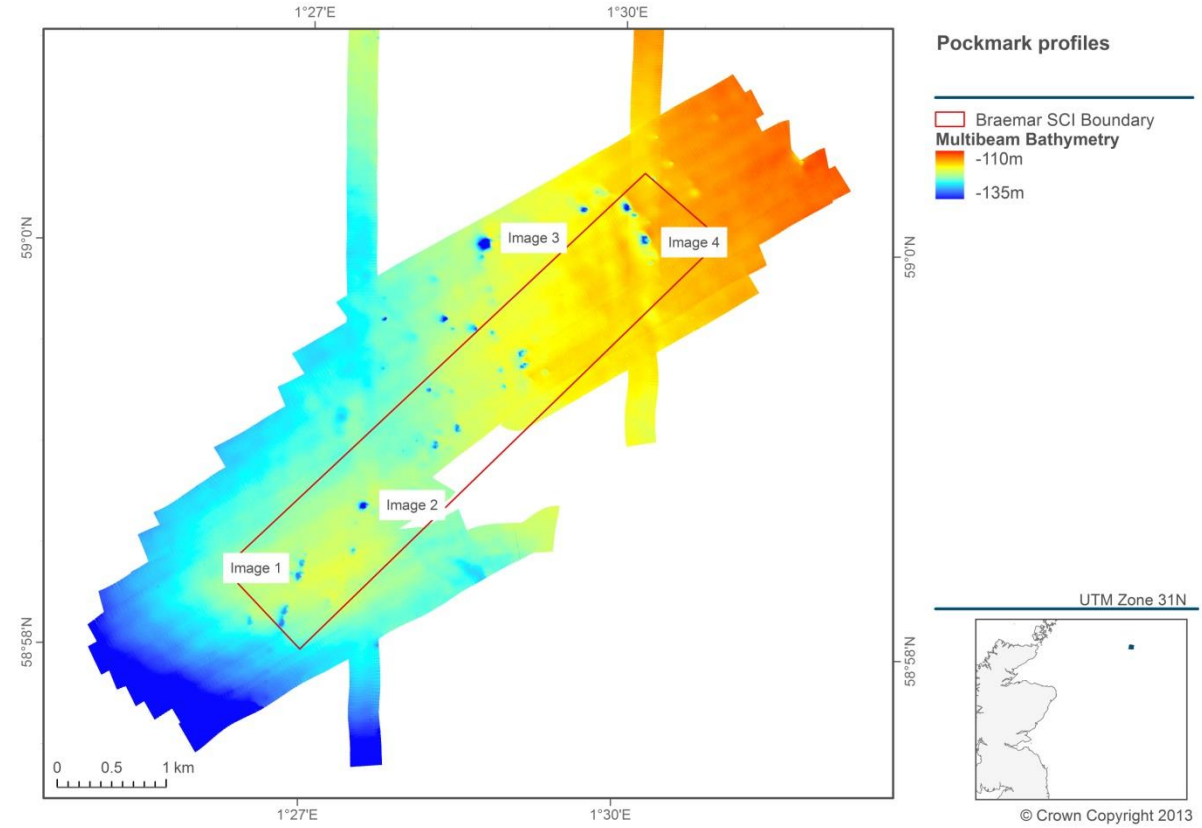

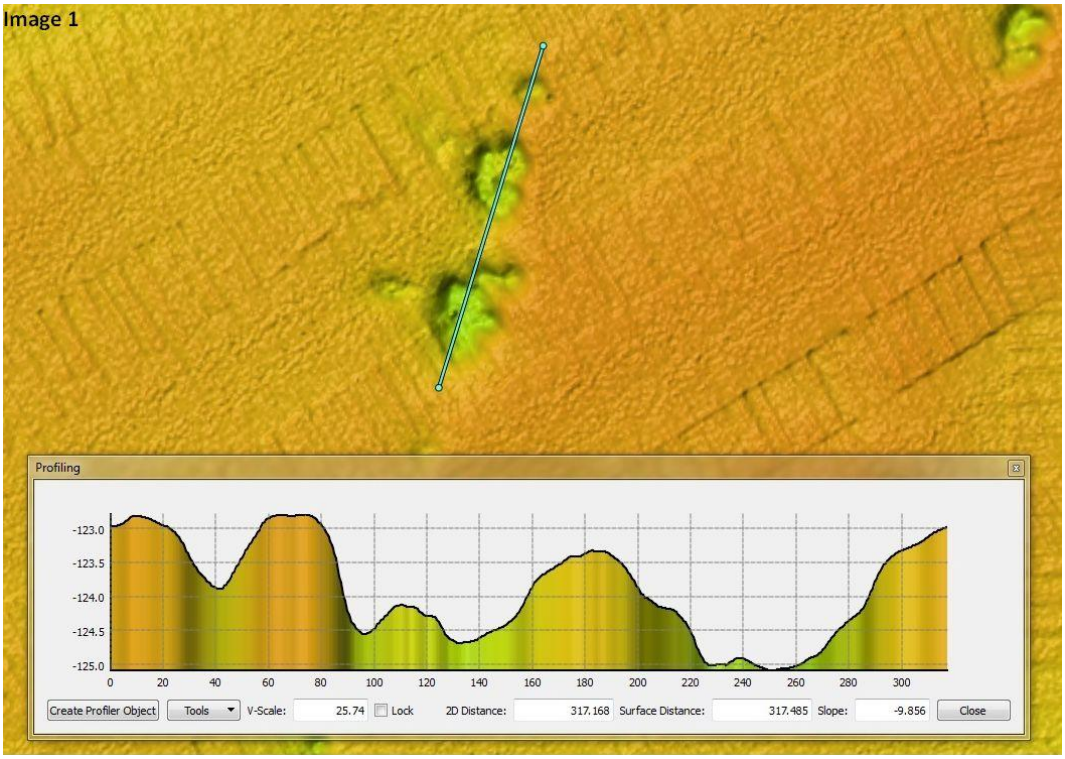

Figure 21. Illustration of profile sections of selected pockmark features within the Braemar Pockmarks SCI. Continues over following page.

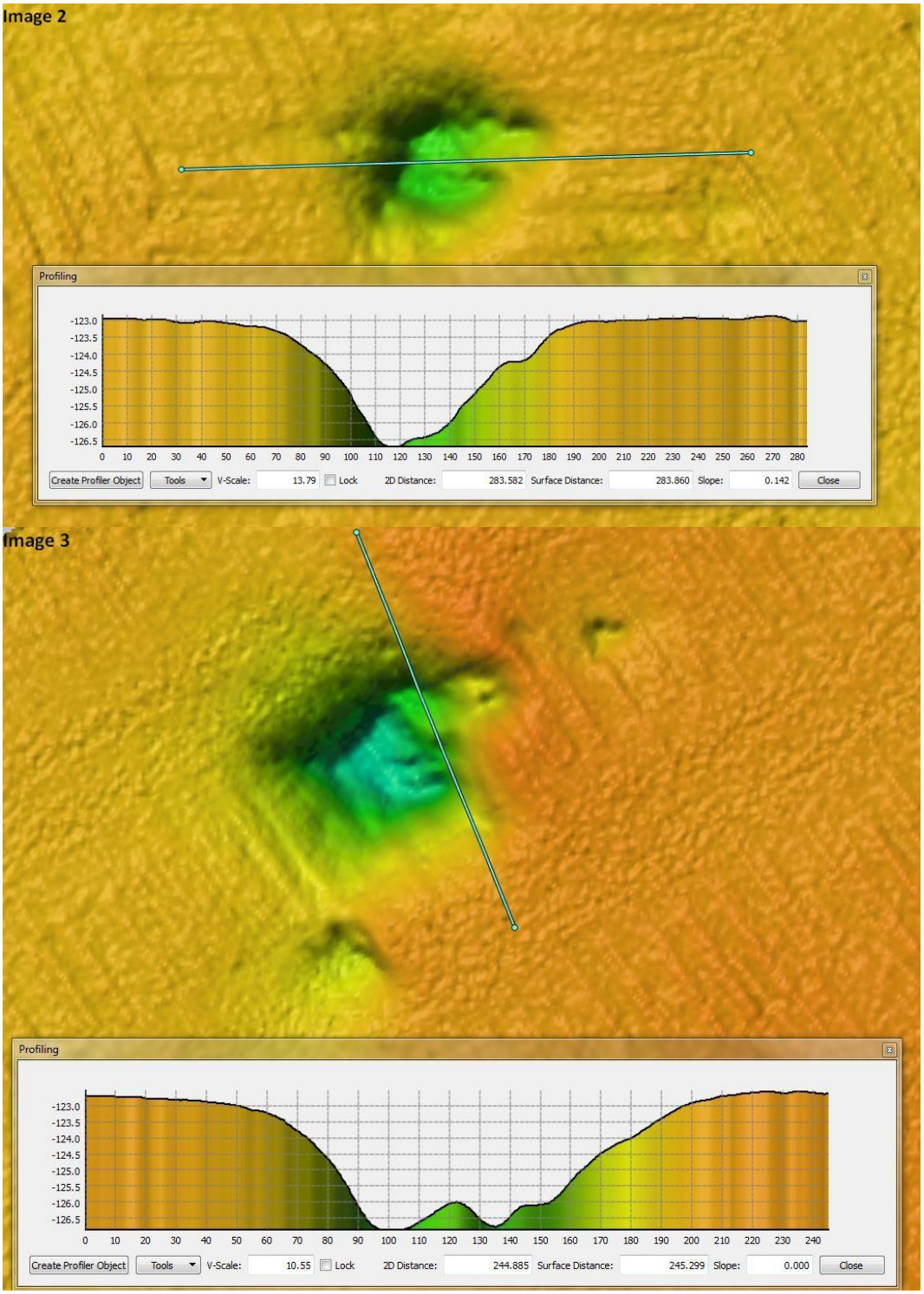

Figure 21 (continued). Illustration of profile sections of selected pockmark features within the Braemar Pockmarks SCI. Continues over following page.

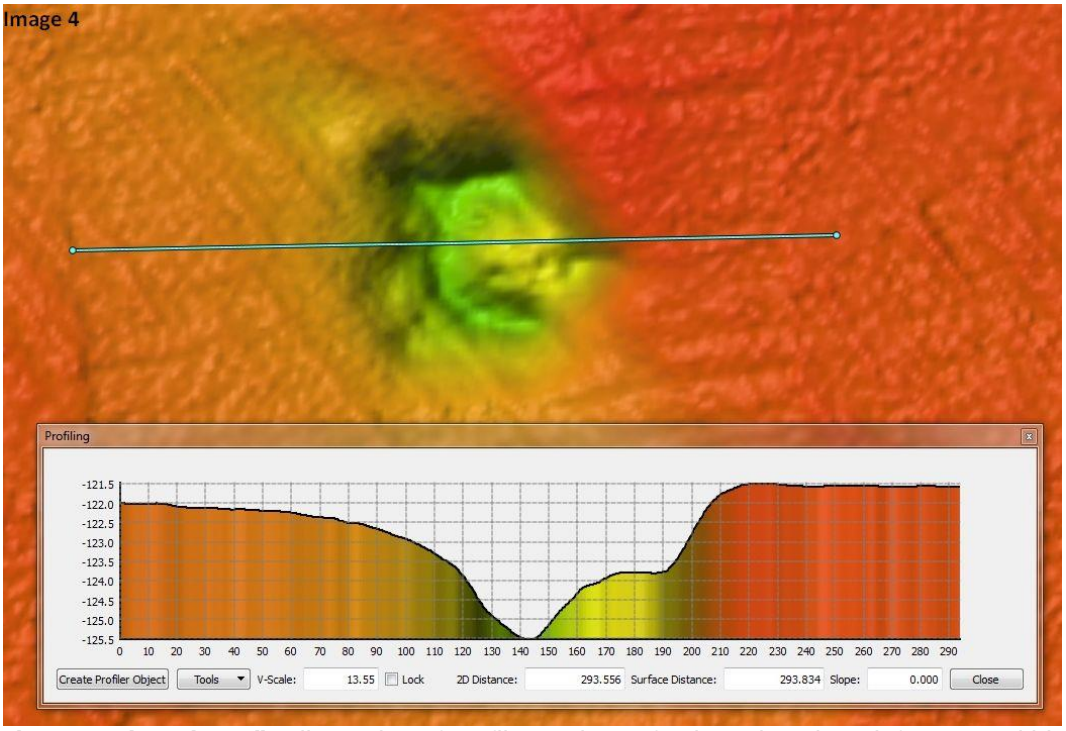

Figure 21 (continued). Illustration of profile sections of selected pockmark features within the Braemar Pockmarks SCI.

4.1.9 Annex I habitats

Analysis of the underwater video footage and observations from grab samples enabled the identification of features within the SCI that could potentially be MDAC. Figure 22 displays the location of the still images captured during the video acquisition, which were identified as having a possible MDAC presence along with the position of grab samples, where possible MDAC samples were recovered.

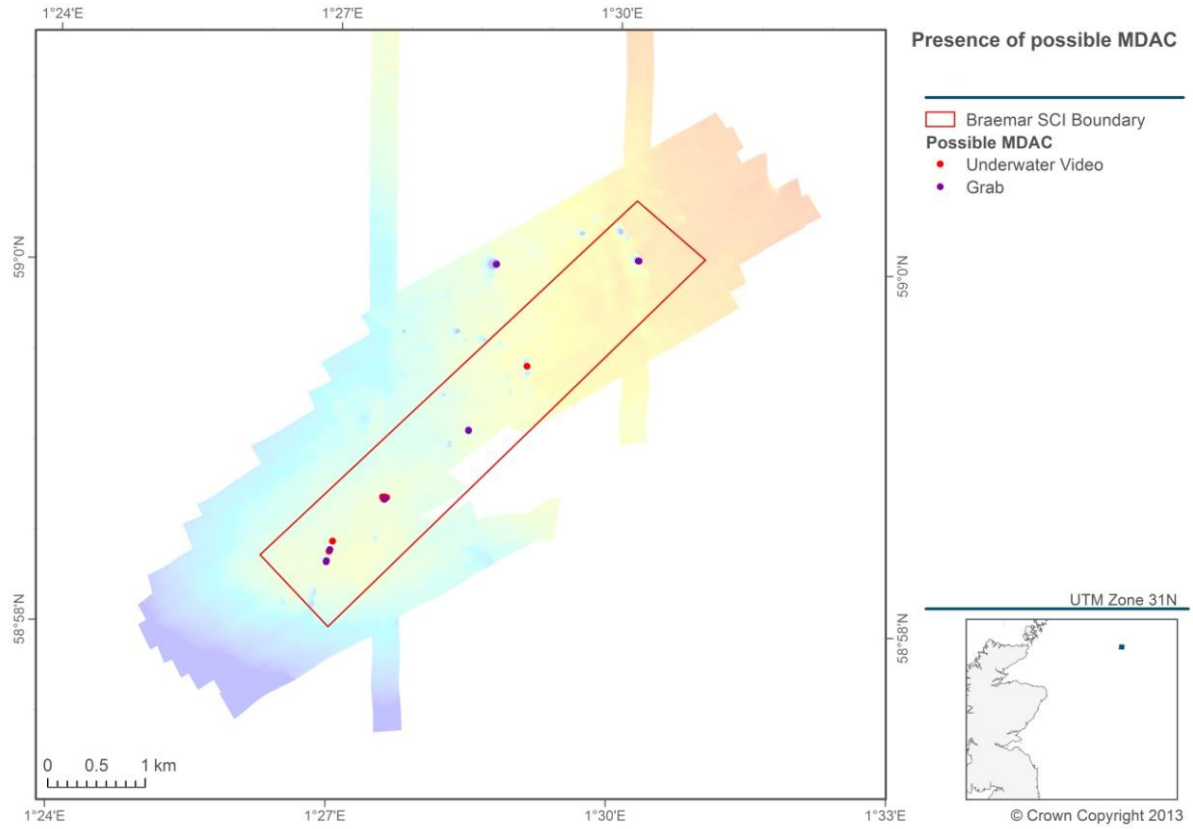

Figure 22. Presence of possible MDAC derived from seabed imagery and grab sample observations, with background bathymetry from Figure 8.

Figure 23 shows a pockmark in the southwest of the Braemar Pockmarks SCI with a distinct high backscatter signature; the position of the corresponding underwater stills has been overlaid to identify the potential presence of possible MDAC. Due to its hardness compared with the surrounding soft seabed sediments, MDAC produces a strong acoustic reflection, which can often be observed in the backscatter data. Still images from BRMR_26-27 Station 8 are displayed below the backscatter data with the corresponding image number. Possible MDAC can be identified in the three images. MDAC can occur as either blocks protruding from the seabed or can be partially covered by sediment; potential examples of both forms can be seen in the images from BRMR_26-27 Station 8.

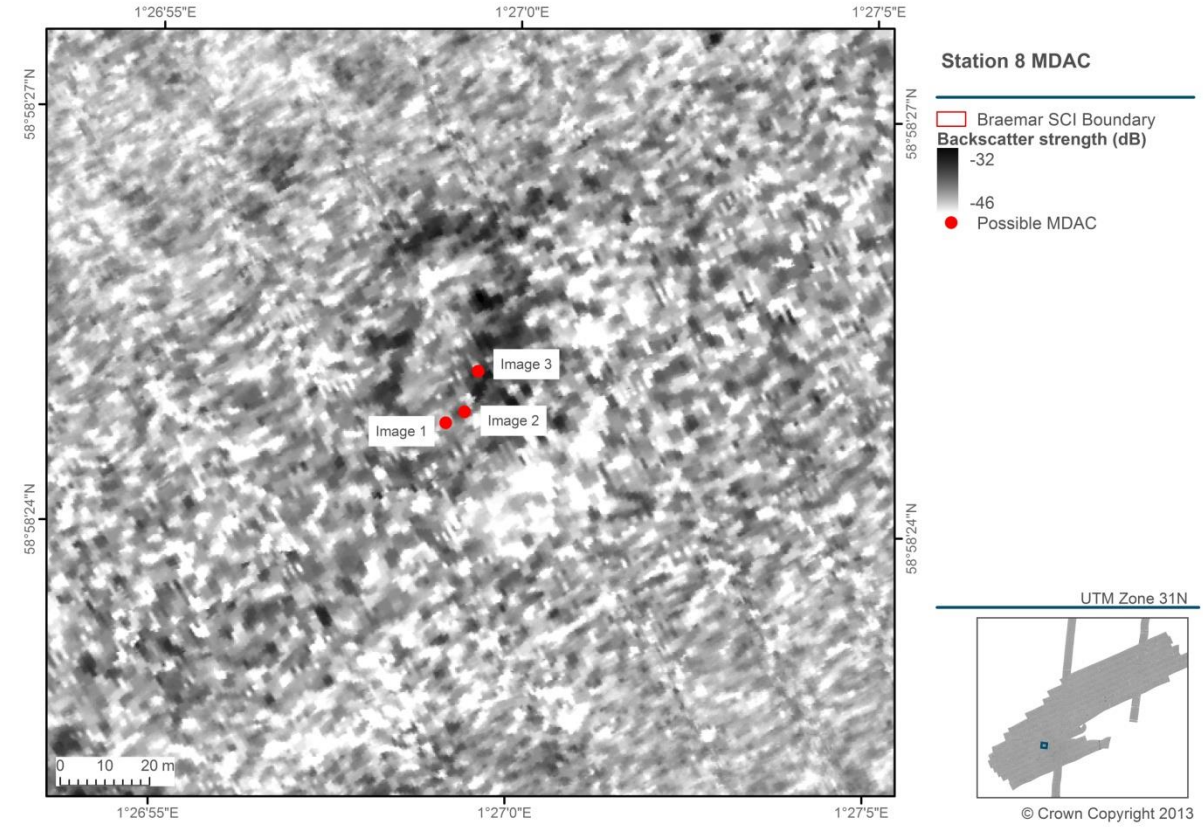

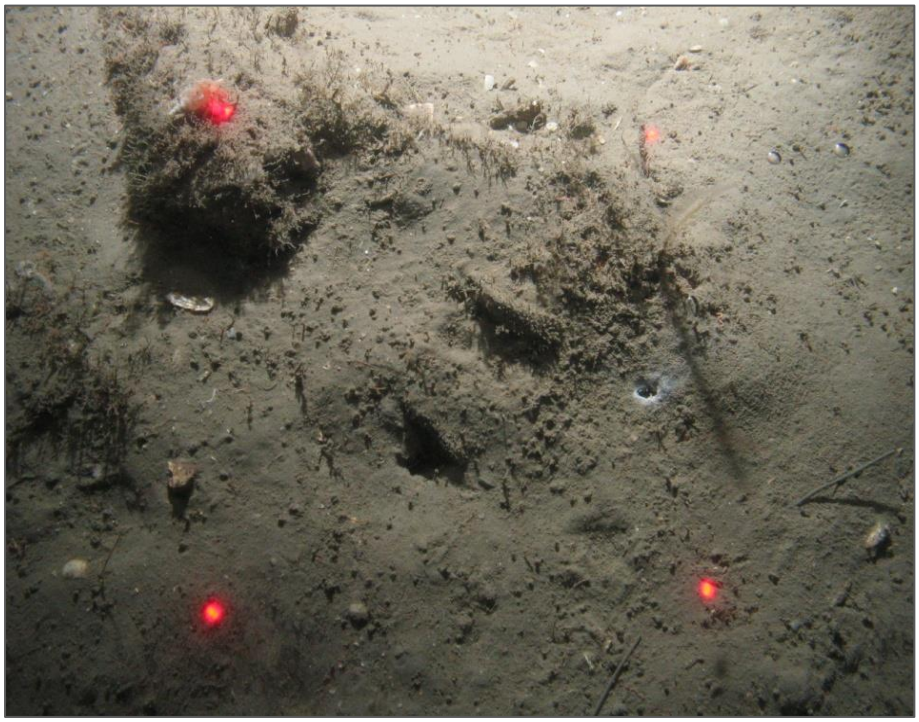

Image 1

Figure 23. Display of multibeam backscatter data at BRMR_26-27 (Station 8) at the Braemar Pockmark SCI, showing possible MDAC as suggested by selected stills. Continues on following page.

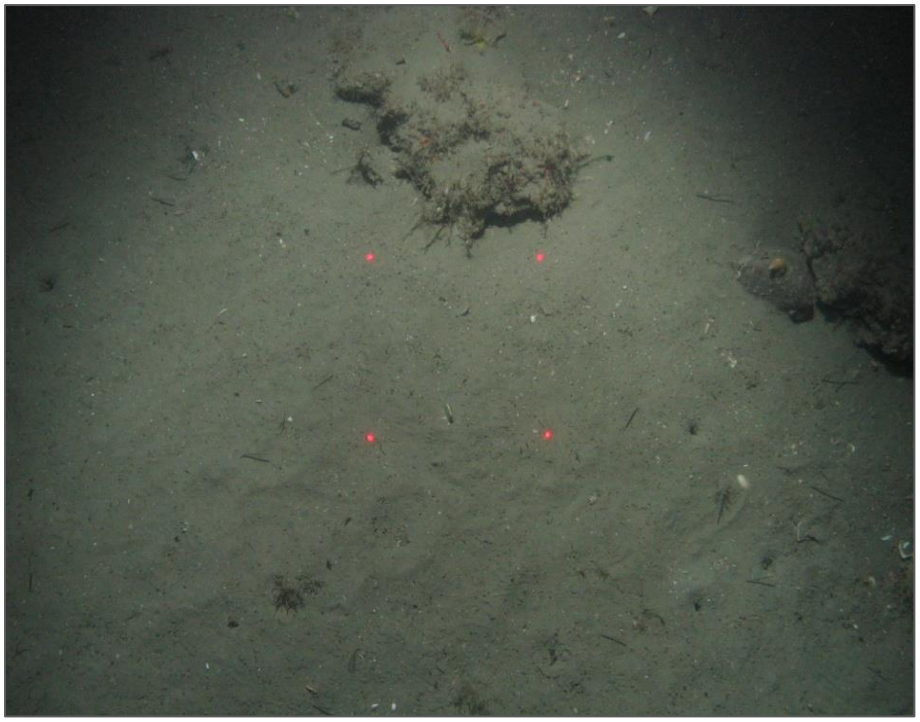

Image 2

Image 3

Figure 23 (continued). Display of multibeam backscatter data at BRMR_26-27 (Station 8) at the Braemar Pockmark SCI, showing possible MDAC as suggested by selected stills.

Faint traces of gas release were identified during the acquisition of sidescan sonar data onboard the survey vessel. Subsequent analysis of the data enabled these gas bubbles to be captured in an image, an example of which can be seen in Figure 24. The image shows streams of bubbles being released into the water column. The pockmark in question is located centrally within the Braemar Pockmark SCI, and possible MDAC was identified from the underwater footage at BRMR_26-27 (Station 13), the still from which can also be seen in the figure. Possible MDAC can be seen in this still image.

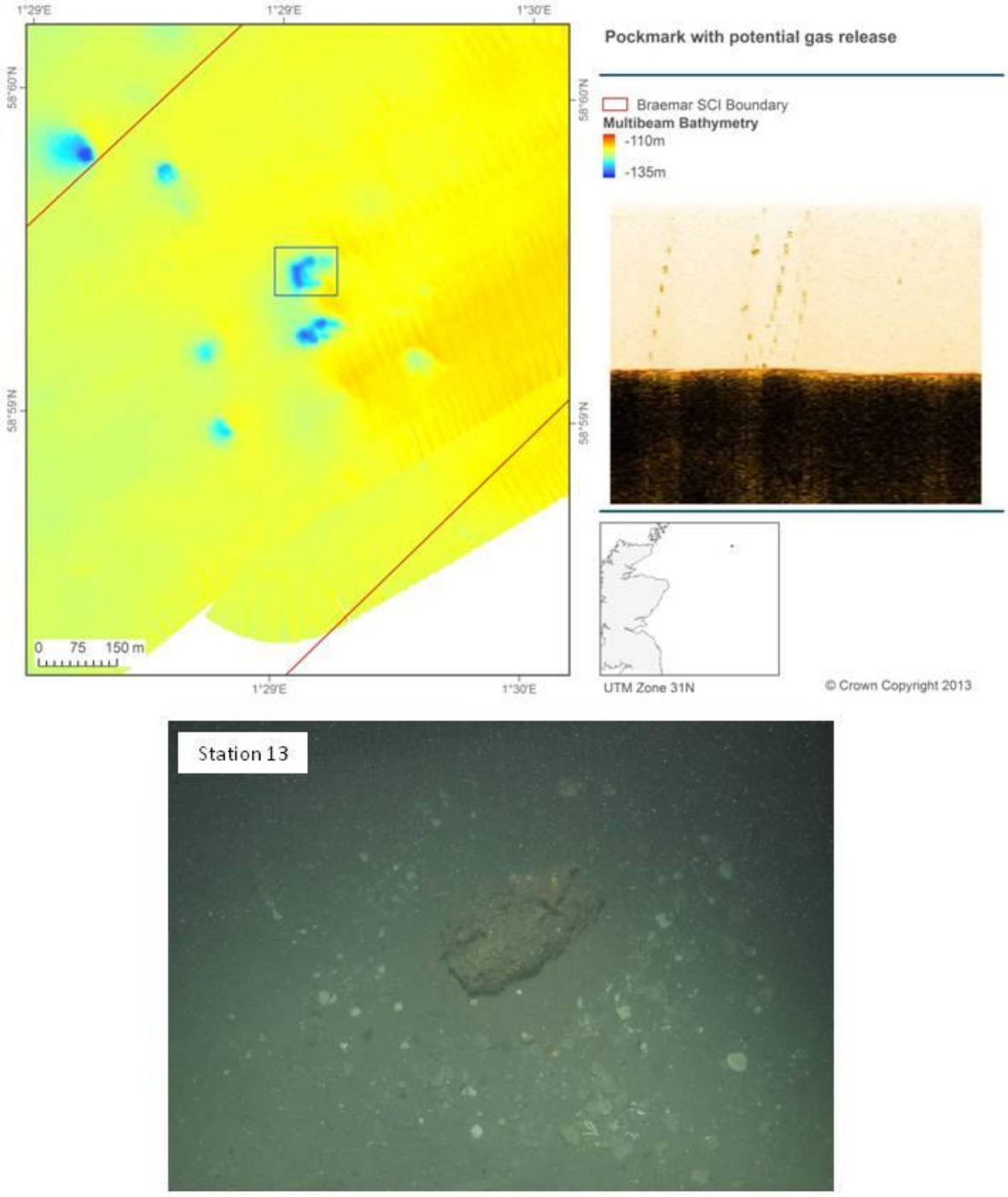

Figure 24. Location of pockmark (Station 13) with potential gas release identified on the sidescan sonar record and a corresponding still image from that station.

4.1.10 Petrographic and stable isotope analysis of potential MDAC samples

Eleven samples of carbonate-cemented sediment recovered from the seabed in the Braemar Pockmark area have been characterised mineralogically and petrographically, and the stable isotope ($\delta^{13}C$ and $\delta^{18}O$) composition of their component carbonate cements has been analysed to describe the nature and evaluate the origin of the carbonate cement. Results from these analyses have revealed that three types of carbonate-cemented sediment can be differentiated: (i) aragonite-dominated cements, (ii) high magnesian calcite-dominated cements, and (iii) dolomite-dominated cements.

Stable carbon isotope analyses showed that the aragonite- and magnesian calcite-dominated cements were highly depleted with respect to ^{13}C, with $\delta^{13}C_{PDB}$ values between -41 to -55‰. This is consistent with a diagenetic origin in which carbonate precipitation is related to methane oxidation, and is characteristic of MDAC deposits described previously from other areas. Therefore, this provides strong evidence to the hypothesis that the aragonite- and magnesian calcite-cemented sandstones and siltstones recovered from the Braemar Pockmark area represent MDAC.

In contrast, the dolomite-dominated cements (from samples HG10 STN29A, HG10 STN29B and HG6 STN 31C) were characterised by $\delta^{13}C_{PDB}$ values between -33.0 and -18.0‰PDB, which were closer to those expected for carbonates produced during bacterial reduction processes. The dolomite-dominated cements in these samples were all very closely associated with the preservation of cellular fabrics that closely resemble mineralised bacterial structures, and with the syngenetic formation of early diagenetic framboidal pyrite. The formation of this micritic dolomite-dominated cement is therefore consistent with the early diagenetic dolomite precipitation within the sulphide-reduction zone close to the sediment surface, or with a significant input of carbonate/bicarbonate ions produced from bacterial sulphide reduction.

Stable oxygen isotope ($\delta^{18}O$) analyses on the aragonite- and magnesian calcite-dominated cements revealed that MDAC formation may have occurred when seawater temperatures were considerably lower (approximately 3 to 10°C colder), possibly during the last ice age, as well as under present day conditions. The dolomitic carbonate cements are similarly heavier than expected with regard to $\delta^{18}O$ for precipitates from present-day seawater. These too could have been formed during cooler marine temperatures than the present day. However, the lighter $\delta^{13}C$ values suggest that these formed with a significant input of carbonate, derived from the bacterial iron and sulphate reduction in the sediment, rather than dominantly from bacterial methane oxidation.

Virtually all of the carbonate-cemented sediment samples examined in this study displayed abraded and well-worn and rounded surfaces. This indicates that most of the pebble- to cobble-sized fragments are clasts of re-worked carbonate-cemented sediment that have eroded from their original source. Therefore, they do not represent in-situ carbonate-cemented rocks. Observations show that the clasts have also been exposed to oxidising conditions on the seafloor during this process.

Further detail on the results from the analysis of MDAC samples from each site can be found in Appendix 7.

4.1.11 Other features of conservation value

Although the Braemar Pockmarks SCI does not fall under the jurisdiction of the SMPA initiative, for the sake of completeness and comparability with the Scanner Pockmark SCI, Table 3lists the search features identified at Braemar Pockmarks SCI (the complete list of SMPA search features is presented in Annex 3).

Table 2. MPA search features recorded as present at Scanner Pockmark SCI.

MPA search feature	**Component habitats/species**
Burrowed mud	Seapens and burrowing megafauna in circalittoral fine mud
	Mud burrowing amphipod *Maera loveni*
Offshore deep sea muds	*Paramphinome jeffreysii, Thyasira* spp. and *Amphiura filiformis* in offshore circalittoral sandy mud

The ocean quahog *Arctica islandica* (designated as a low or limited mobility species) was recorded at the Braemar Pockmarks SCI, although this species was not observed to occur in

aggregations. Burrowed mud and Offshore deep sea muds (identified as habitat features in Scottish offshore waters; see Annex 2) covered the majority of the survey area. Burrows were observed in 84% of all video samples, and seapens were recorded in 16% of video samples. *Ampharete falcata* were observed in all but one of the distinct macrofaunal assemblages identified in Figure 16 (assemblages *b*, *c*, *d*, *e* and *f*). Similarly, *Levinsenia gracilis* was also absent from a single assemblage (assemblage *f*). *Paramphinome jeffreysii* was the macrofaunal species with the highest average abundance across all macrofaunal samples (Appendix 2). *Thyasira* spp. and *Amphiura filiformis* were also present in all or most assemblages identified in Figure 16.

4.1.12 Anthropogenic impacts

Low-frequency sidescan data showed linear track-like features, indicative of seabed disturbance from bottom-trawling activity (Figure 25). The lines indicate where scars, consistent with those created by fishing trawl gear, were observed on sidescan data records, with the majority of activity located to the north and outside of the Braemar Pockmarks SCI boundary.

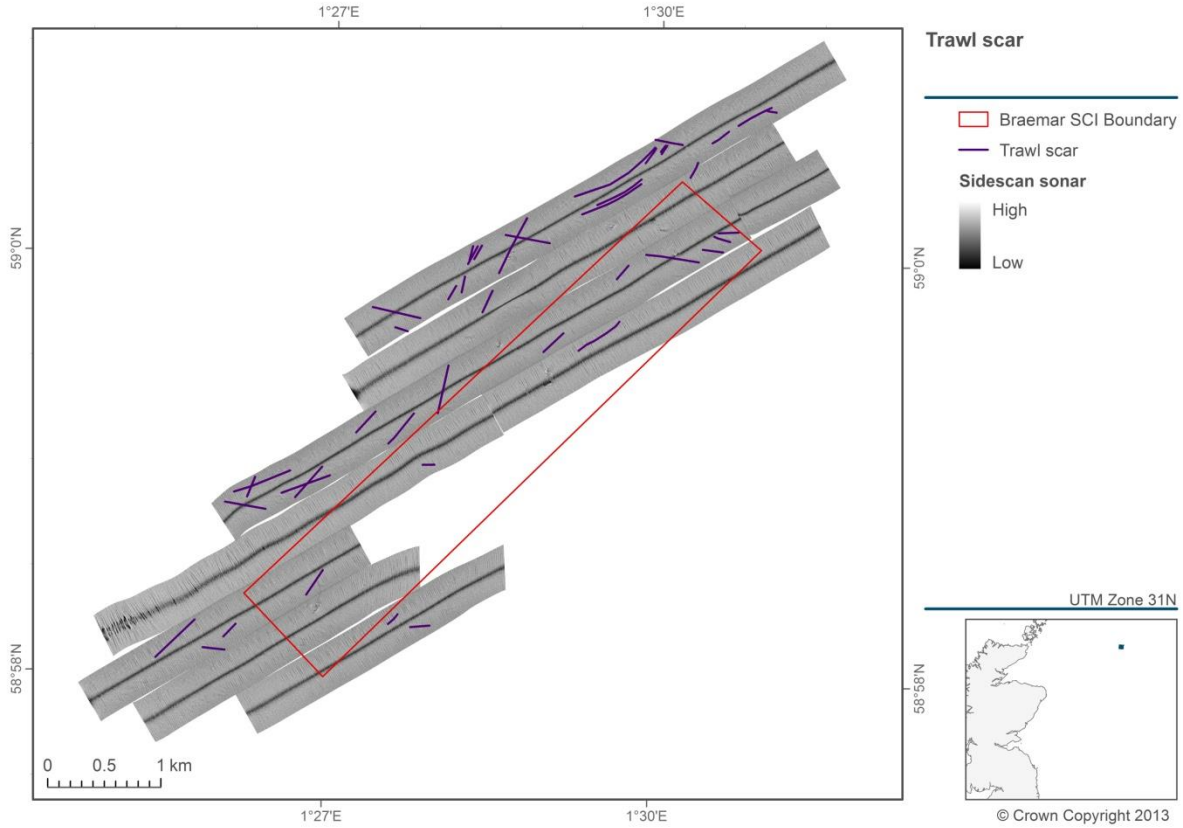

Figure 25. Interpretation of sidescan sonar data to identify trawl scars at Braemar Pockmarks SCI.

Figure 26 identifies a trawl scar within the SCI boundary, located centrally near one of the larger pockmark features. The scar is highlighted by a blue box.

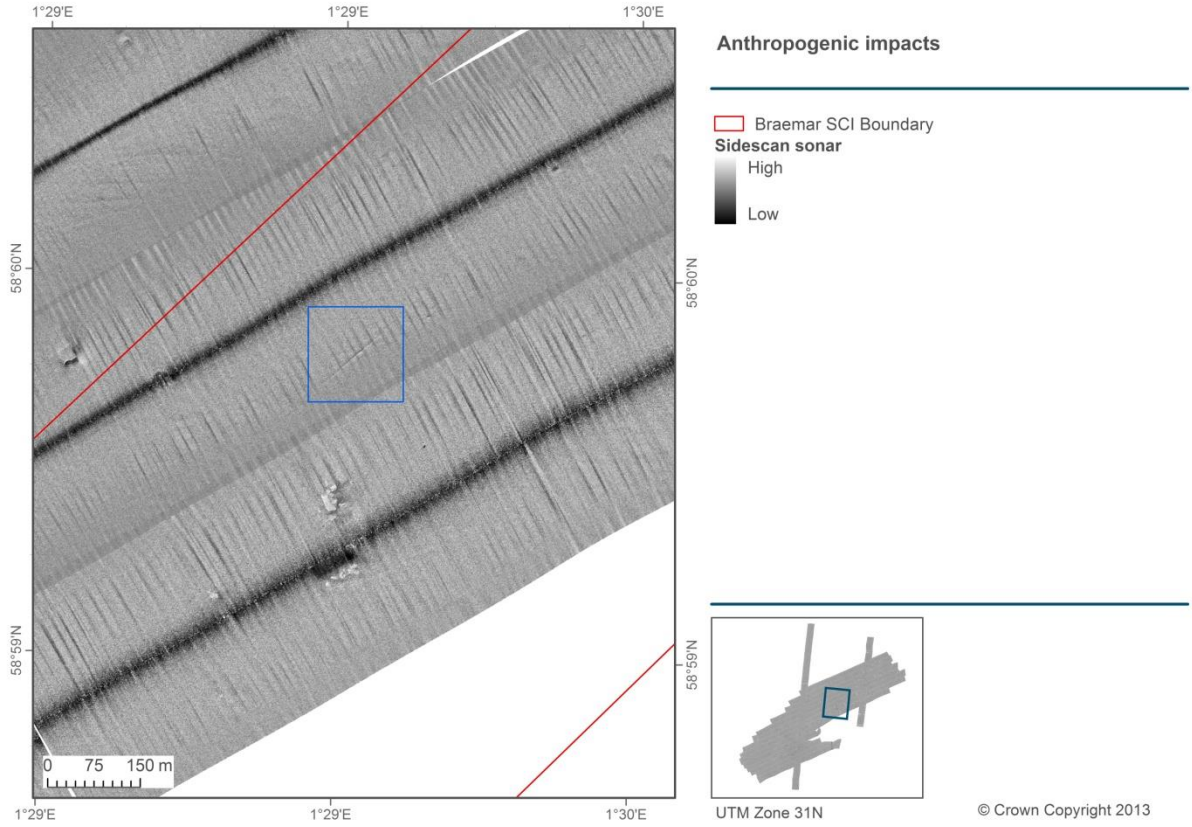

Figure 26. Trawl scar identified on the sidescan sonar low frequency data.

In additon to trawl scars, another anthropogenic impact was indentified on the seabed at the Braemar Pockmarks SCI, namely an abandoned wellhead (Figure 27). Faint channels can be seen in the multibeam bathymetry and occur in radial and geometrically regular intervals, believed to be the result of anchor mooring cables on the seabed.

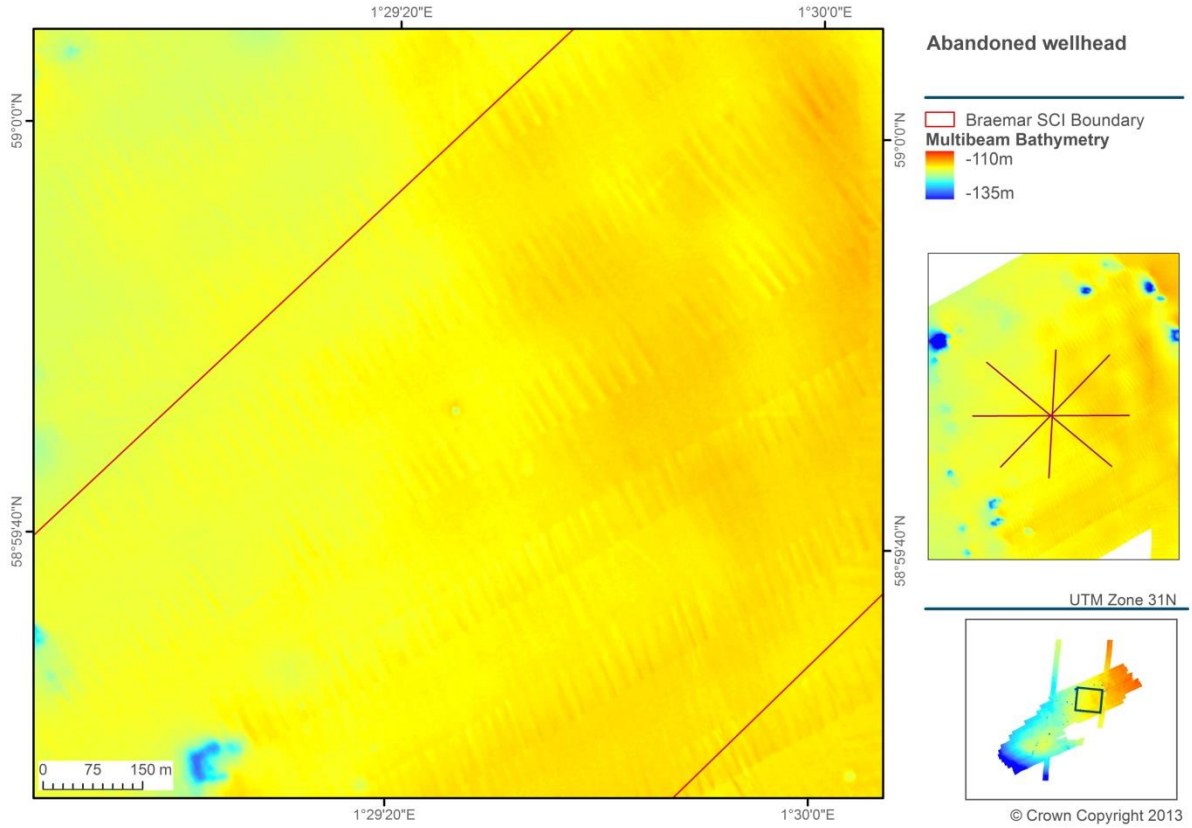

Figure 27. Abandoned wellhead identified within the Braemar Pockmarks SCI. The red lines on the inset map highlight the feint channels visible on the multibeam bathymetry around the wellhead, possibly created by anchor chains.

4.2 Scanner Pockmark SCI

4.2.1 Multibeam bathymetry and backscatter

Full coverage multibeam bathymetry and backscatter data were acquired at the Scanner Pockmark SCI, extending slightly beyond the SCI boundary. The average water depth at the Scanner Pockmark SCI is approximately 150m (CD); the shallowest depth recorded is 145m. The data revealed the presence of large pockmarks within and to the northwest of the site, which include the Scotia, Challenger and Scanner Pockmark Complex (Figure 28). These depressions are up to 17m deeper than the surrounding seabed and approximately 500m in diameter. Smaller unit pockmarks are present throughout the area and are roughly 1-2m in depth and <5m in diameter.

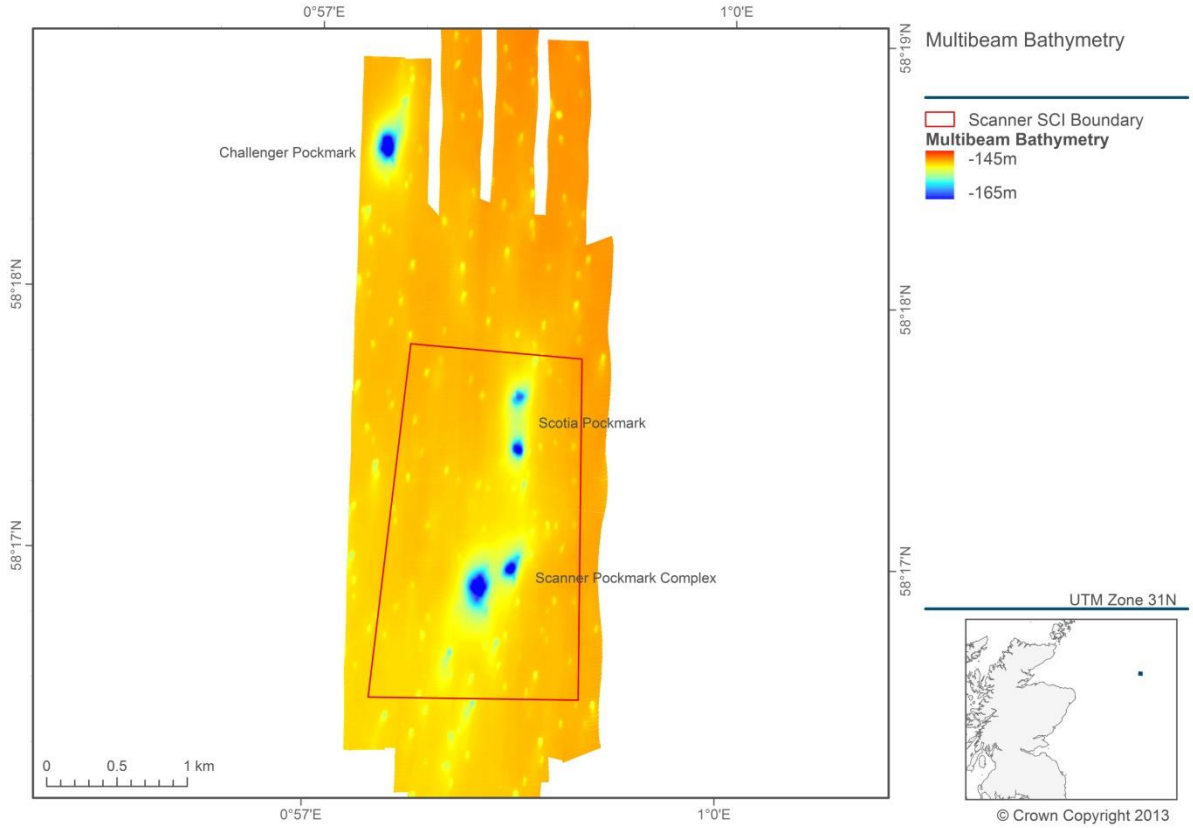

Figure 28. Display of multibeam bathymetry data at the Scanner Pockmark SCI.

The multibeam backscatter data (Figure 29) confirms the presence of a relatively homogeneous seabed with numerous pockmark features scattered across the SCI and surrounding seafloor. The majority of the seafloor has a low backscatter return, indicative of a soft substrate. The pockmarks themselves have a higher backscatter signature, suggesting a substrate with a coarser nature compared with the surrounding sediments.

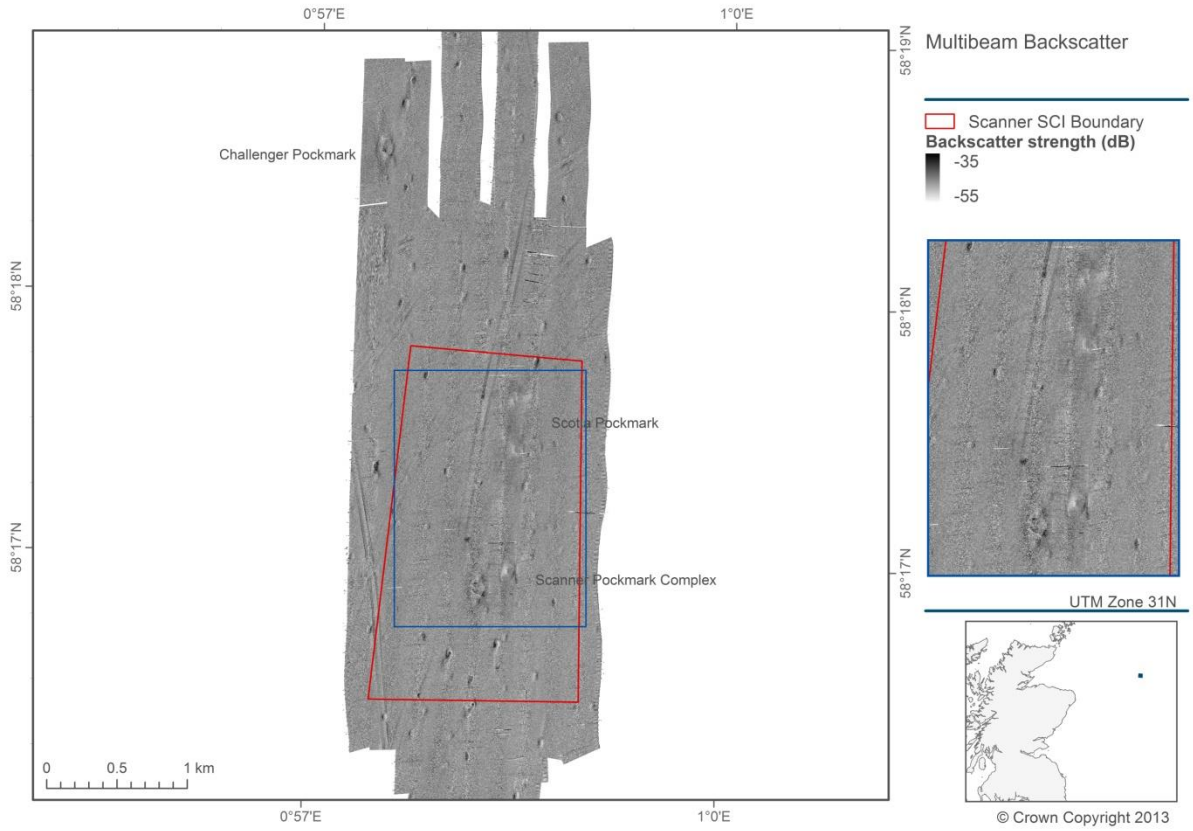

Figure 29. Display of multibeam backscatter data from the Scanner Pockmark SCI.

4.2.2 Sidescan sonar

Sidescan sonar data were acquired to further aid identification of the features of interest, and to enable the high resolution interpretation of possible anthropogenic impacts such as trawl scars. The high and low frequency data were processed onboard and the low frequency output, which was less impacted on by the poor weather conditions, can be seen in Figure 30. The large pockmarks seen on the multibeam bathymetry and backscatter are also distinguishable on the sidescan sonar records. Detail of the Scanner pockmark complex is presented in Figure 31.

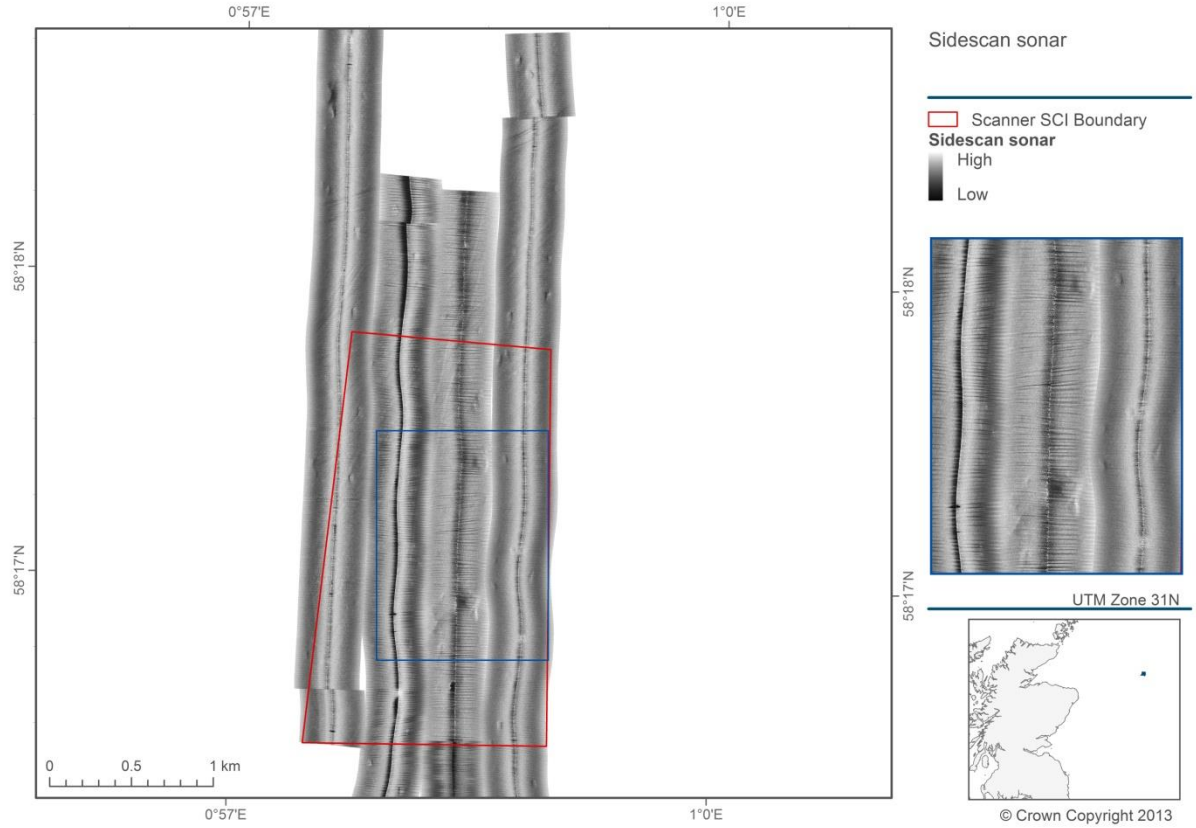

Figure 30. Display of sidescan sonar data at the Scanner Pockmark SCI.

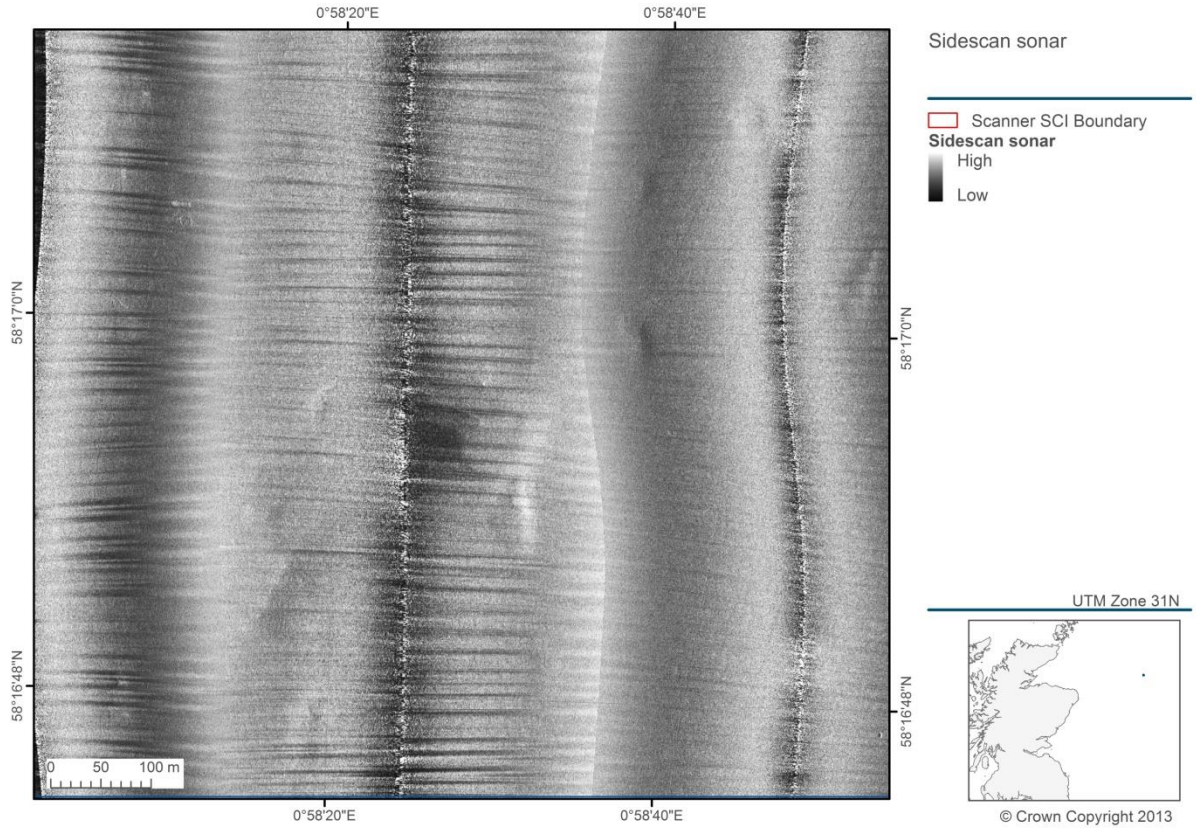

Figure 31. Detail of the Scanner Pockmark Complex on the sidescan sonar data.

4.2.3 Surficical sediments

The acoustic and groundtruthing data collected at the Scanner Pockmark SCI enabled the categorisation of sediment type. Observations of the samples made during their acquisition indicated a seabed consisting of mud and sandy mud. This is supported by the PSA results which indicate a mud content of >80% within the samples (Figure 32 and Figure 33). Additionally, the underwater video and still images show a similar result of subtidal mud across the survey area.

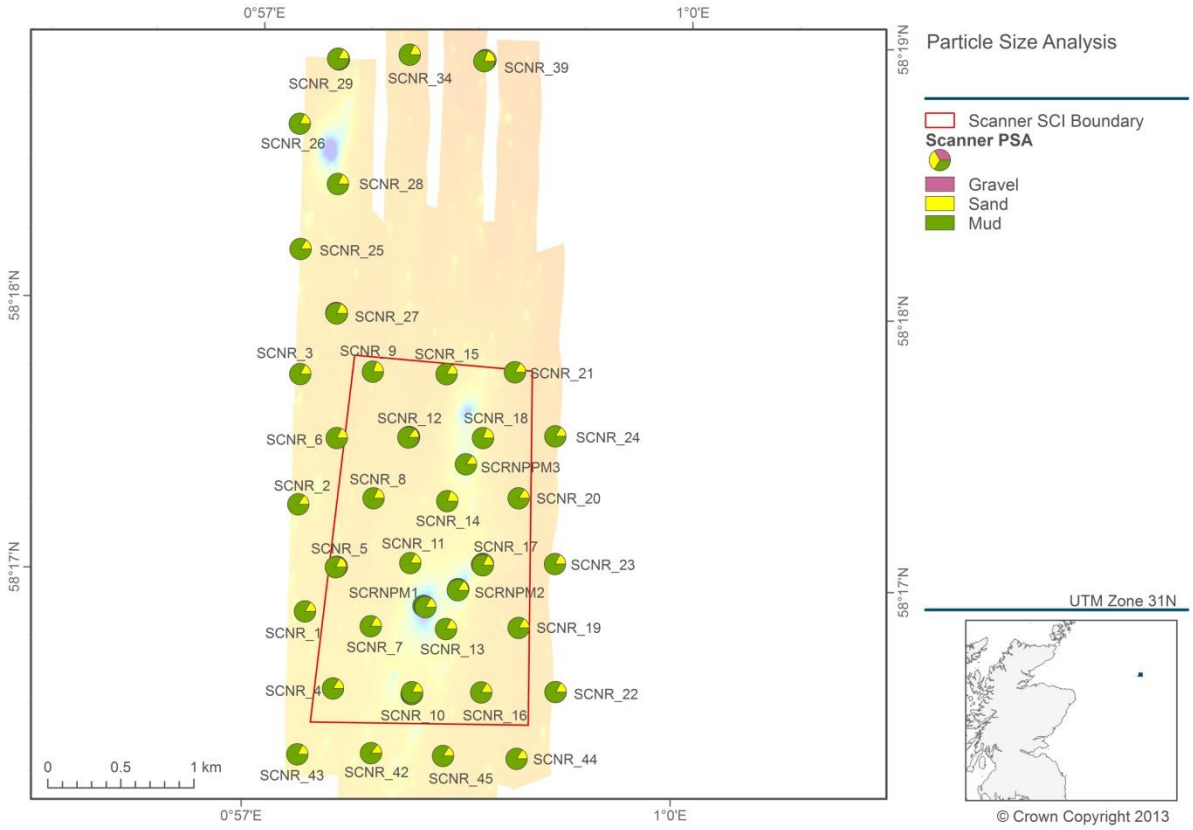

Figure 32. Results from PSA displayed as pie charts for the Scanner Pockmark SCI. Underlying background bathymetry is that shown in Figure 28.

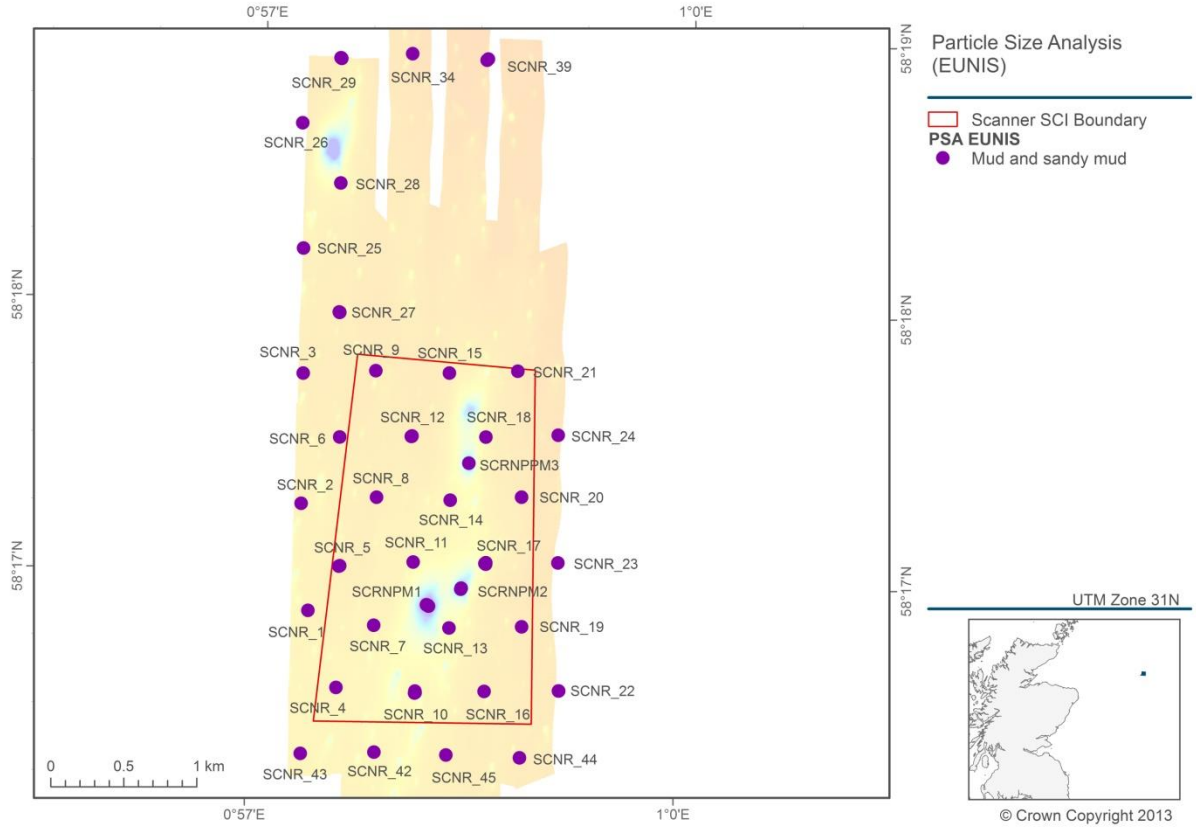

Figure 33. Results from PSA displayed according to the EUNIS classification for the Scanner Pockmark SCI. Underlying background bathymetry is that shown in Figure 28.

Due to the homogeneous nature of the sediments within the Scanner Pockmark SCI, the distinction of ground type within the Scanner Pockmark SCI using eCognition was assisted by applying some assumptions to the decision-making process. It was assumed that the areas with a high multibeam backscatter would have a comparable sediment composition to those identified at the Braemar Pockmarks SCI, and therefore were classed as mixed/coarse (see Figure 34).

Long (1986) noted that seabed sediments dominated by sandy mud tend to have a higher pockmark density yet smaller diameter (<50m), and seabed sediments containing solely mud tend to be larger in diameter (>50m) with a lower pockmark density (Judd 2001). The Scanner Pockmark SCI comprises mainly mud, and the numerous pockmark features have a sediment type of mixed/coarse attributed to them (Figure 34). The coarse material associated with the unit pockmark is widespread at the site.

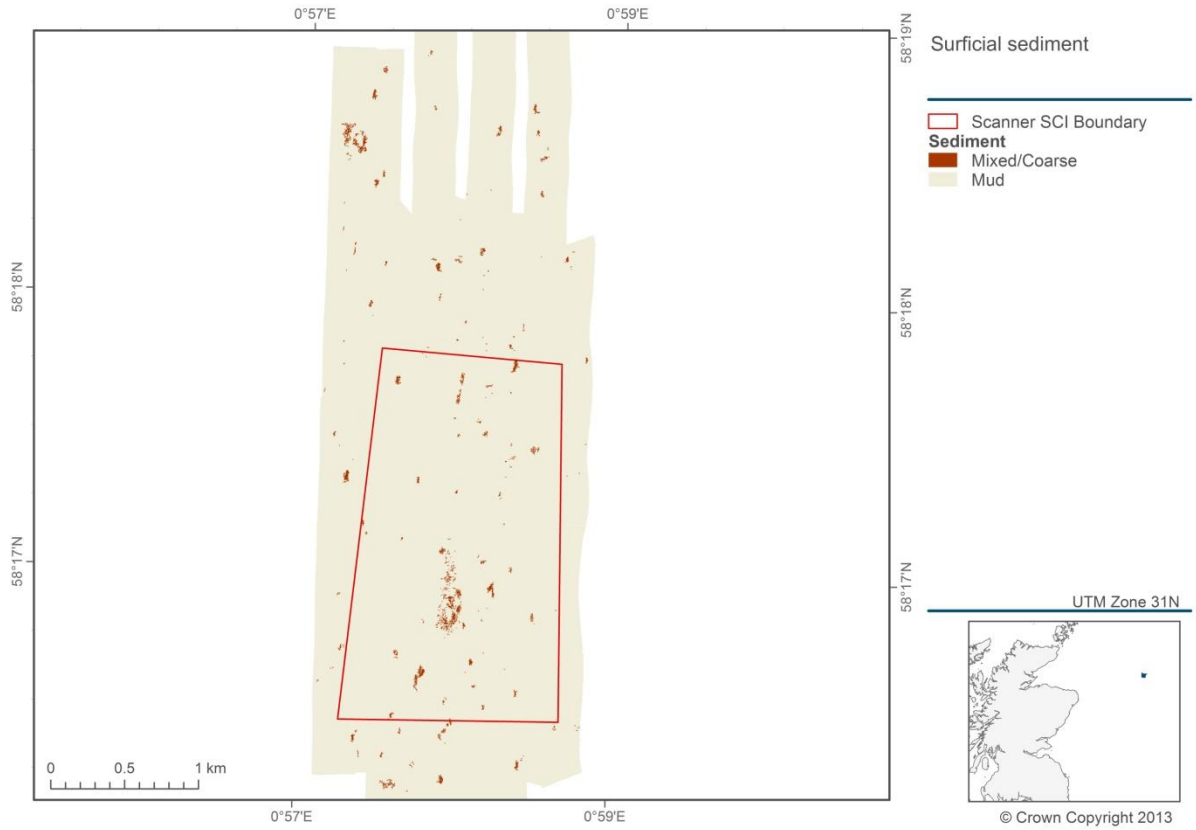

Figure 34. Sediment classification map based on the combination of acoustic and groundtruthing data.

4.2.4 Grab sample analysis

All samples collected at the Scanner Pockmark SCI were acquired using a Day grab. Ten out of all 38 sampling stations were sampled three times, a single station was sampled twice, and all remaining stations were sampled once.

Macrofaunal abundance values per sample ranged between 47 and 292 individuals. The lowest and highest recorded number of taxa per sample were 17 and 37, respectively. Wet weight biomass ranged from 0.43g to 25.08g per sample. Taxon diversity was between 5.4 and 24.9 per sample. All calculated metrics per sample are presented in Appendix 1. The distribution of selected calculated metrics across the Scanner Pockmark SCI is displayed in Figure 35, Figure 36 and Figure 37. At sampling stations where replicate grabs were taken, an average across replicates has been calculated for each metric at each station.

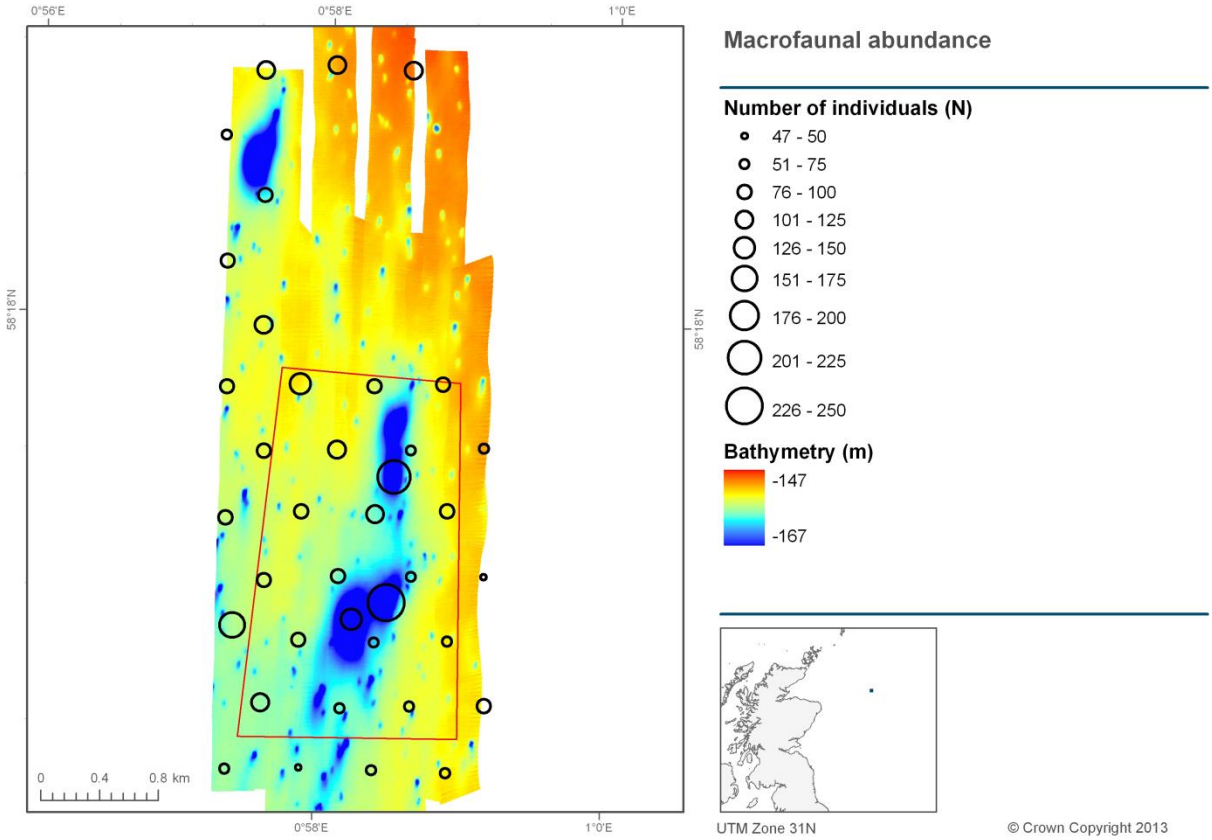

Figure 35. Spatial distribution of mean macrofaunal abundance values per station at the Scanner Pockmark SCI. The red line marks the Scanner Pockmark SCI boundary.

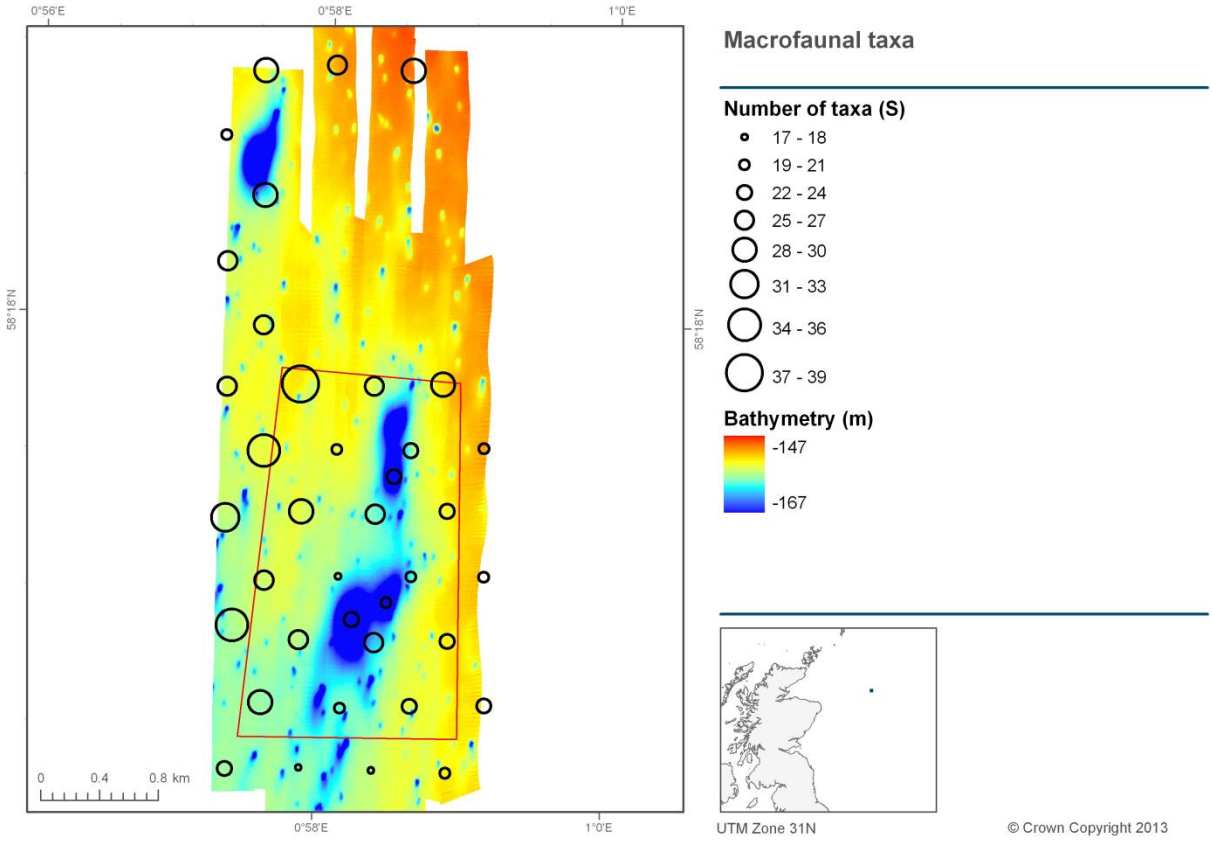

Figure 36. Spatial distribution of the mean number of macrofaunal taxa recorded per station at the Scanner Pockmark SCI. The red line marks the Scanner Pockmark SCI boundary.

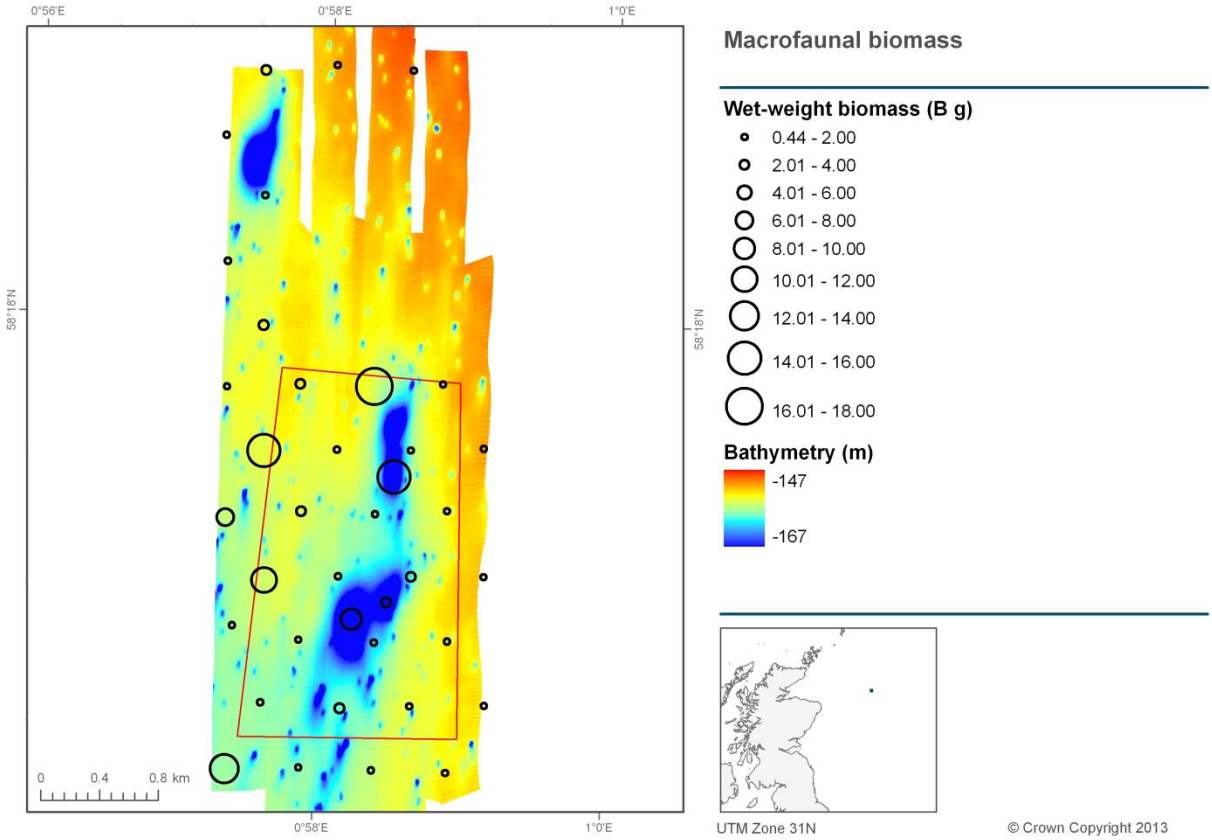

Figure 37. Spatial distribution of the mean wet-weight biomass recorded per station at the Scanner Pockmark SCI. The red line marks the Scanner Pockmark SCI boundary.

Within the boundaries of the Scanner Pockmark SCI, the highest abundance values per sample were observed within the pockmark features. Smallest values for macrofaunal abundance were observed outside the SCI boundary (Figure 35). Conversely, relatively few taxa were observed within the pockmark features whereas in the surrounding areas both high and low numbers of taxa were observed (Figure 36). The distribution of diversity across the survey area followed the same pattern as the number of taxa (data not shown). Wet-weight biomass per sample was generally low across the survey area, except for a handful of sites, most of which falling outside the pockmark feature (Figure 37). With the exception of the number of taxa per sample, the difference between the values of calculated assemblage metrics between inside and outside the pockmark feature was statistically significant ($p<0.05$).

Multivariate analyses were performed on the first replicate sample acquired from each sampling station, to avoid detecting any pattern caused by unequal sampling effort across the sampling stations. Analyses revealed seven distinct macrofaunal assemblages (*a* to *g*), four of which were represented by a single sample (*a*, *b*, *d* and *e*). Assemblage *c* was represented at three sampling stations towards the south of the survey area. Assemblage *f*, represented by four sampling stations corresponded broadly with those falling within the pockmark feature. Assemblage *g* was the most widespread, represented at 27 sampling stations (Figure 38). Taxa characterising each of the assemblages identified are listed in Appendix 3.

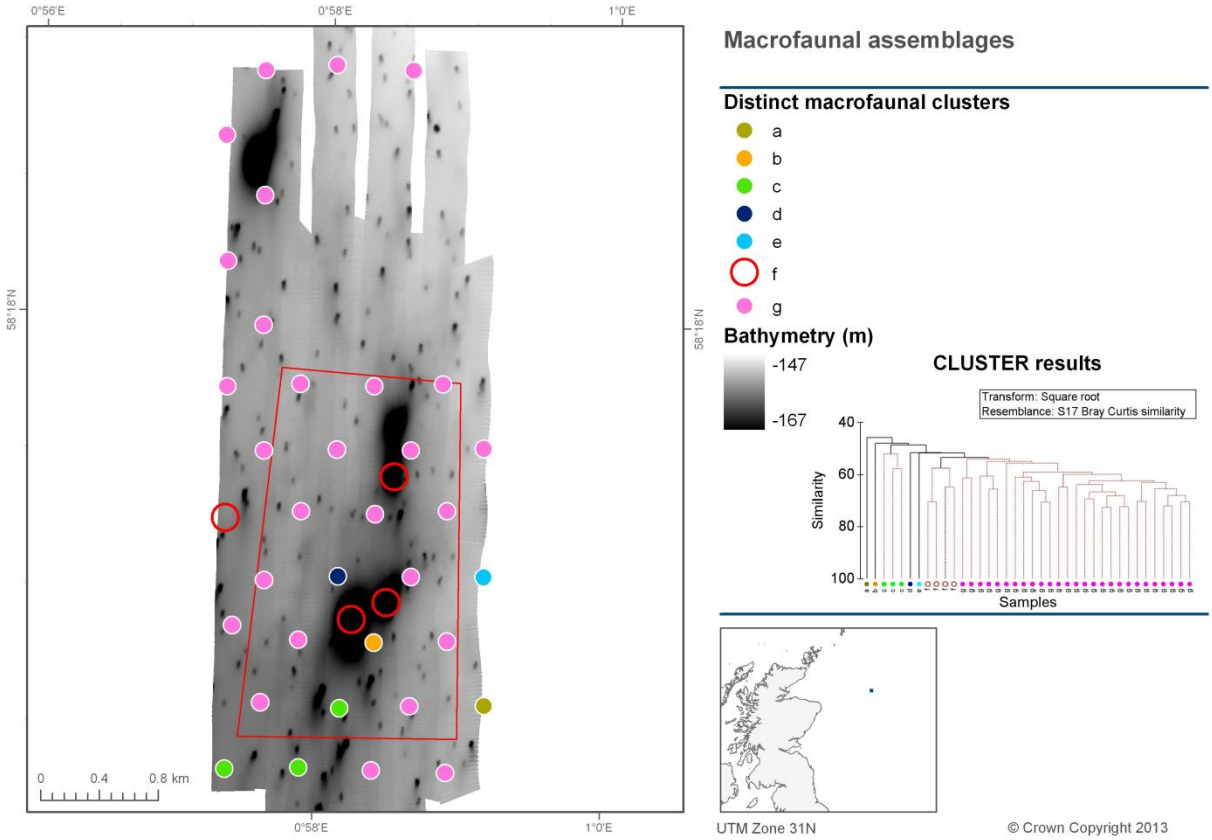

Figure 38. Spatial distribution of the distinct macrofaunal assemblages identified at the Scanner Pockmark SCI. The straight red line marks the Scanner Pockmark SCI boundary.

An ANOSIM test to investigate whether there was a difference in assemblage composition between samples falling within and outside the pockmark features revealed no significant difference between the two test treatments.

Multivariate analyses on particle size distribution data (averaged across replicates from the same sampling station) revealed several statistically distinct clusters of stations (Figure 39). No distinct cluster appeared to represent pockmark features exclusively, and more than one distinct cluster of samples was represented within pockmark features (notably, clusters *b* and *k*). Clusters *b* and *k* were characterised by slightly coarser sediments than those represented in the rest of the survey area, containing a larger proportion of fine gravel. None of the distinct clusters identified appeared to define any spatially obvious pattern in their distribution, suggesting that the whole survey area is a relatively homogeneous, although there are isolated patches of seabed with slightly different sediment particle size composition; the slight variation in the different proportions of variously sized particles are responsible for the distinctness of clusters identified.

The Principle Component Analysis (PCA) plot (see insert in Figure 39) also revealed no clear pattern in the separation of sampling stations based on PSA. Only 57% of the variation in samples was captured by both plotted axes. This finding supports the notion of a relatively homogeneous seabed, but with some patches with a slightly different proportion of the various sediment particle size classes comprising the predominantly slightly sandy mud substrate.

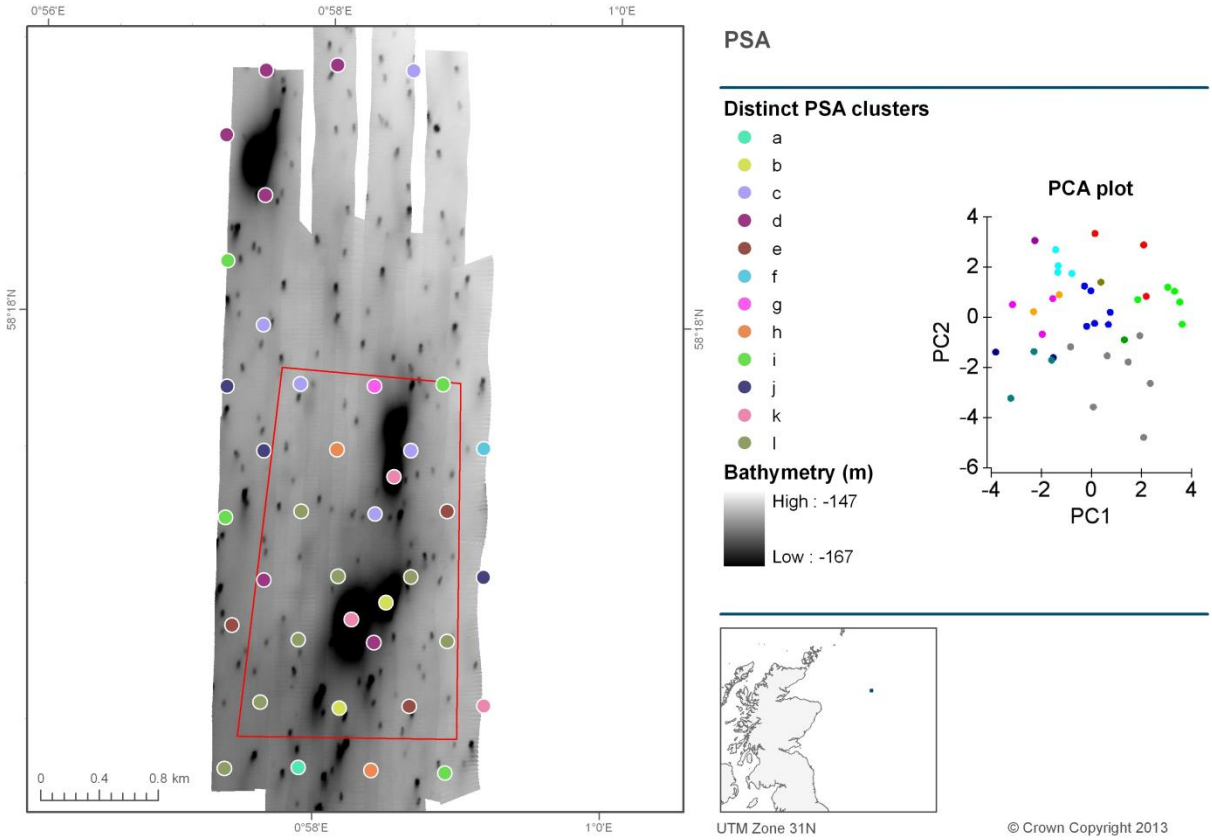

Figure 39. Distribution of distinct clusters of sampling stations based on multivariate PSA. Insert Principle Component Analysis (PCA) plot of stations. The red line marks the Scanner Pockmark SCI boundary.

The sediment fraction showing the highest correlation with the pattern in macrofaunal distribution was very fine gravel (rho value: 0.241), however the relatively low correlation value, superseded by that of several combinations of up to five different variables across the particle size spectrum (data not shown), suggests that differences in particle size composition across the survey area were of very little influence over the patterns observed in the resident macrofaunal assemblage. The coarsest sediment component identified, fine gravel, showed the lowest correlation with any pattern observed in the macrofaunal data (rho value: -0.061), suggesting that the limited proportion of this fraction in the sediments had no influence whatsoever on the resident macrofaunal assemblage.

4.2.5 Video and still sample analysis

A total of 16 video clips and 401 stills were analysed from in and around the Scanner Pockmark SCI. Many of the images analysed had moderate or poor visibility due to the sediment being disturbed and/or the camera being too far from the seafloor. Analysis of the video tows showed the habitat type to be the same across the whole survey area. The biotope identified was Circalittoral Fine Mud (SS.SMu.CFiMu). An additional biotope was recorded during the analysis of stills that was not observed on the video samples; this was Seapens and Burrowing Megafauna in Circalittoral Fine Mud (SS.SMu.CFiMu.SpnMeg). However, the density of seapens was not considered sufficient to change the assignment of the biotope from that designated from the video samples.

Other notable taxa that were recorded included the burrowing crustacean *Nephrops norvegicus* and the anemone *Arachnanthus sarsi*. A complete list of taxa recorded from video and stills samples is presented in Appendix 5.

4.2.6 Meiofaunal analysis

At the Scanner Pockmark SCI, 94 nematode taxa were recorded, and the whole area had an average Simpson's diversity index value of 26.25 (Physalia 2013). This diversity index value was almost half of that recorded at the Braemar Pockmarks SCI, however, it is likely that the high abundance/dominance of a single species in the samples from around the Scanner Pockmark, namely *Astomonema southwardarum*, may have brought down the value of the diversity index.

A. southwardarum occurred in all samples collected within and around the Scanner Pockmark SCI. It was recorded at a maximum density of 14,904 individuals per litre of sediment in sample SCNR_80A. In this case it accounted for 54% of the total nematode assemblage. This species was originally described from the Scanner area by Austen *et al* (1993) and is a characteristic species of methane seep habitats. The adults possess degenerate alimentary canals and they appear to derive nutrients from the endosymbiotic, chemoautotrophic bacteria that are contained within their body cavity (see Tchesunov *et al* 2012).

4.2.7 Biotopes

An assessment of the acoustic data with the associated benthic habitats was undertaken to enable the allocation of EUNIS Level 4 biotopes at Scanner Pockmark SCI.
The two classifications used to distinguish the surficial sediment map have been integrated to allocate the EUNIS classifications shown in Figure 40. Two biotopes were identified in the biotope map, namely A5.36 Circalittoral Fine Mud and A5.44 Circalittoral Mixed Sediment. The site is predominantly circalittoral fine mud with scattering of mixed sediment, associated mostly with the pockmarks and unit pockmarks.

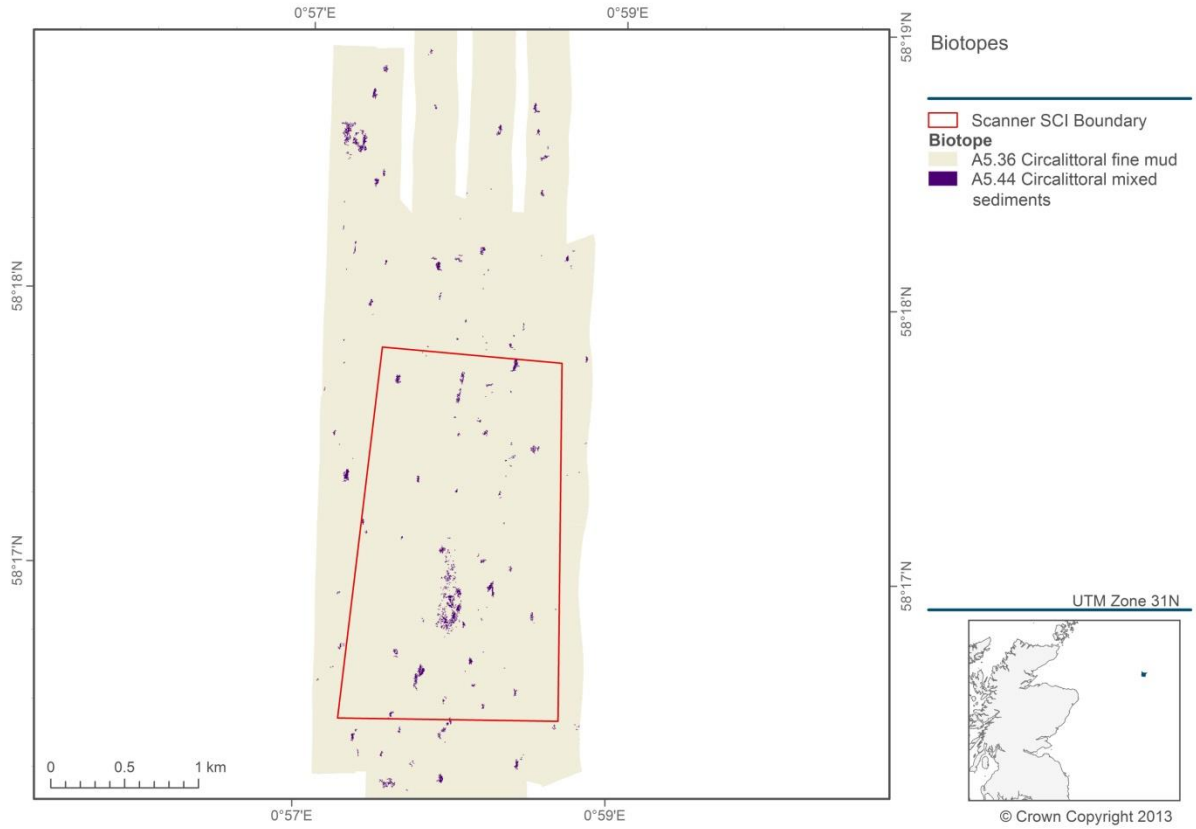

Figure 40. Biotope map based on Scanner Pockmark SCI acoustic and groundtruthing data.

4.2.8 SMPA Priority Marine Features

Table 3 lists the search features identified at Scanner Pockmark SCI (the complete list of features is presented in Annex 2).

Table 3. MPA search features recorded as present at Scanner Pockmark SCI.

MPA search feature	Component habitats/species
Burrowed mud	Seapens and burrowing megafauna in circalittoral fine mud
	Mud burrowing amphipod *Maera loveni*
Offshore deep sea muds	*Levinsenia gracilis* and *Heteromastus filiformis* in offshore circalittoral mud and sandy mud
	Paramphinome jeffreysii, Thyasira spp. and *Amphiura filiformis* in offshore circalittoral sandy mud

No low or limited mobility species (listed in Annex 3) were recorded from the Scanner Pockmark SCI survey.

Burrowed mud and Offshore deep sea muds were represented throughout the whole survey area. Burrows were recorded in 100% of all video samples and 70% of all stills (Appendix 5). Seapens were observed in 69% of video samples, and *Maera loveni* was a constituent species (in low abundance) of the most widespread macrofaunal assemblage identified in Figure 38 (assemblage *g*). *Levinsenia gracilis* was represented in the most widespread macrofaunal assemblages identified in Figure 38 (assemblages *f* and *g*; Appendix 3). Conversely, *Paramphinume jeffreysii* and *Thyasira* spp. were members of assemblages that were only represented at a single sampling station (*d*, *b*, *a* and *e*; Figure 38 and Appendix 3).

4.2.9 Pockmark features

The features of interest at the Scanner Pockmark SCI are a number of crater-like depressions. A range of BPI20 and BPI50 outputs were used to identify likely pockmark signatures. The site has four large pockmarks within its boundary and one large pockmark to the north east outside of the SCI (Figure 41). These larger pockmarks include the Scotia, Challenger and Scanner pockmark complex.

The site is also scattered with smaller unit pockmarks. These unit pockmarks are circular depressions roughly <5m in diameter and have been a recognised feature since the 1980s (Hovland *et al* 2010). The unit pockmarks are abundant across the site and not only form in clusters around the more prominent pockmarks but also occur in linear strings, roughly 200m apart.

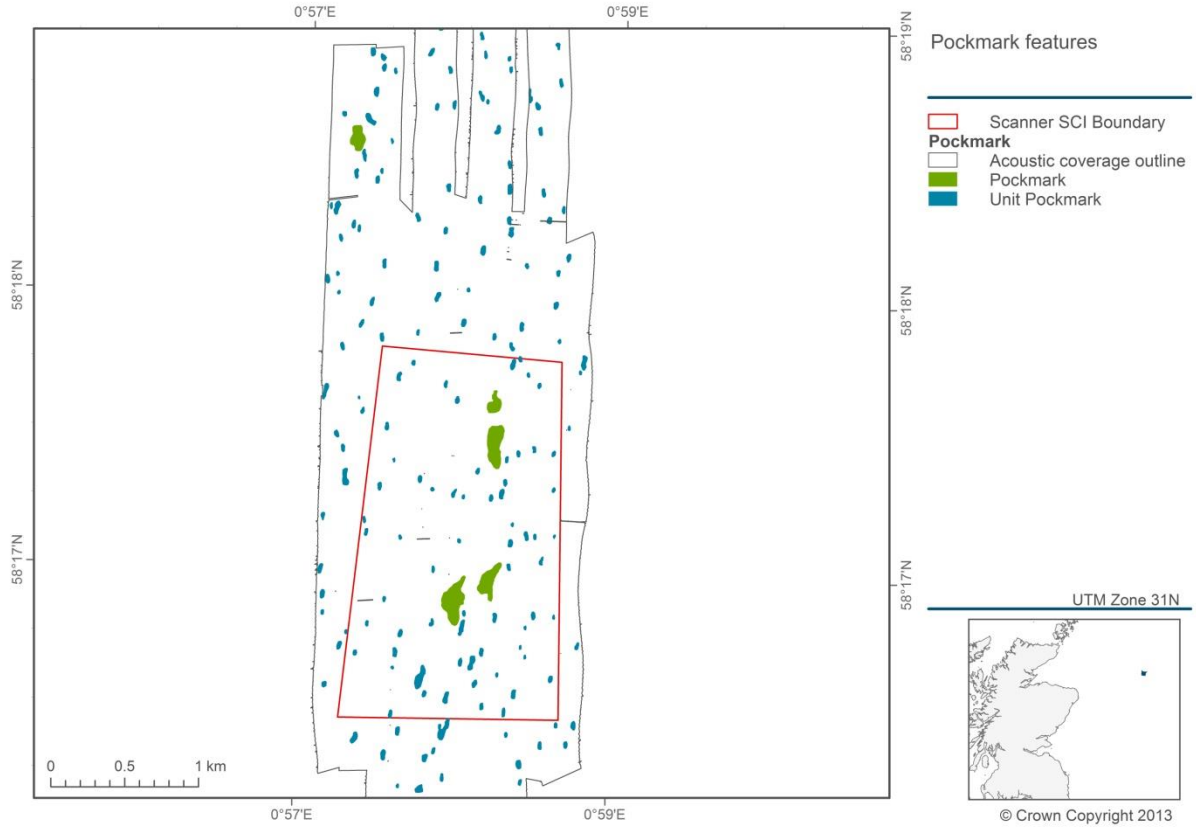

Figure 41. Pockmark and unit pockmark distribution map at the Scanner Pockmark SCI.

Profiles of the Scotia, Challenger and Scanner pockmark complexes within the Scanner Pockmark SCI have been created in Fledermaus v7 (Figure 42). Image 1 shows an example of a unit pockmark located to the south of the Scanner complex. The pockmark is 4m deep and approximately 40m in diameter. The Scanner complex itself is shown in Image 2 and illustrates the extent and depth of the pockmarks. With a diameter of approximately 100m and a depth of up to 14m, the pockmarks are considered extremely large.

The Scotia pockmark can be seen in Image 3 and consists of two depressions, up to 10m deeper than the surrounding seabed. The depressions are narrower than their neighbouring pockmarks with a diameter of up to 50m. Finally, the Challenger pockmark, positioned outside of the Scanner Pockmark SCI boundary, can be seen in Image 4. The singular pockmark is 12m deeper than its surroundings and extends to around 150m in diameter, making it the largest of the four main pockmarks in the area.

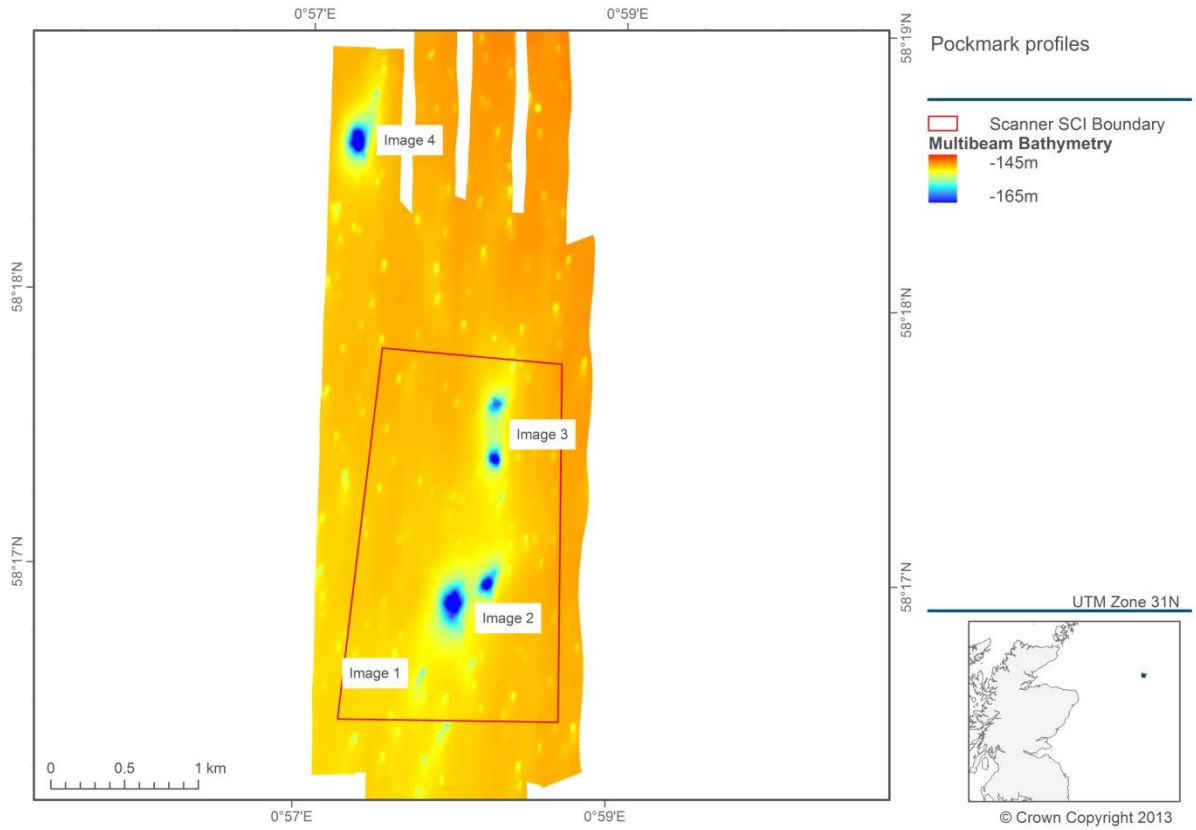

Figure 42. Illustration of profile sections of selected pockmark features within the Braemar Pockmarks SCI. Continues over following page.

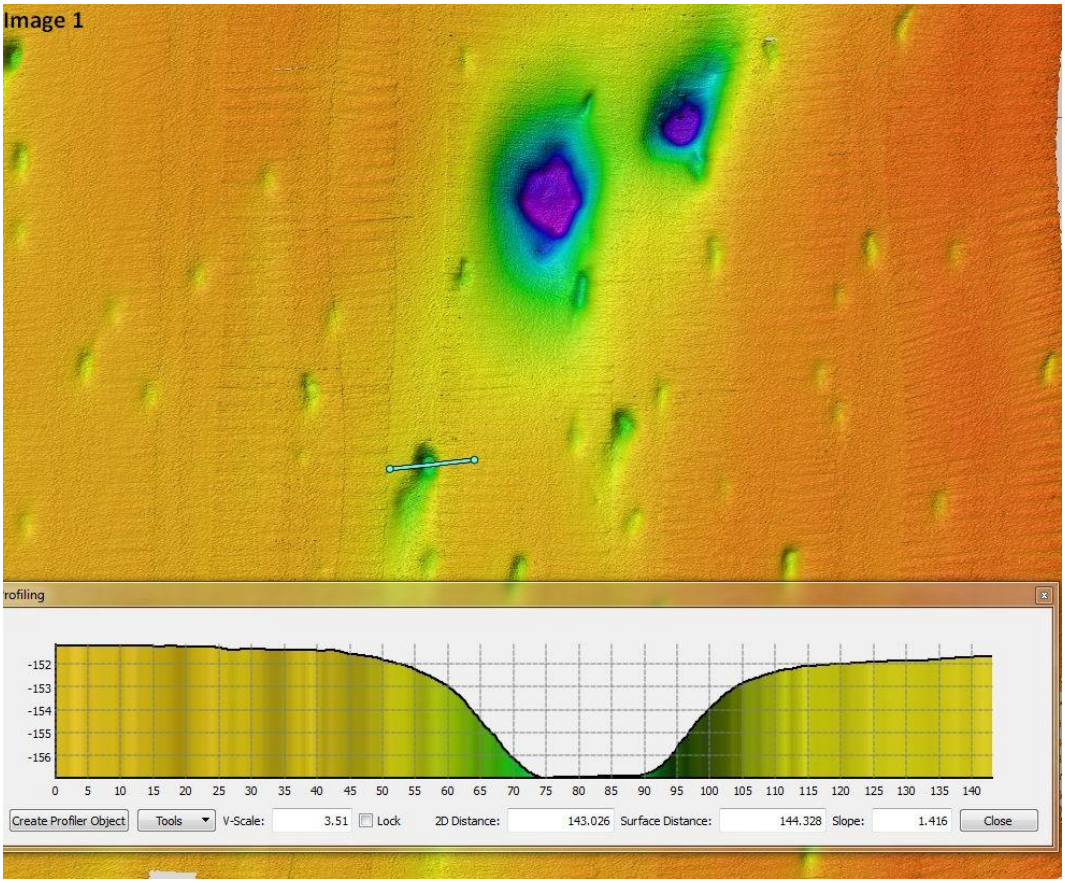

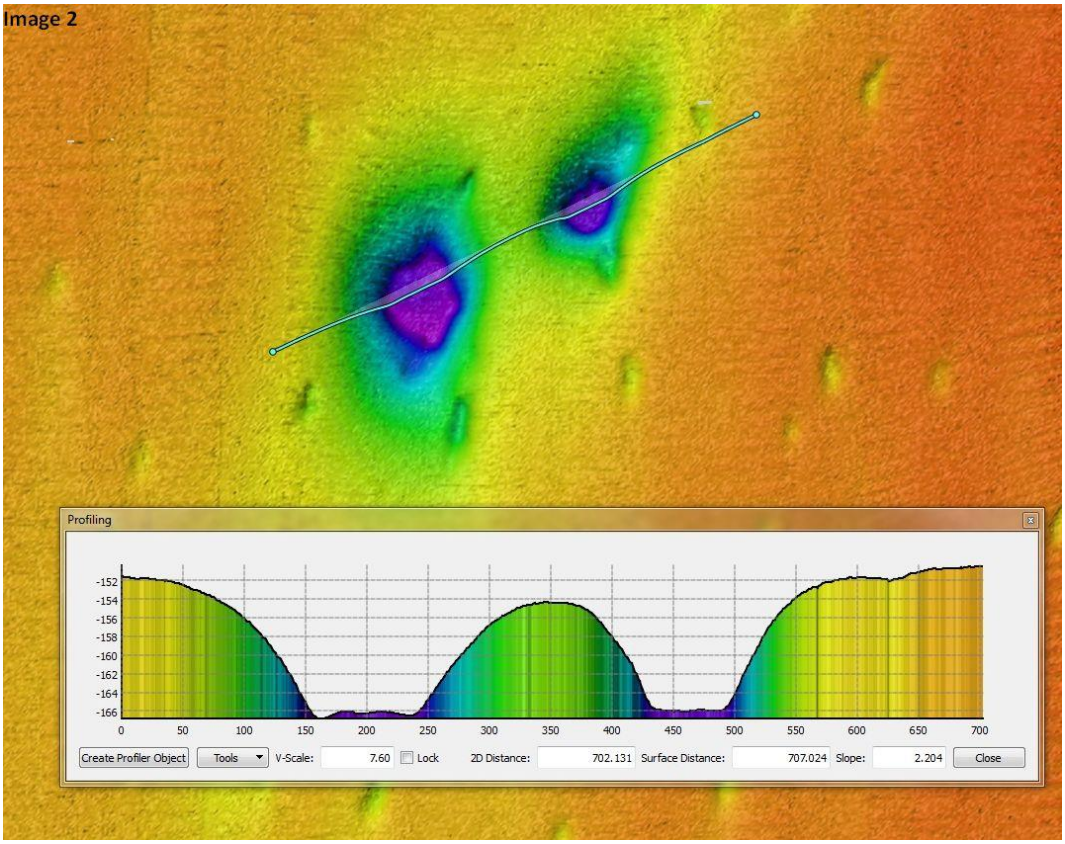

Figure 42 (continued). Illustration of profile sections of selected pockmark features within the Braemar Pockmarks SCI. Continues over following page.

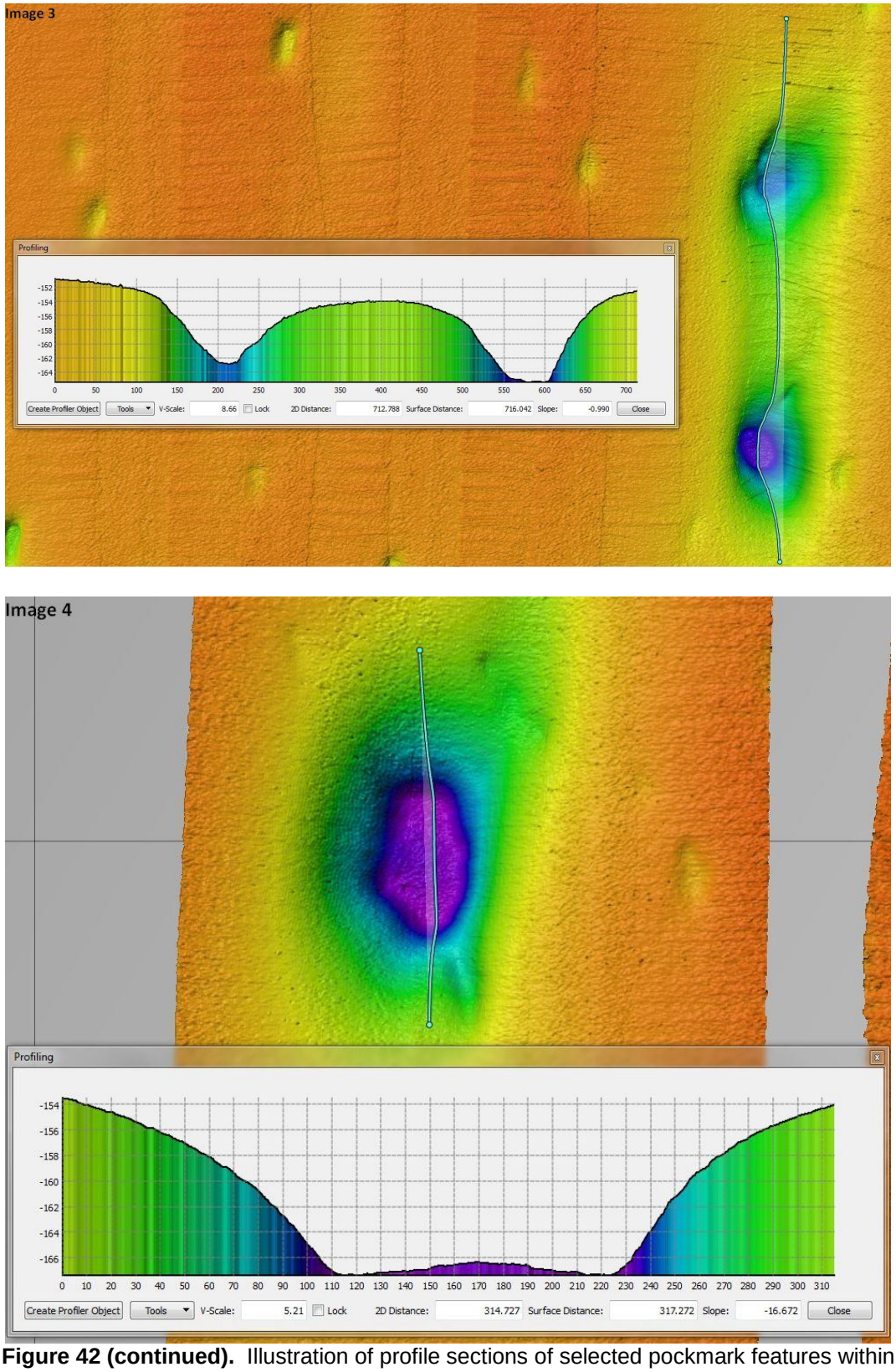

Figure 42 (continued). Illustration of profile sections of selected pockmark features within the Braemar Pockmarks SCI.

No definitive evidence was observed of the presence of possible MDAC within the sampled pockmark features. A single still image from Station 92 (SCDC06) on the edge of a pockmark feature revealed a small area of seabed which was slightly elevated from the surrounding area by a few centimetres (Figure 43). It is impossible to tell from the available evidence what might be the exact cause of this feature. Possible causes may be an exposed

ledge of harder substrate (although it shows signs of being burrowed), or a slump of a small area of seabed due to a collapse of a subsurface hollow, such as a network of burrows.

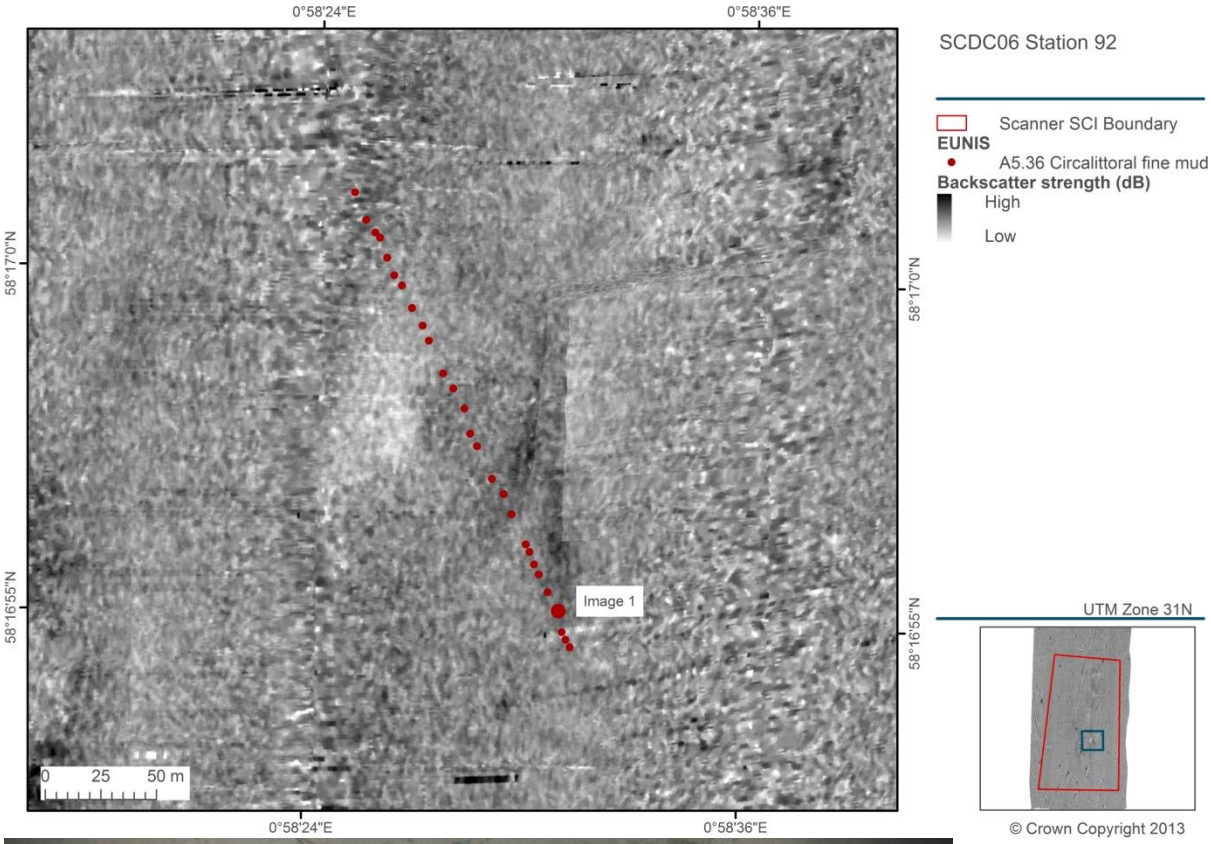

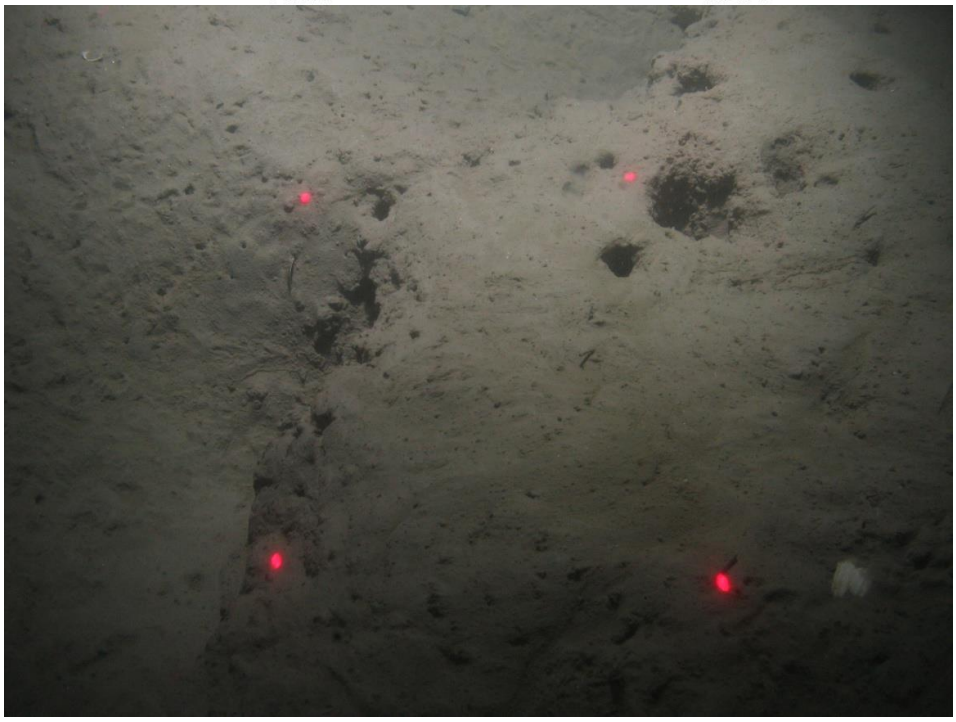

Image 1

Figure 43. Close-up detail of Station 92 within the Scanner Pockmark SCI. Still image shows an abrupt change in seabed elevation at the scale of a few centimetres.

4.2.10 Annex I habitats

Although pockmarks have been identified at the Scanner Pockmark SCI, evidence of MDAC within the pockmark craters has not been detected. Since it is the MDAC itself that constitutes the Annex I definition of 'Submarine structures made by leaking gases', it cannot be stated that Annex I habitat has been observed within the Scanner Pockmark SCI during this survey.

4.2.11 Anthropogenic impacts

The acoustic data shows evidence that bottom-contact fishing activities have occurred in the area. Several scars from trawls are present on the seafloor in and around the Scanner Pockmark SCI boundary, see Figure 45. The majority of the scars are orientated north to south.

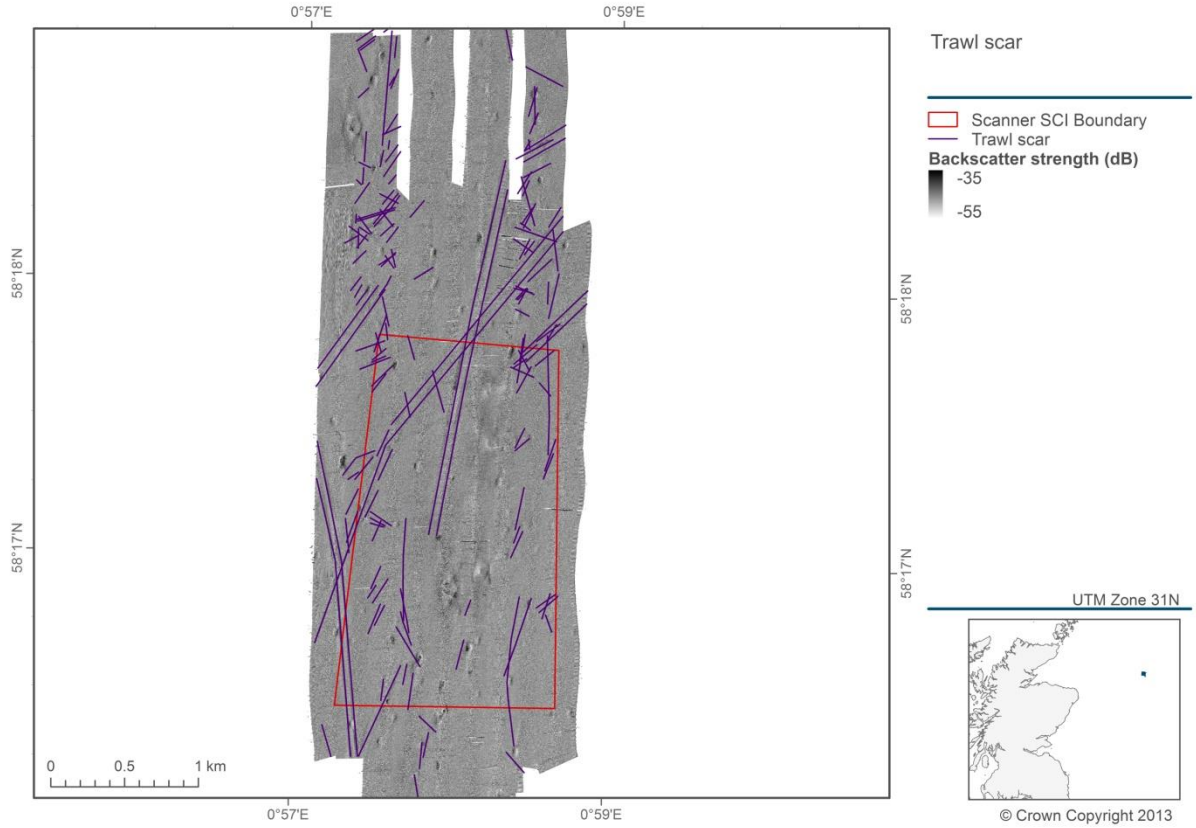

Figure 44. Interpretation of the sidescan sonar and multibeam backscatter data to identify trawl scars at Scanner Pockmark SCI.

Figure 45 displays a detailed view of an area within the Scanner Pockmark SCI boundary; bottom trawl scars can be seen clearly on the multibeam backscatter data.

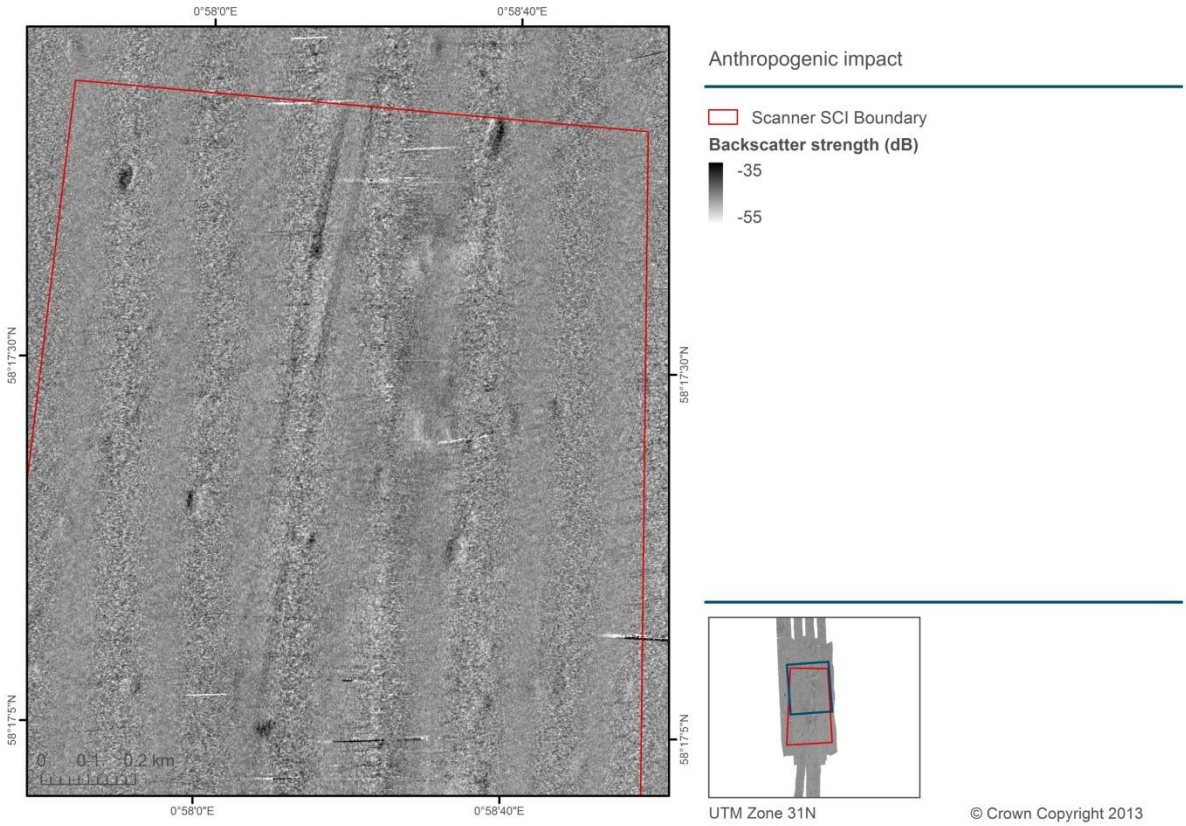

Figure 45. Display of multibeam backscatter data from the northern extent of the Scanner Pockmark SCI showing numerous trawl scars.

5 Conclusion

5.1 Summary of habitats and features of interest recorded

The presence and extent of the Annex I habitat 'Submarine structures made by leaking gases' has been assessed within the Braemar Pockmarks and Scanner Pockmark SCIs using a combination of acoustic and groundtruthing data (including underwater video, still and grab sample analysis) collected during a dedicated survey in November 2012. The surveys conducted at both SCIs confirmed the presence of pockmark features on the seabed within both sites. The pockmarks encountered show considerable variability with respect to their size, density and distribution.

5.1.1 Braemar Pockmarks SCI

The Braemar Pockmarks SCI contains a series of crater-like depressions and pockmarks within a relatively homogeneous area of seabed. The predominant biotope identified within the SCI itself is A5.36 Circalittoral Fine Mud, with the pockmarks themselves identified as A5.44 Circalittoral Mixed Sediment. The mixed sediment includes shell hash and possible MDAC fragments observed in the video tows and grab samples. Petrological and stable isotope analysis of these MDAC fragments confirmed their diagenetic origin, either by the authigenic precipitation of carbonate through methane oxidation or by its precipitation within the sulphide-reduction zone closely associated with bacterial metabolism. It is apparent that MDAC formation has occurred in the present geological age, as well as in periods of cooler sea temperatures, such as during the last ice age. None of the MDAC fragments acquired represented previously undisturbed, *in-situ* carbonate-cemented rocks.

Presence of the Annex I habitat 'Submarine structures made by leaking gases' within the site was verified through observations made using the video and still image data and the confirmed presence of MDAC in a number of the grab samples (following laboratory analysis). Sidescan sonar records provided evidence of gas bubbles in the water column, which appeared to be venting from one of the pockmarks. This may suggest that methane seeps within the Braemar Pockmark SCI are currently active, although this would need further confirmation through a dedicated water sampling/gas sampling regime. Similarly, observations from the video and stills data of 'presumed chemosynthetic' white bacterial mats on the seabed surface supports the hypothesis that methane seeps within this area are currently active. It is stressed though that further specific sampling of these bacterial mats would be beneficial to confirm their type.

5.1.2 Scanner Pockmark SCI

The Scanner Pockmark SCI has four large pockmark features and a high abundance of smaller unit pockmarks within its boundary. There is no obvious pattern to the formation or distribution of the unit pockmarks but their overall geometry indicates a predominance of a north to south orientation. No evidence of Annex I habitat 'Submarine structures made by leaking gases' was observed within this site. No observations of possible MDAC were made from the underwater video and still images and no MDAC fragments were found in the grab samples collected within this site. Similarly, no observations of bacterial mats were made from the video and still images acquired. However, the nematode species *Astomonema southwardarum* known to host endosymbiotic, chemoautotrophic bacteria within their body cavity were ubiquitous across the survey area. No fluid seepage was observed during the survey.

5.2 Data limitations

The overall quality of the acoustic data was considered to be very good. The multibeam bathymetry and backscatter data were cleaned and tidally corrected. The extent of the acoustic coverage was also satisfactory. Unfortunately, at the Braemar Pockmarks SCI, the presence of a well-head presented an obstruction to data collection, which led to a small gap in the data record within the SCI boundary. The quality of the sidescan sonar data was less favourable and, due to a combination of weather conditions during acquisition and water depth, the quality of the high-frequency sidescan sonar record was adversely affected. Numerous groundtruthing samples were collected at both SCIs, enabling a thorough analysis of the faunal assemblages to be made. However, weather conditions during a limited period of the survey did affect the quality of the video and stills data acquired at a sub-set of sampling stations. This, in turn, affected the ability to accurately assign seabed images to a given classifications and also affected the resolution of species identification in a limited number of instances.

5.3 Survey limitations

The surveys were designed and executed within the time allocated and enabled the collection of extensive acoustic and groundtruthing data of high quality.

Acknowledgements

We thank Dr Sue Ware and Koen Vanstaen (Cefas) for editing the text of the earlier drafts of this report. We acknowledge the valuable contributions made by all sub-contractors whose data and analyses have contributed to this report.

References

Addison, P. (2010). Quality Assurance in Marine Biological Monitoring. Environment Agency/Joint Nature Conservation Committee, 8pp. http://www.nmbaqcs.org/qa-standards/qa-in-marine-biological-monitoring.aspx

Astrium. (2011). Creation of a high resolution Digital Elevation Model (DEM) of the British Isles continental shelf: Final Report. Prepared for Defra, Contract Reference: 13820, 26pp.
Austen, M.C., Warwick, R.M. & Ryan, K.P. (1993). *Astomonema southwardorum* sp. nov., a gutless nematode dominant in a methane seep area in the North Sea. *Journal of the Marine Biological Association, UK*, **73**: 627-634.

Blaschke, T. (2010). Object based image analysis for remote sensing. *ISPRS International Journal of Photogrammetry and Remote Sensing*, **65**(1): 2-16.

Boetius, A., Ravensclag, K., Shubert, C.J., Rickert, D., Widdel, F., Glieseke, A., Amann, R., Jørgensen, B.B., Witte, U. & Pfannkuche, O. (2000). A marine microbial consortium apparently mediating anaerobic methane oxidation. *Nature*, **407**: 623-626.

Boulton, G.S., Peacock, J.D. & Sutherland, D.G. (2002). Quaternary. Iin Trewin NH (Ed.). *The Geology of Scotland*, Geological Society London, pp. 407-430.

Cefas and JNCC (2013). Braemar cSAC, Scanner cSAC and Turbot Bank SMPA Search Location Cruise Report. JNCC 132pp.

Clarke, K.R. & Gorley, R.N. (2006). PRIMER v6: User Manual/Tutorial. PRIMER-E, Plymouth.

Coggan, R. & Howell, K. (2005). Draft SOP for the collection and analysis of video and still images for groundtruthing an acoustic basemap. Video survey SOP version 5. 10pp.

Coggan, R., Mitchell, A., White, J. & Golding, N. (2007) (not published). Recommended operating guidelines (ROG) for underwater video and photographic imaging techniques. www.searchmesh.net/pdf/GMHM3_Video_ROG.pdf.

Dando, P.R. (2001). A review of pockmarks in the UK part of the North Sea, with particular respect to their biology. Technical report produced for Strategic Environmental Assessment – SEA2. UK: Department of Trade and Industry.

Dando, P.R., Austen, M.C., Burke Jnr, R.J., Kendall, M.A., Kennicutt II, M.C., Judd, A.G., Moore, D.C., O'Hara, S.C.M., Schmaljohann, R. & Southward, A.J. (1991). Ecology of a North Sea pockmark with an active methane seep. *Marine Ecology Progress Series*, **70**, 49-63.

Hartley, J.P. (2005). Seabed Investigations of Pockmark Features in UKCS Block 16/3. Report to Joint Nature Conservation Committee. Hartley Anderson Limited, Aberdeen.
Hill, M.O. (1973). Diversity and evenness: a unifying notation and its consequences. *Ecology*, **54**, 427-432.

Hovland, M. (1989). The formation of pockmarks and their potential influence on offshore formation. *Quarterly Journal of Engineering Geology*, **22**: 131-138.

Hovland, M., Heggland, R., De Vries, M.H. & Tjelta, T.I. (2010). Unit pockmarks and their potential significance for predicting fluid flow. *Marine and Petroleum Geology*, **27**: 1190-1199.

Hovland, M. & Judd, A.G. (1988). Seabed pockmarks and seepages: impact on geology, biology and the marine environment. Graham and Trotman, London.

Hovland, M., Svensen, H., Forsberg, C.F., Johansen, C.F., Fossa, J.G., Jonsson, R. & Rueslatten, H. (2005). Complex pockmarks with carbonate ridges off mid Norwat: Products of sediment degassing. *Marine Geology*, **218**: 191-206.

ICES. (2004). Biological Monitoring: General Guidelines for Quality Assurance. In Rees. H. (ed.) ICES Techniques in Marine Environmental Sciences, No. 32. 44pp. http://www.marbef.org/qa/documents/PKG85.pdf

JNCC. (2008). Offshore Special Area of Conservation: Scanner Pockmark. SAC Selection Assessment, Version 4.0 (1st July 2008). JNCC 12pp. http://jncc.defra.gov.uk/PDF/ScannerPockmark_SelectionAssessment_4.0.pdf

JNCC. (2011a). Braemar Pockmarks Natura 2000 Data Form. Produced by JNCC 27/07/11, 3pp.

JNCC. (2011b). Scanner Pockmark Natura 2000 Data Form. Produced by JNCC 27/07/11, 3pp.

JNCC. (2012a). Offshore Special Area of Conservation: Braemar Pockmarks. SAC Selection Assessment, Version 4.1 (9th January 2012), 15pp. http://jncc.defra.gov.uk/PDF/BraemarPockmarks_SelectionAssessment_4.1.pdf.

JNCC. (2012b). Offshore Special Area of Conservation: Braemar Pockmarks. Conservation Objectives and Advice on Operations, Version 4.0 (March 2012), 24pp. http://jncc.defra.gov.uk/PDF/BraemarPockmarks_ConservationObjectives_AdviceonOperations_4.0.pdf.

JNCC. (2012c). Offshore Special Area of Conservation: Scanner Pockmark. Conservation Objectives and Advice on Operations, Version 4.0 (March 2012), 24pp. http://jncc.defra.gov.uk/PDF/ScannerPockmarks_ConservationObjectives_AdviceonOperations_4.0.pdf.

Judd, A., Long, D. & Sankey, M. (1994). Pockmark formation and activity, UK block 15/25, North Sea. *Bulletin of the Geological Society of Denmark*, **41**: 34-49.

Judd, A.G. (2001). Pockmarks in the UK Sector of the North Sea. Technical report (TR_002) produced for Strategic Environmental Assessment - SEA2. Department of Trade and Industry, UK.

Judd, A.G. & Hovland, M. (2007). Seabed fluid flow: the impact on geology, biology and the marine environment. Cambridge University Press, Cambridge.

Long, D. (1986). Seabed Sediments: Fladen Sheet 58°N-00°, British Geological Survey 1:250,000 Series.

Long, D. (2006). BGS detailed explanation of seabed sediment modified folk classification. MESH.

http://www.searchmesh.net/PDF/BGS%20detailed%20explanation%20of%20seabed%20sediment%20modified%20folk%20classification.pdf.

Mason, C. (2011). Particle Size Analysis (PSA) for Supporting Biological Analysis. NMBAQC's Best Practice Guidance, 72pp.

Milodowski, A.E. & Sloane, H. 2013. Petrography and stable isotope study of methane-derived authigenic carbonates (MDAC) from the Braemar Pockmark Area, North Sea. British Geological Survey Commissioned Report, CR/13/078, 111pp.

Physalia. (2013). Taxonomic Analysis of Meiofaunal Nematode Samples Collected From Marine Methane Seeps - Scanner and Braemar Pockmarks cSAC/SCI Sites. A factual report prepared for CEFAS by Physalia Ltd, Consultant & Forensic Ecologists, Harpenden.

Stoker, M.S. (1981). Pockmark morphology: a preliminary description. Evidence for slumping and doming. Report no. 77/12 of the Institute of Geological Sciences, UK.

Stoker, M.S. & Bent, A.J.A. (1987). Lower Pleistocene deltaic and marine sediments in boreholes from the central North Sea. *Journal of Quaternary Science*, **2**(2): 87-96

Stoker, M.S., Long, D. & Fyfe, J.A. (1985). The Quaternary succession in the central North Sea. *Newsletters on Stratigraphy*, **14**: 119-128.

Tchesunov, A.V., Ingels, J. & Popova, E.V. (2012). Marine free-living nematodes associated with symbiotic bacteria in deep-sea canyons of north-east Atlantic Ocean. *Journal of the Marine Biological Associaltion of the UK*. FirstView: 15 pp.

Trewin, N.H. (Ed.) (2002). *The Geology of Scotland*. Geological Society London, 576pp.

Worsfold, T.M., Hall, D.J. & O'Reilly, M. (2010). Guidelines for processing marine macrobenthic invertebrate samples: a processing requirements protocol version 1 (June 2010). Unicomarine Report NMBAQCMbPRP to the NMBAQC Committee, 33pp.

Annexes

Annex 1. Geological context

The Scanner pockmark complex lies within the Witch Ground Graben, a major structural feature that formed between Triassic and early Cretaceous times. The graben was a depositional site during the late Jurassic and early Cretaceous and was subsequently infilled by a thick sequence of Tertiary and Quaternary sediments (Andrews *et al* 1990, quoted by Judd *et al* 1994). An exploration well analysed by Judd *et al* (1994) revealed the presence of a thin sequence of Mesozoic sediments lying unconformably on the Lower Carboniferous strata and the presence of about 2000m Tertiary succession dominated by clays, but also sandstone and limestone beds. The Quaternary sequence comprises about 350-400m of sediments belonging to the Aberdeen Ground Formation, Coal Pit Formation, Witch Ground Formation and Swatchway Formation (Judd *et al* 1994). The Aberdeen Ground Formation comprises muds and sands of deltaic environments (Stoker & Bent 1987). The irregular erosion surfaces at the top of the Aberdeen Formation are associated with the presence of furrows similar to those created by iceberg keels drifting into shallow waters over the seabed sediments (Boulton *et al*, in Trewin 2002, p. 418). The Coal Pit Formation comprises dark-grey to brownish-grey, muddy, pebbly sands and sandy muds deposited during a Pleistocene glacial-interglacial-glacial cycle (Stoker *et al* 1985, quoted by Judd *et al* 1994). The Swatchway Formation comprises silty sandy clays with rare pebbles (Stoker *et al* 1985) and is interpreted as a reworked glaciomarine deposit (Andrews *et al* 1990). The Witch Ground Formation comprises very soft to soft clays and silts with sandy horizons and rare pebbles, and has been interpreted as a Pleistocene-Holocene glaciomarine deposit (Stoker *et al* 1985). The irregular base of the Witch Ground Formation is interpreted to be a transition within the environmental history of the area between a landscape heavily shaped by glacial depositional and erosional processes since the last glacial maximum about 18,000 years ago dominated by the mechanical action of sea-ice cover, iceberg as well as temperatures, and a landscape less shaped by glacial processes due to rising temperatures and sea level and more characterised by rapid sedimentation beneath the sea-ice cover.

From the last glacial maximum approximately 18,000 years ago to 15,000 years ago, the area has been heavily shaped by glacial depositional and erosional processes associated to the low temperatures and to the mechanical action of sea-ice cover and icebergs (Judd *et al* 1994). Approximately 15,000 years ago, as the temperatures began to rise, the sea level rose, the sea ice cover became thinner and the seabed was no longer disturbed by the iceberg keels. This transition between geomorphic processes is represented by the irregular base of the Witch Ground Formation, characterised by the last sea ice plough marks (Judd *et al* 1994). Up to 13,000 years ago, a rapid sedimentation beneath the sea ice cover led to the formation of the well-layered Fladen Formation. Judd *et al* (1995) suggested that 13,000 years ago a rapid increase in seawater temperature occurred due to the northwards migration of the polar front and the entering of warmer North Atlantic waters. British Geological Survey (BGS) geophysical data show that the formation of the Scanner pockmark occurred most probably at this time when large quantities of gas escaped to the seabed and the eruption displaced the Fladen Member sediments. After 13,000 years ago, marine sedimentation continued with the short-term return of ice between 11,000-10,000 years ago (Judd *et al* 1994). The analysis of sediments within the Witch Ground Basin suggests that since the early Holocene (8,000 BP) sedimentation has been almost non-existent. Today, sedimentation is restricted to the re-working of the Witch Member in the formation of the Glenn Member during pockmark formation (Judd *et al* 1994). As anticipated earlier, gas escape during pockmark formation sorts the near-surface sediment leading to the formation of a very thin layer of very well-sorted silt.

Pockmark features in the Witch Ground Basin (northern North Sea) are approximately circular to ellipsoidal with a length-width ratio of 1-1.25 or more and the longer axes aligned with the dominant tidal current direction. Their perimeters are not regular but complicated by indentations and lobes, and the pockmark floor is undulating. The smaller pockmark features at Scanner exhibit a tail whose orientation is south or slightly southeast and southwest. These asymmetrical pockmarks are more common than circular shaped pockmarks in the Witch Ground Basin and the orientation of their asymmetry varies considerably within the basin (Stoker 1981; Judd & Hovland 2007).

The pockmark features are believed to be formed by the expulsion of fluids through seabed sediments (Hovland 1989; Dando 2001). The escaping fluid is gas in the majority of cases, but may also be groundwater (Judd 2001). The gas may be microbial or thermogenic. In the first case, the gas forms because of microbial decomposition of organic matter within the near-seabed sediments (Judd 2001). In the second case, the gas originates from the thermocatalytic destruction of kerogens deep within the sediments. The gas is typically composed principally by methane (>95%) and, if thermogenic, ethane, butane, propane and pentane may also be present (Judd 2001).

Inactive pockmarks show no signs of gas seepage (Dando 2001). However, the gas seepage observed in active pockmarks is generally a gentle bubbling and is insufficient to erode the seabed sediments (Judd 2001) and justify the presence of the crater shape. A conceptual model has been suggested by Hovland and Judd (1988) for the formation of pockmarks. During the first stage, the gas accumulates beneath the seabed and the fluid pressure may inflate the sediments to form a dome. In a second stage, the gas is released in a single event that fluidises the sediment in the water column: fine-grained sediments drift away with the currents, while coarse sediment falls back to the pockmark floor that is often found to be covered by a lag deposit of coarse sediment and shell hash (Judd 2001). The event that triggers the gas expulsion may be an earthquake or any disturbance of the seabed, e.g. iceberg ploughing (Judd 2001). If the gas continues to migrate from deeper sediments, gas seepage may continue or the gas may be periodically trapped within a sequence of inter-bedded fine and coarse sediment layers so that gas escape becomes intermittent and gives rise to polycyclic pockmarks (Judd 2001).

There is not a scientific consensus on the origin of the gas in the Witch Ground Basin; it could equally be that it originates from a shallow biogenic source, a deep thermogenic source, or from both. However, based on the review of isotopic analyses found in literature, Stoker and Holmes (2005) concluded that, the gas is predominantly of biological origin. Judd *et al* (1994) suggested that the Tertiary lignites are the most likely source of the gas; they also suggested that gas generation started earlier than the deposition of the Quaternary sediments in which it is accumulated and that is still forming, providing a continuous supply. In the largest pockmark, the gas seepages are fed from a laterally almost continuous deposit of gas-charged sediments situated between the margins of a buried sub-glacial channel approximately 120m below seabed (Stoker & Holmes 2005).

Methane-derived authigenic carbonate (MDAC) is a deposit of carbonate formed through a process of precipitation during the oxygenation of seeping methane gas. MDAC concretions may occur as crusts, slabs or lumps. The carbonate is a high-magnesian calcite, aragonite or dolomite. Carbon isotope studies demonstrated that the source of carbon is methane, rather than sea water or sediment porewater. The carbonate precipitation is mediated by a microbial association of archaea and sulphate reducing bacteria (Boetius *et al* 2000, quoted by Judd 2001). The presence of MDAC is indicative of methane seepage, but not necessarily of an active seepage unless there are other evidences like bacterial mats or gas bubbles. The rate of MDAC formation is unknown; however, the presence of crusts over certain anthropogenic material indicates that the formation has occurred on a human timescale (Judd (2001), data collected by the offshore energy industry).

Annex 2. List of EC Habitats Directive Annex I habitats

Atlantic salt meadows

Estuaries

Lagoons

Large shallow inlets and bays

Mediterranean and thermo-Atlantic halophilious scrubs

Mudflats and sandflats not covered by seawater at low tide

Reefs

Salicornia and other annuals colonising mud and sand

Sandbanks which are slightly covered by seawater all the time

Spartina swards

Submerged or partially submerged caves

Submarine structures made by leaking gases

Annex 3. List of SMPA seabed habitat search features/priority marine features in Scottish offshore waters

MPA search feature	Component habitats/species
Burrowed mud	Seapens and burrowing megafauna in circalittoral fine mud
	Burrowing megafauna and *Maxmuelleria lankesteri* in circalittoral mud
	Tall seapen *Funiculina quadrangularis*
	Fireworks anemone *Pachycerianthus multiplicatus*
	Mud burrowing amphipod *Maera loveni*
Carbonate mound communities	Carbonate mound communities
Cold-water coral reefs	Coral reefs
Coral gardens	Coral gardens
Deep sea sponge aggregations	Deep sea sponge aggregations
Northern sea fan and sponge communities	Northern sea fan *Swiftia pallida*
Offshore deep sea muds	*Ampharete falcata* turf with *Parvicardium ovale* on cohesive muddy sediment near margins of deep stratified seas
	Formaniferans and *Thyasira* sp. in deep circalittoral fine mud
	Levinsenia gracilis and *Heteromastus filiformis* in offshore circalittoral mud and sandy mud
	Paramphinome jeffreysii, *Thyasira* spp. and *Amphiura filiformis* in offshore circalittoral sandy mud
	Myrtea spinifera and polychaetes in offshore circalittoral sandy mud
Offshore subtidal sands and gravels	*Glycera lapidum*, *Thyasira* spp. and *Amythasides macroglossus* in offshore gravelly sand
	Hesionura elongata and *Protodorvillea kefersteini* in offshore coarse sand
	Echinocyamus pusillus, *Ophelia borealis* and *Abra prismatica* in circalittoral fine sand
	Abra prismatica, Bathyproeia elegans and polychaetes in circalittoral fine sand
	Maldanid polychaetes and *Eudorellopsis deformis* in offshore circalittoral sand or muddy sand
	Owenia fusiformis and *Amphiura filiformis* in offshore circalittoral sand or muddy sand
Seamount communities	Seamount communities
Submarine structures made by leaking gases	Submarine structures made by leaking gases

Annex 4. List of low or limited mobility species in Scottish offshore waters

MPA search feature	Species name	Taxon group
Northern feather star aggregations on mixed substrata	*Leptometra celtica*	Starfish and feather stars
Fan mussel aggregations	*Atrina pectinata*	Snails, clams, mussels and oysters
Ocean quahog aggregations	*Arctica islandica*	Snails, clams, mussels and oysters

Annex 5. Modified Folk trigon (Long 2006)

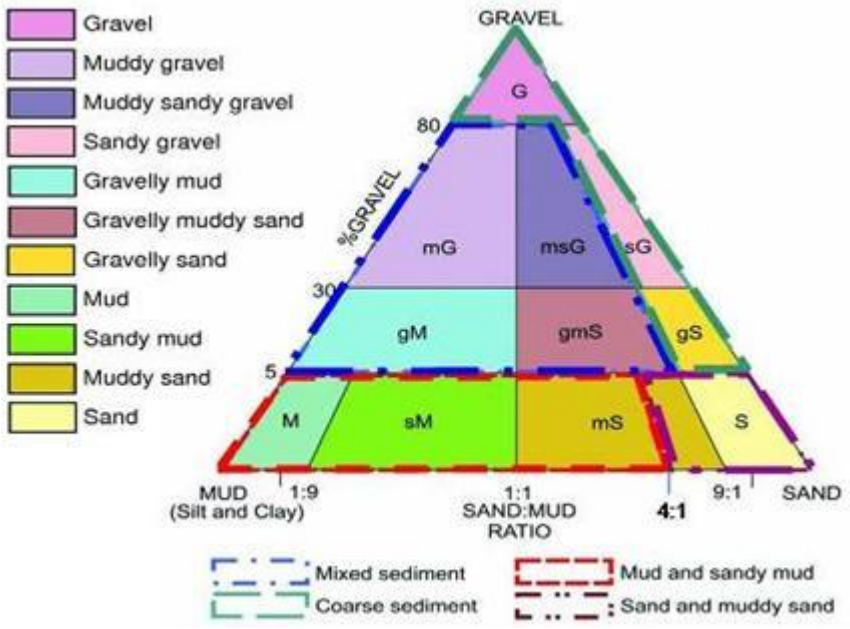

Appendices

Appendix 1. Macrofaunal assemblage metrics calculated for each grab sample at both Braemar Pockmarks and Scanner Pockmark SCI

Sample	Gear	Stn Code	Stn No	Replicate	SCI	S	N	N1	B (g)
HG11 23B	HC	HG11	23	B	Braemar	38	113	22.8	1.581
HG11 23A	HC	HG11	23	A	Braemar	54	209	27.3	5.231
BRMR_01 24A	DG	BRMR_01	24	A	Braemar	54	226	33.6	112.318
BRMR_02 25A	DG	BRMR_02	25	A	Braemar	57	280	25.7	52.385
BRMR_05 26A	DG	BRMR_05	26	A	Braemar	53	265	27.1	**284.738**
BRMR_04 27A	DG	BRMR_04	27	A	Braemar	58	213	29.9	184.135
BRMR_03 28A	DG	BRMR_03	28	A	Braemar	44	136	33.4	16.807
HG10 29B	HC	HG10	29	B	Braemar	43	116	29.7	1.660
HG10 29A	HC	HG10	29	A	Braemar	50	182	32.6	1.845
HG09 30B	HC	HG09	30	B	Braemar	35	96	20.8	0.468
HG09 30A	HC	HG09	30	A	Braemar	52	164	26.3	6.989
HG06 31A	HC	HG06	31	A	Braemar	20	56	12.4	2.559
HG06 31C	HC	HG06	31	C	Braemar	**72**	**422**	31.0	5.390
HG06 31B	HC	HG06	31	B	Braemar	64	269	33.6	11.787
BRMR_07 32A	DG	BRMR_07	32	A	Braemar	40	124	24.1	48.644
BRMR_06 33A	DG	BRMR_06	33	A	Braemar	47	168	24.5	56.109
BRMR_08 34A	DG	BRMR_08	34	A	Braemar	60	267	33.2	22.961
BRMR_10 35A	DG	BRMR_10	35	A	Braemar	59	251	35.1	109.578
HG12 36C	HC	HG12	36	C	Braemar	35	89	26.2	85.030
HG12 36A	HC	HG12	36	A	Braemar	44	147	30.7	92.708
HG12 36B	HC	HG12	36	B	Braemar	46	118	33.7	56.159
HG08 37C	HC	HG08	37	C	Braemar	46	180	15.8	2.544
HG08 37B	HC	HG08	37	B	Braemar	42	140	20.2	3.583
HG08 37A	HC	HG08	37	A	Braemar	44	167	28.6	1.183
BRMR_13 38A	DG	BRMR_13	38	A	Braemar	55	239	32.4	80.574
BRMR_12 39A	DG	BRMR_12	39	A	Braemar	52	176	34.1	55.890
BRMR_17 40A	DG	BRMR_17	40	A	Braemar	58	247	35.1	92.350
BRMR_16 41A	DG	BRMR_16	41	A	Braemar	66	303	35.3	34.019
HG03 42C	HC	HG03	42	C	Braemar	**14**	**22**	**11.9**	**0.404**
HG03 42B	HC	HG03	42	B	Braemar	32	80	19.6	3.700
HG03 42A	HC	HG03	42	A	Braemar	38	123	22.2	7.279
BRMR_18 43A	DG	BRMR_18	43	A	Braemar	56	250	31.3	33.549
BRMR_19 44A	DG	BRMR_19	44	A	Braemar	58	209	28.1	25.256
BRMR_22 45A	DG	BRMR_22	45	A	Braemar	49	133	35.2	2.283
HG02 46B	HC	HG02	46	B	Braemar	34	81	22.1	1.790
HG02 46A	HC	HG02	46	A	Braemar	53	271	25.4	5.446
HG02 46C	HC	HG02	46	C	Braemar	49	177	31.6	2.223
BRMR_21 47A	DG	BRMR_21	47	A	Braemar	66	209	**41.0**	21.383
BRMR_23 48A	DG	BRMR_23	48	A	Braemar	57	226	35.5	24.303
BRMR_24 49A	DG	BRMR_24	49	A	Braemar	53	157	33.9	1.591
SCNR_39 54B	DG	SCNR_39	54	B	Scanner	30	154	14.0	1.701
SCNR_39 54A	DG	SCNR_39	54	A	Scanner	26	83	17.0	1.812
SCNR_39 54C	DG	SCNR_39	54	C	Scanner	29	67	22.7	1.846

Sample	Gear	Stn Code	Stn No	Replicate	SCI	S	N	N1	B (g)
SCNR_34 55A	DG	SCNR_34	55	A	Scanner	25	121	11.4	1.509
SCNR_29 56B	DG	SCNR_29	56	B	Scanner	20	76	12.0	0.632
SCNR_29 56A	DG	SCNR_29	56	A	Scanner	31	121	20.0	3.063
SCNR_29 56C	DG	SCNR_29	56	C	Scanner	32	152	17.4	4.921
SCNR_26 57A	DG	SCNR_26	57	A	Scanner	20	60	12.5	0.438
SCNR_28 58A	DG	SCNR_28	58	A	Scanner	29	87	20.7	0.991
SCNR_25 59A	DG	SCNR_25	59	A	Scanner	27	94	16.9	1.323
SCNR_27 60B	DG	SCNR_27	60	B	Scanner	27	81	15.8	0.770
SCNR_27 60C	DG	SCNR_27	60	C	Scanner	26	105	14.8	1.498
SCNR_27 60A	DG	SCNR_27	60	A	Scanner	28	124	11.4	5.898
SCNR_3 61A	DG	SCNR_3	61	A	Scanner	27	89	17.6	1.663
SCNR_6 62A	DG	SCNR_6	62	A	Scanner	36	99	24.9	15.818
SCNR_2 63A	DG	SCNR_2	63	A	Scanner	32	97	18.0	7.151
SCNR_5 64A	DG	SCNR_5	64	A	Scanner	21	90	9.5	1.173
SCNR_5 64B	DG	SCNR_5	64	B	Scanner	29	110	16.6	3.844
SCNR_5 64C	DG	SCNR_5	64	C	Scanner	23	76	14.6	25.082
SCNR_1 65A	DG	SCNR_1	65	A	Scanner	36	151	15.1	1.013
SCNR_4 66A	DG	SCNR_4	66	A	Scanner	30	115	15.8	1.952
SCNR43 67A	DG	SCNR43	67	A	Scanner	24	57	17.5	12.427
SCNR42 68A	DG	SCNR42	68	A	Scanner	17	47	10.7	1.681
SCNR10 69B	DG	SCNR10	69	B	Scanner	25	90	11.2	1.184
SCNR10 69A	DG	SCNR10	69	A	Scanner	19	49	15.1	1.261
SCNR10 69C	DG	SCNR10	69	C	Scanner	18	59	8.8	5.085
SCNR7 70A	DG	SCNR7	70	A	Scanner	26	94	15.6	0.896
SCNR11 71A	DG	SCNR11	71	A	Scanner	18	81	8.9	0.799
SCNR8 72A	DG	SCNR8	72	A	Scanner	30	81	18.8	2.668
SCNR12 73C	DG	SCNR12	73	C	Scanner	22	102	9.9	1.014
SCNR12 73B	DG	SCNR12	73	B	Scanner	20	94	13.0	1.089
SCNR12 73A	DG	SCNR12	73	A	Scanner	20	106	10.7	3.282
SCNR9 74A	DG	SCNR9	74	A	Scanner	37	138	21.2	3.040
SCNR15 75A	DG	SCNR15	75	A	Scanner	26	86	17.2	17.083
SCNR18 76A	DG	SCNR18	76	A	Scanner	23	64	12.9	0.947
SCNR14 77A	DG	SCNR14	77	A	Scanner	26	119	12.6	1.740
SCNR17 78B	DG	SCNR17	78	B	Scanner	17	53	9.2	0.496
SCNR17 78A	DG	SCNR17	78	A	Scanner	20	65	12.1	1.565
SCNR17 78C	DG	SCNR17	78	C	Scanner	20	62	10.6	4.128
SCNR13 79A	DG	SCNR13	79	A	Scanner	26	59	18.3	1.464
SCNR16 80A	DG	SCNR16	80	A	Scanner	22	65	14.3	0.485
SCNR45 81A	DG	SCNR45	81	A	Scanner	18	51	14.6	1.685
SCNR44 82A	DG	SCNR44	82	A	Scanner	20	72	13.6	0.484
SCNR22 83C	DG	SCNR22	83	C	Scanner	26	100	13.5	0.444
SCNR22 83B	DG	SCNR22	83	B	Scanner	26	86	12.5	2.255
SCNR22 83A	DG	SCNR22	83	A	Scanner	19	51	13.5	2.289
SCNR19 84A	DG	SCNR19	84	A	Scanner	23	71	14.4	0.528
SCNR23 85A	DG	SCNR23	85	A	Scanner	19	50	11.5	0.890
SCNR20 86A	DG	SCNR20	86	A	Scanner	24	98	14.9	1.151
SCNR24 87A	DG	SCNR24	87	A	Scanner	20	72	11.8	1.118
SCNR21 88A	DG	SCNR21	88	A	Scanner	29	77	20.7	1.430

Sample	Gear	Stn Code	Stn No	Replicate	SCI	S	N	N1	B (g)
SCRNPM2 10B	DG	SCRNPM2	107	B	Scanner	24	185	7.0	1.137
SCRNPM1 10A	DG	SCRNPM1	107	A	Scanner	21	96	8.1	8.802
SCRNPM3 10C	DG	SCRNPM3	107	C	Scanner	21	110	11.2	15.570
SCRNM2 10B	DG	SCRNM2	108	B	Scanner	18	258	6.1	2.084
SCRNM2 10A	DG	SCRNM2	108	A	Scanner	18	188	**5.4**	2.146
SCRNM2 10C	DG	SCRNM2	108	C	Scanner	25	**292**	7.9	4.237
SCRNPM3 10A	DG	SCRNPM3	109	A	Scanner	21	222	5.6	7.721
SCRNPM3 10B	DG	SCRNPM3	109	B	Scanner	24	220	8.8	22.137

DG = Day Grab; HC = HamCam; S = number of taxa; N = abundance; N1 = diversity; B = wet-weight biomass. Lowest and highest values for each calculated variable within each SCI are given in blue and red, respectively.

Appendix 2. Table of taxa characterising each distinct macrofaunal assemblage identified at Braemar Pockmarks SCI

	Assemblage					
Taxa	**a**	**b**	**c**	**d**	**e**	**f**
Paramphinome jeffreysii	1.4	4.1	2.8	4.5	5.3	2.1
Galathowenia oculata	2.0	2.8	1.4	2.6	3.3	2.9
Amphiuridae	2.0	2.5	1.8	2.9	2.4	1.3
Spiophanes kroyeri	1.0	1.6	2.3	2.3	3.0	1.3
Nematoda	2.0	5.2	1.4	1.8	1.5	0.5
Terebellides stroemii	1.0	2.1	2.3	1.1	2.8	2.1
Lagis koreni	1.0	0.7	3.2	0.6	2.0	2.5
Glycera lapidum	1.0	1.5	2.0	1.2	2.0	1.6
Mendicula ferruginosa	1.4	2.4	1.6	1.2	1.7	1.2
Lumbrineris aniara	1.0	1.7	1.7	1.3	1.9	0.6
Spatagonida	1.0	0.2	1.6	1.3	2.8	1.1
Cerianthus lloydii		2.0	5.3	2.9	4.0	3.0
Pterolysippe vanelli		3.3	2.4	2.2	2.7	1.6
Thyasira equalis		1.9	1.8	2.6	2.9	2.0
Amphiura chiajei		2.1	1.9	1.7	2.4	2.1
Diplocirrus glaucus		2.1	2.0	1.2	2.3	2.3
Ampharete falcata		1.5	2.0	1.7	2.1	2.2
Axinulus croulinensis		2.6	1.2	1.9	2.2	0.9
Abyssoninoe hibernica		1.1	1.7	2.2	1.3	1.3
Notomastus		1.3	1.0	1.3	2.1	1.2
Praxillella affinis		1.7	0.5	1.7	1.9	0.9
Levinsenia gracilis	1.4	1.0	2.0	1.4	1.4	
Spiophanes bombyx	3.9	1.3	1.0		1.6	1.7
Abra nitida		0.8	1.0	1.4	1.4	0.9
Chone		1.5	0.7	0.7	1.0	1.4
Laonice sarsi		0.7	0.9	1.6	1.1	0.9
Amaeana trilobata		1.0	1.4	0.8	1.2	0.7
Cerebratulus		0.2	1.4	1.3	0.9	0.9
Typhlotanais aequiremis		0.8	1.2	0.8	0.7	1.0
Streblosoma		1.0	0.5	1.3	1.1	0.3
Trichobranchus roseus		0.8	0.5	1.0	1.1	0.3
Phoronis		0.5	1.0	0.5	1.1	0.5
Ophiuridae	1.7	1.4		0.3	0.6	0.3
Heteromastus	1.0	0.5		0.3	0.8	0.8
Turbellaria		0.2	0.5	0.6	0.5	0.3
Gnathiidae		0.4	0.5	0.7	0.2	0.3
Nephasoma minutum		3.2		2.8	1.8	3.5
Arctica islandica			2.1	0.5	2.0	1.5
Dipolydora coeca		1.0		1.5	1.0	0.9
Scalibregma inflatum			1.2	0.3	0.7	1.3
Echinoida		0.2	1.9	0.8	0.5	
Thyasira obsoleta		0.4		1.1	0.6	0.9
Tubulanus polymorphus		0.4		1.3	0.9	0.3
Brissopsis lyrifera		0.8		0.9	0.2	0.7
Harpinia antennaria		0.5		1.1	0.4	0.5
Amphiura filiformis		0.3	1.0	0.3	0.7	
Minuspio cirrifera		0.7		0.3	1.0	0.3
Haliella stenostoma		0.5		0.8	0.2	0.8
Pista cristata sensu Jirkov		0.9		0.3	0.5	0.6
Phtisica marina		0.5	0.7	0.3	0.5	
Astacilla		0.2		0.8	0.6	0.3
Rhodine loveni		0.3		0.7	0.5	0.5

	Assemblage					
Taxa	**a**	**b**	**c**	**d**	**e**	**f**
Owenia fusiformis	1.0	0.5		0.6	0.7	
Haploops tubicola		0.2		0.7	0.2	0.7
Poecilochaetus serpens		0.7	0.5	0.3	0.2	
Apseudes spinosus		0.2	0.5	0.5	0.5	
Polycirrus		0.2	0.5	0.5	0.3	
Sthenelais limicola	1.0	0.8	0.5		0.2	
Eunereis longissima		0.2		0.3	0.3	0.3
Gnathia vorax		0.2	0.5	0.3	0.1	
Pholoe pallida		0.2		0.3	0.2	0.3
Leucon nasica			1.2	0.9	2.0	
Scolelepis korsuni			0.5	0.8	0.8	
Westwoodilla caecula		1.0	0.5		0.3	
Orbinia norvegica				0.8	0.3	0.7
Maera loveni		0.3		1.0	0.5	
Nephtys incisa			0.5	0.7	0.5	
Eriopisa elongata		0.7			0.6	0.3
Amphictene auricoma		0.8	0.5		0.3	
Nemertea	1.0	0.7			0.8	
Byblis gaimardii		0.2			0.5	0.8
Peringia ulvae		0.6		0.5	0.3	
Ampelisca gibba		0.4	0.5		0.4	
Philine scabra		0.2		0.3	0.7	
Cuspidaria cuspidata			0.5		0.3	0.3
Natatolana borealis		0.4		0.3	0.3	
Ennucula tenuis	1.0		0.7		0.2	
Augeneria tentaculata		0.2			0.4	0.3
Praxillura longissima		0.2		0.5	0.2	
Phascolion (Phascolion) strombus strombus		0.2			0.3	0.3
Virgularia mirabilis				0.3	0.1	0.3
Amythasides macroglossus		0.3		0.3	0.1	
Copepoda		0.2		0.3	0.2	
Phyllodoce groenlandica		0.2		0.3	0.2	
Amphipholis squamata			0.9	1.2		
Diastylis cornuta		0.4		1.0		
Tmetonyx			1.0		0.2	
Lysippe sexcirrata		0.9			0.2	
Siboglinum		0.5			0.5	
Streblosoma bairdi		0.3			0.7	
Pseudopolydora paucibranchiata		0.2	0.7			
Acidostoma obesum				0.7	0.2	
Aspidosiphon muelleri		0.2	0.5			
Nyctiphanes couchii		0.2	0.5			
Thelepus cincinnatus		0.2		0.5		
Anobothrus gracilis		0.4			0.2	
Nephtys hystricis					0.3	0.3
Diastyloides biplicata				0.3	0.2	
Loxosomella varians					0.2	0.3
Tryphosites longipes				0.5	0.1	
Lucinoma borealis		0.2				0.3
Ophiocten affinis		0.4			0.1	
Roxania utriculus		0.3			0.2	
Euclymene sp A					0.1	0.3
Myodocopodia				0.3	0.1	
Tellimya ferruginosa				0.3	0.1	
Leucothoe lilljeborgi		0.2			0.2	

	Assemblage					
Taxa	**a**	**b**	**c**	**d**	**e**	**f**
Harpinia pectinata		0.3			0.1	
Euclymene droebachiensis		0.2			0.2	
Harmothoe antilopes		0.2			0.2	
Liocarcinus		0.2			0.2	
Paradoneis eliasoni		0.2			0.2	
Sarsinebalia urgorrii		0.2			0.1	
Eudorella truncatula		0.2			0.1	
Eumida bahusiensis		0.2			0.1	
Ophelina acuminata			0.7			
Abra prismatica						0.7
Enteropneusta					0.6	
Tubificoides amplivasatus		0.5				
Amphipoda			0.5			
Glycera alba			0.5			
Malacobdella grossa			0.5			
Podocopida			0.5			
Nicippe tumida					0.4	
Harpinia crenulata					0.4	
Mytilus edulis						0.3
Ophiodromus flexuosus				0.3		
Processa modica modica						0.3
Pseudopolydora pulchra				0.3		
Thracia convexa				0.3		
Timoclea ovata				0.3		
Tryphosella nanoides						0.3
Harmothoe impar agg					0.3	
Pholoe assimilis		0.3				
Sosane wahrbergi		0.3				
Astropecten irregularis					0.3	
Aphelochaeta					0.2	
Aricidea catherinae					0.2	
Euchone					0.2	
Bougainvillidae		0.2				
Dasybranchus		0.2				
Diastylis lucifera		0.2				
Eulimella acicula		0.2				
Eumida sanguinea		0.2				
Halecium		0.2				
Hyalinoecia tubicola		0.2				
Kurtiella bidentata		0.2				
Limatula gwyni		0.2				
Nuculana minuta		0.2				
Ophelina cylindricaudata		0.2				
Panthalis oerstedi		0.2				
Perioculodes longimanus		0.2				
Pholoe baltica		0.2				
Stenothoe marina		0.2				
Syllis cornuta		0.2				
Turritella communis		0.2				
Vitreolina philippi		0.2				
Aporrhais serresianus					0.2	
Chaetoderma nitidulum					0.2	
Orbinia kupfferi					0.2	
Phaxas pellucidus					0.2	
Campylaspis rubicunda					0.2	

	Assemblage					
Taxa	**a**	**b**	**c**	**d**	**e**	**f**
Desmosoma lineare					0.2	
Ditrupa arietina					0.2	
Gattyana cirrhosa					0.2	
Sige fusigera					0.2	
Cuspidaria rostrata					0.1	
Paguridae					0.1	
Tellimya tenella					0.1	
Amphicteis gunneri					0.1	
Antalis entalis					0.1	
Aoridae					0.1	
Aphrodita aculeata					0.1	
Apistobranchus tullbergi					0.1	
Ascidea					0.1	
Brada villosa					0.1	
Clymenura					0.1	
Epitonium trevelyanum					0.1	
Ericthonius					0.1	
Falcidens crossotus					0.1	
Golfingia vulgaris					0.1	
Goniada maculata					0.1	
Goniada norvegica					0.1	
Hiatella arctica					0.1	
Hyperia galba					0.1	
Jasmineira candela					0.1	
Labidoplax media					0.1	
Lanice conchilega					0.1	
Leptognathia breviremis					0.1	
Lysilla loveni					0.1	
Macrochaeta					0.1	
Melinnacheres steenstrupi					0.1	
Nephtys paradoxa					0.1	
Ophryotrocha					0.1	
Pectinidae					0.1	
Prionospio dubia					0.1	
Scoletoma magnidentata					0.1	
Spio armata					0.1	
Spiochaetopterus					0.1	
Thyasira sarsi	3.0					

Colour coding reflects relative abundance (red = high, yellow = medium, green = low).

Appendix 3. Table of taxa characterising each distinct macrofaunal assemblage identified at Scanner Pockmark SCI

	Assemblage						
Taxa	**d**	**b**	**a**	**e**	**c**	**f**	**g**
Abyssoninoe hibernica	1.41	1.73	1.41		1.05	7.41	2.59
Amphiura chiajei	1.00	1.00		1.00	0.94	1.75	1.13
Ampharete lindstroemi		1.73		1.00	2.49	1.41	1.85
Amphiura	2.00	2.00			0.91	1.9	1.27
Orbinia (Phylo) grubei	2.65	1.41	2.00	1.41			0.07
Cerianthus lloydii	1.73		1.41		0.67	0.68	0.73
Byblis gaimardi		1.00	1.00		0.91	0.85	0.59
Leucon nasica		1.41	1.41	1.00	0.33		0.04
Chaetoderma nitidulum		1.00		1.00	0.33	0.85	0.9
Cuspidaria cuspidata		1.00	1.41		0.33	0.68	0.4
Leiochone johnstoni	1.00	1.00		1.00		0.35	0.05
Diplocirrus glaucum	1.00	1.00			0.67	0.25	0.41
Thyasira obsoleta	4.80	3.46	3.61	2.83			
Paramphinome jeffreysii	4.80	1.00		3.87			0.07
Amphictene auricoma		1.00			1.63	1.77	2.03
Apseudes spinosus			2.00		1.96	0.96	0.78
Polycirrus medusa	1.00		2.24	2.00			0.04
Spiophanes kroyeri	1.41	2.45	1.00				0.04
Nemertea	1.41		1.00	1.73			0.19
Nephtys paradoxa	1.41	1.00	1.41				0.13
Mediomastus fragilis			2.00	1.41		0.25	0.04
Eriopisa elongata			1.41	1.00	0.8		0.43
Cirratulus cirratus	1.00			1.00		0.68	0.89
Goniada maculata			1.00		0.33	0.25	0.27
Abra nitida					3.16	5.58	3.54
Ampelisca typica					1.05	3.77	4.19
Amphicteis gunneri					1.72	2.16	1.8
Harpinia antennaria			1.41	1.73	0.67		
Arrhis phyllonyx					1.49	0.5	1.2
Astropecten irregularis					1.28	0.6	1.23
Ophelina norvegica	2.00			1.00			0.11
Ceratocephale loveni		1.00				0.71	1.38
Brissopsis lyrifera					0.47	0.87	1.71
Echinocardium		1.73				0.43	0.82
Laonice sarsi		1.00		1.00		0.5	
Mendicula ferruginea		1.00		1.00			0.29
Callianassa					0.67	0.35	1.17
Campylaspis rubicunda					0.8	0.75	0.6
Chaetoparia nilssoni					0.67	0.6	0.5
Harpinia pectinata		1.00				0.5	0.16
Levinsenia gracilis		1.00				0.25	0.11
Ditrupa arietina					0.47	0.5	0.36
Eudorella truncatula					0.33	0.75	0.13
Eunereis longissima					0.33	0.6	0.27
Glycera lapidum					0.33	0.25	0.43
Golfingia vulgaris					0.33	0.25	0.27
Terebellides stroemi	1.00	2.00					
Campylaspis costata						0.96	1.22
Praxillella affinis		1.73					0.04
Platyhelminthes				1.41			0.04
Pseudopolydora antennata	1.41						0.04
Edwardsia claparedii					0.33		0.9

	Assemblage						
Taxa	**d**	**b**	**a**	**e**	**c**	**f**	**g**
Eulima bilineata					0.33		0.87
Gammaropsis					0.67		0.46
Ophiodromus flexuosus			1.00				0.1
Panthalis oerstedi			1.00				0.07
Pennatula phosphorea		1.00					0.07
Philine aperta				1.00			0.07
Polynoidae	1.00						0.04
Streblosoma intestinalis			1.00				0.04
Gnathia oxyuraea						0.75	0.26
Gnathia pranizae						0.75	0.19
Goniada norvegica					0.33		0.5
Lagis koreni					0.33		0.31
Leucothoe lilljeborgi						0.25	0.11
Lumbrineris fragilis						0.25	0.07
Lumbrineris gracilis						0.25	0.07
Trichobranchus rosea		1.41					
Lumbineris latreilli					0.33		
Maera loveni							0.31
Minuspio cirrifera							0.26
Myriochele heeri						0.25	
Natatolana borealis							0.2
Nephtys longosetosa							0.16
Nereimyra punctata							0.11
Nicomache lumbricalis							0.11
Notomastus latericeus							0.11
Nucula nitidosa							0.11
Ophelina acuminata							0.11
Orbinia (O.) cf. latreilli							0.09
Orbinia (O.) sertulata							0.07
Pholoe assimilis							0.07
Pholoe pallida							0.05
Pista cristata							0.04
Pseudopolydora pulchra							0.04
Pterolysippe cf. vanelli							0.04
Sabellidae							0.04
Scalibregma inflatum							0.04
Sipuncula							0.04
Spadella cephaloptera							0.04
Spiochaetopterus cf. typicus							0.04
Spiophanes bombyx							0.04
Talochlamys pusio							0.04

Colour coding reflects relative abundance (red = high, yellow = medium, green = low).

Appendix 4. Tables of taxa identified from the analysis of video and still samples from Braemar Pockmarks SCI

Taxon/feature - VIDEO	% occurrence
Sabella	87
Burrows	84
Pagurus	81
Mysida	77
Asterias rubens	71
Gadidae	58
Echinus acutus	55
Myxinidae	55
Virgularia mirabilis	55
Hydrozoa	45
Anthozoa	42
Trisopterus luscus	42
Pollachius	39
Asteroidea	32
Cnidaria	32
Caridea	23
Pennatula phosphorea	16
Pleuronectiformes	16
Buccinidae	10
Urticina	10
Glyptocephalus cynoglossus	6
Hippasteria phrygiana	6
Nephrops norvegicus	6
Bacterial mat	6
Crustacea	3
Lophius piscatorius	3
Ophiuroidea	3
Pectinidae	3

Taxon/feature – STILLS	% occurrence
Sabella	94
Unidentified megafauna	79
Pagurus	16
Echinus acutus	13
Pollachius virens	12
Hydrozoa	10
Asterias rubens	7
Mysidae	5
Caridea	5
Gadidae	4

Taxon/feature – STILLS	% occurrence
Virgularia mirabilis	4
Mysida	4
Pisces	4
Asteroidea	3
Unidentified tube	2
Echinoidea	2
Pleuronectiformes	2
Myxinidae	2
Anthozoa	1
Trisopterus luscus	1
Urticina	1
Echinus	1
Pennatula phosphorea	1
Actiniaria	1
Bacterial mat	1
Gastropoda	1
Ophiura albida	1
Astropecten	1
Buccinum undatum	1
Pseudamussium septemradiatum	1
Buccinidae	1
Myxine glutinosa	1
Pomatoceros	1
Amphiura	<1
Calliactis parasitica	<1
Crustacea	<1
Hippasteria phrygiana	<1
Nephrops norvegicus	<1
Aporrhais pespelecani	<1
Arctica	<1
Glyptocephalus cynoglossus	<1
Lophius piscatorius	<1
Merlangius merlangus	<1
Nephrops	<1
Ophiotrichidae	<1
Ophiuroidea	<1
Pectinidae	<1
Pelecypoda	<1
Scophthalmus rhombus	<1

Appendix 5. Table of taxa identified from the analysis of video and still samples from Scanner Pockmark SCI

Taxon/feature - VIDEO	% occurrence
Burrows	100
Ditrupa	94
Sabella	94
Caridea	88
Myxine glutinosa	81
Asteroidea	75
Pagurus	75
Pennatula phosphorea	69
Actiniaria	56
Pisces	50
Cerianthus lloydii	31
Nephrops norvegicus	31
Pleuronectiformes	31
Virgularia mirabilis	31
Pollachius	19
Arachnanthus sarsi	13
Ceriantharia	13
Gadidae	13
Aequipecten opercularis	6
Astropecten irregularis	6
Gobiidae	6
Lithodes maia	6
Naticidae	6
Trisopterus	6
Unidentifiable megafauna	6

Taxon/feature - STILLS	% occurrence
Burrows	70
Sabella	52
Ditrupa	28
Actiniaria	5
Pagurus	5
Myxine glutinosa	4
Caridea	4
Asteroidea	3
Gadidae	3
Unidentifiable burrowing fauna	3
Pennatula phosphorea	3
Pisces	2
Virgularia mirabilis	2
Cerianthus lloydii	2
Nephrops norvegicus	1
Anthozoa	1
Astropecten irregularis	1
Pleuronectiformes	1
Arachnanthus sarsi	<1
Ophiura	<1
Aequipecten opercularis	<1
Gobiidae	<1
Luidia sarsi	<1
Mollusca	<1
Naticidae	<1
Pleuronectidae	<1
Polychaeta	<1
Trisopterus luscus	<1
Tunicata	<1

Appendix 6. Taxonomic analysis of meiofaunal nematode samples collected from marine methane seeps: Scanner & Braemar Pockmark cSAC/SCI Sites

Report available as PDF file alongside this report.

Appendix 7. Petrography and stable isotope study of methane-derived authigenic carbonates (MDAC) from the Braemar Pockmark Area, North Sea

Report available as PDF file alongside this report.

JNCC/Cefas Partnership Report Series. *CEND 19x/12: Offshore seabed survey of Braemar Pockmarks SCI and Scanner Pockmark SCI*, **No. 14**. Rance, J., Barrio Froján, C. & Schinaia, S. March 2017. ISSN 2051-6711